Moisture Susceptibility Testing for Hot Mix Asphalt Pavements in New England

Eshan V. Dave, Principal Investigator
University of New Hampshire (UNH)

Jo Sias Daniel, Co-Principal Investigator
University of New Hampshire (WPI)
Rajib B. Mallick, Co-Principal Investigator
Worcester Polytechnic Institute (WPI)

Christopher DeCarlo, Research Assistant (UNH)

Ram Kumar Veeraragavan, Research Assistant (WPI)

Nivedya Madankara Kottayi, Post-Doctoral Research Associate (WPI)

Prepared for

The New England Transportation Consortium

August 2018

NETCR109 Project No. 15-3

ACKNOWLEDGEMENTS

The following are the members of the Technical Committee that developed the scope of work for the project and provided technical oversight throughout the course of the research:

- Derek Nener-Plante (TC Chairperson), Maine Department of Transportation
- Beran Black, New Hampshire Department of Transportation
- Mark Brum, Massachusetts Department of Transportation
- Eliana Carlson, Connecticut Department of Transportation
- Scott DaRosa, Rhode Island Department of Transportation
- Andy Willette, Vermont Agency of Transportation

Technical Report Documentation Page

1. Report No.	2. Government Accession No.	3. Recipient's Catalog No.
NETCR109	N/A	N/A

4. Title and Subtitle	5. Report Date
Moisture Susceptibility Testing for Hot Mix Asphalt Pavements in New England	August 2018
	6. Performing Organization Code: N/A

7. Author(s)	8. Performing Organization Report No.
Eshan Dave, Jo Sias Daniel, Rajib Mallick, Christopher DeCarlo, Ram Kumar Veeraragavan, Nivedya Madankara Kottayi	NETCR109

9. Performing Organization Name and Address	10. Work Unit No. (TRAIS)
University of New Hampshire 105 Main Street Durham, NH, 03824	N/A
	11. Contract or Grant No.: N/A

12. Sponsoring Agency Name and Address	13. Type of Report and Period Covered
New England Transportation Consortium C/O Transportation Research Center University of Vermont, Farrell Hall 210 Colchester Avenue Burlington, VT 05405	Final Report
	14. Sponsoring Agency Code: NETC 15-3. A study conducted in cooperation with the U.S. DOT

15. Supplementary Notes

16. Abstract

Moisture damage in asphalt mixtures is a common and challenging distress for pavements in wet climates such as New England. Moisture damage is typically addressed with laboratory tests as a part of the mixture design process where the main point of the test is to determine the potential for the material to experience moisture related damage, known as moisture susceptibility. The long established standard moisture susceptibility test method, AASHTO T-283, has been widely criticized concerning its ability to accurately and reliably predict field results. This problem has been experienced in the New England region where multiple high profile moisture failures have occurred on roadways. The primary objective of this research was to evaluate multiple different moisture susceptibility test methods to determine the most reliable and accurate replacement for current test methods in New England. A total of ten asphalt mixtures with varying historical performance in terms of moisture damage (poor, moderate, and good) were sampled and extensively tested in lab. On basis of lab testing and analysis, recommendations for lab tests are developed for New England agencies to adopt as part of their asphalt mix design and acceptance procedures. Hamburg wheel tracking test is recommended to be adopted due to its most clear distinction between poor and good performers, ultra-sonic pulse velocity non-destructive test is also recommended as a low cost screen tool to be used during mix design process.

17. Key Words	18. Distribution Statement
Asphalt, moisture susceptibility, modified Lottman test, MiST, Hamburg Wheel Tracker, Ultra-sonic pulse velocity, semi-circular bend test, disk-shaped compact tension test, multi-cycle freeze-thaw, ME pavement analysis.	No restriction. This document is available to the public through the National Technical Information Service, Springfield, Virginia 22161

19. Security Classif. (of this report)	20. Security Classif. (of this page)	21. No. of Pages	22. Price
Unclassified	Unclassified	164	N/A

SI* (MODERN METRIC) CONVERSION FACTORS

APPROXIMATE CONVERSIONS TO SI UNITS

SYMBOL	WHEN YOU KNOW	MULTIPLY BY	TO FIND	SYMBOL
		LENGTH		
in	inches	25.4	millimeters	mm
ft	feet	0.305	meters	m
yd	yards	0.914	meters	m
mi	miles	1.61	kilometers	km
		AREA		
in^2	square inches	645.2	square millimeters	mm^2
ft^2	square feet	0.093	square meters	m^2
yd^2	square yard	0.836	square meters	m^2
ac	acres	0.405	hectares	ha
mi^2	square miles	2.59	square kilometers	km^2
		VOLUME		
fl oz	fluid ounces	29.57	milliliters	mL
gal	gallons	3.785	liters	L
ft^3	cubic feet	0.028	cubic meters	m^3
yd^3	cubic yards	0.765	cubic meters	m^3
	NOTE: volumes greater than 1000 L shall be shown in m^3			
		MASS		
oz	ounces	28.35	grams	g
lb	pounds	0.454	kilograms	kg
T	short tons (2000 lb)	0.907	megagrams (or "metric ton")	Mg (or "t")
		TEMPERATURE (exact degrees)		
°F	Fahrenheit	5 (F-32)/9 or (F-32)/1.8	Celsius	°C
		ILLUMINATION		
fc	foot-candles	10.76	lux	lx
fl	foot-Lamberts	3.426	candela/m^2	cd/m^2
		FORCE and PRESSURE or STRESS		
lbf	poundforce	4.45	newtons	N
lbf/in^2	poundforce per square inch	6.89	kilopascals	kPa

APPROXIMATE CONVERSIONS FROM SI UNITS

SYMBOL	WHEN YOU KNOW	MULTIPLY BY	TO FIND	SYMBOL
		LENGTH		
mm	millimeters	0.039	inches	in
m	meters	3.28	feet	ft
m	meters	1.09	yards	yd
km	kilometers	0.621	miles	mi
		AREA		
mm^2	square millimeters	0.0016	square inches	in^2
m^2	square meters	10.764	square feet	ft^2
m^2	square meters	1.195	square yards	yd^2
ha	hectares	2.47	acres	ac
km^2	square kilometers	0.386	square miles	mi^2
		VOLUME		
mL	milliliters	0.034	fluid ounces	fl oz
L	liters	0.264	gallons	gal
m^3	cubic meters	35.314	cubic feet	ft^3
m^3	cubic meters	1.307	cubic yards	yd^3
		MASS		
g	grams	0.035	ounces	oz
kg	kilograms	2.202	pounds	lb
Mg (or "t")	megagrams (or "metric ton")	1.103	short tons (2000 lb)	T
		TEMPERATURE (exact degrees)		
°C	Celsius	1.8C+32	Fahrenheit	°F
		ILLUMINATION		
lx	lux	0.0929	foot-candles	fc
cd/m^2	candela/m^2	0.2919	foot-Lamberts	fl
		FORCE and PRESSURE or STRESS		
N	newtons	0.225	poundforce	lbf
kPa	kilopascals	0.145	poundforce per square inch	lbf/in^2

*SI is the symbol for the International System of Units. Appropriate rounding should be made to comply with Section 4 of ASTM E380.

Table of Contents

List of Tables

List of Figures

1. Introduction

The loss of asphalt mixture durability and load carrying capacity due to the presence of moisture is commonly referred to as moisture-induced damage. This damage can result in significantly inferior performance of asphalt pavements, resulting in a reduced life span that will have a considerable economic impact on the transportation agencies. The extent to which an asphalt mixture is prone to moisture-induced damage is commonly known as moisture susceptibility. A number of experimental procedures have been proposed for conditioning asphalt mixtures to simulate moisture conditions experienced in the field and to measure loss of durability or strength through use of mechanical or non-destructive tests. Often, these procedures also establish threshold values that are used to determine whether remedial actions, such as use of anti-stripping additives, are needed. While a number of procedures exist in literature, mixed success with these procedures, including the AASHTO T-283 method (most widely adopted), has been reported by many state transportation agencies. At present, no single comprehensive study has compared different moisture conditioning methods, different methods to assess the loss of mixture durability and load carrying capacity, and actual field durability. Furthermore, while a few studies have had several of these attributes, these have not been assessed on asphalt mixtures commonly used in the New England region. The project presented in this report is designed to address the primary challenge of incorporating reliable moisture susceptibility in mix design, design acceptance and project acceptance stages. The project also builds the framework for addressing the secondary challenges of determining service life reductions from moisture induced damage and incorporating it in the pavement design process.

The objectives of this project, as outlined in the original proposal, were defined as:

- Evaluate good and poor performing asphalt mixtures in New England and determine mechanisms responsible for poor performing mixtures
- Determine impacts of remedial measures in reducing moisture susceptibility of poor performing mixtures
- Assess impacts of moisture induced-damage on pavement performance and service life
- Recommend an evaluation framework consisting of appropriate test procedure(s), specifications, and analysis procedure verified with field performance data that is reliable and suitable for moisture susceptibility testing of asphalt mixtures used in New England

This report details the main tasks and accomplishments of the NETC 15-3 project. This report is organized into four main sections, each of which details the key findings from each of the projects tasks outlined in the proposal. Task 1 focused on a review of current practice and documented research on moisture susceptibility testing for hot mix asphalt. Task 2 detailed the choices made by the research team with respect to the methodology, including material sampling, specimen preparation, and laboratory testing, for the project. Task 3 contains the laboratory testing results

and associated discussion, while Task 4 covers the final conclusions and recommendations from the project. The Appendices contain supplemental information pertinent to the project.

2. Task 1: State of the Practice and Literature Review

The first part of the following section details the literature review conducted by the research team as a precursor to developing the methodology and testing plan for the project. This review is an overview of current practice in New England and the United States with respect to moisture susceptibility testing for hot mix asphalt as well as pertinent research related to the topic. The second part of this section summarizes findings from a survey sent to the New England transportation agencies focusing on their experience with moisture susceptibility. The focus of this survey was to gain an understanding of how significant the issue of moisture susceptibility is to New England transportation agencies as well as determining what the various agencies are interested in learning through the research project. The key findings from the review and survey are presented here.

2.1 Asphalt Moisture Susceptibility Testing

Testing for moisture susceptibility can be divided into two main categories: (a) tests on loose mix; and, (b) tests on compacted mixtures.

A number of visual rating based testing procedures have been used in the past for testing loose mixes. These include boiling water test (ASTM D3625), Texas boiling water test (Kennedy et al. 1984), static immersion test (previously AASHTO T-182, now removed) and rolling bottle test (European standard EN 12697-11). Tests of loose mixes have been criticized for two reasons, firstly the use of subjective visual evaluations in these methods often times increases variability and lowers consistency in multi-operator settings. Secondly, while these tests might be able to distinguish moisture susceptibility in terms of component materials (aggregates and affinity between aggregate and binder), the tests do not assess moisture induced damage in compacted asphalt mixtures. This limits the ability of these tests to reliably predict pavement performance impacts and does not take into account variations between mix designs and air void distribution. Finally, the tests on loose mixes usually focus only on the moisture-induced adhesive failures without considering cohesive failure within asphalt mastic.

Laboratory moisture susceptibility tests on compacted asphalt specimens can be further divided into two categories, the first approach is where the specimens are divided into control and moisture conditioned groups, both are tested (typically to measure mechanical response of the material) and the results are compared to determine moisture susceptibility of the mixture. Examples of this first approach include the modified Lottman procedure (AASHTO T-283), Moisture induced stress tester (MiST) conditioning followed by dynamic modulus and direct tension cyclic fatigue test using asphalt mixture performance tester (AMPT), incremental repeated permanent deformation test (iRLPD) and repeated freeze-thaw conditioning followed by creep, strength and fracture energy testing. The second approach is where moisture conditioning and testing for material property occurs simultaneously. A commonly adopted test in this category is Hamburg wheel tracking (HWT) test (AASHTO T-324).

2.2 Laboratory Procedures for Moisture Conditioning

2.2.1 Modified Lottman Procedure/AASHTO T283

The modified Lottman test procedure (AASHTO T-283) is the most widely accepted method for evaluation of moisture susceptibility of asphalt mixtures. Dave and Koktan (2011) reported that 36 out of 50 State Department of Transportation in United States use this procedure in their asphalt mixture specifications. The original procedure was formalized by Lottman (1978, 1982) and has since undergone several iterations of refinements (i.e. such as Epps et al. 2000). The moisture conditioning for the AASHTO T-283 procedure includes moisture saturation of specimens to a level of 70-80%. The saturated samples are conditioned at -18°C for 16 hours followed by a thawing period at 60°C for 24 hours. The specimens are thereafter placed in a water bath at 25°C and tested in indirect tensile mode at 25°C. Many states allow a deviation on this procedure by exempting the freezing portion of the conditioning.

While commonly adopted, the AASHTO T-283 procedure has received substantial criticism for not being able to distinguish mixtures that may be susceptible to moisture damage in field (Solaimanian et al. 2007), not being able to capture moisture damage seen from actions of traffic (Epps et al. 2000; Mallick et al. 2003; Pinkham et al. 2013) or in regions of colder climates (Dave and Baker 2013) and being non-fundamental in nature (Kringos et al. 2011). Due to these limitations, and on the basis of mixed success realized by State highway agencies with use of the Lottman approach, research has continued to refine the procedures and to investigate other alternatives.

The AASHTO T-283 procedure requires asphalt specimens to be vacuum saturated prior to freezing them. Jacques (2013) compared the vacuum saturation with the normal inundation procedure with four Maine DOT asphalt mixtures. His results showed that the loss of dynamic modulus of asphalt specimens using vacuum saturation creates a greater amount of damage than normal inundation.

2.2.2 Environmental Conditioning System

As part of the Strategic Highway Research Program (SHRP), Al-Swailmi and Terrel (1994) proposed the Environmental Conditioning System (ECS) for assessing the moisture susceptibility of HMA mixes. The ECS was subsequently standardized as AASHTO TP-34, "Determining Moisture Sensitivity of Compacted Bituminous Mixtures Subjected to Hot and Cold Climate Conditions." This procedure was designed to determine the moisture sensitivity of compacted asphalt specimens under conditions of temperature, moisture saturation, and dynamic loading similar to those found in pavements. Although the ECS showed promise, the results from this type of conditioning system were not significantly more precise or accurate than those of the AASHTO

T-283. The NCHRP 9-34 study by Solaimanian et al. (2007), further evaluated ECS. The NCHRP project utilized a modified ECS system on basis of work by Tandon and Nazarian (2001). The modified and improved ECS was used in conjunction with dynamic modulus of asphalt mixture as a way to determine the extent of moisture induced damage in asphalt mixtures. In spite of the advantages of procedure, the researchers found several shortcomings that needed to be addressed before the ECS/dynamic modulus procedure can be used as a routine mix design test to identify the moisture damage susceptibility of a mix. The main problems were associated with the duration of water/load conditioning, temperature requirements at the time of conditioning, and the magnitude of the conditioning load.

2.2.3 Moisture Induced Stress Tester

The Moisture Induced Stress Tester (MiST), shown in Figure 1: MiST DeviceFigure 1, was developed as a simulation (conditioning) method for moisture damage to asphalt concretes. It uses a hydraulic system to create alternative pressure and vacuum cycles inside the test chamber, thereby forcing water into and out of the pores of HMA specimens. This process is intended to mimic the effect of hydraulic scouring, one of the most common forms of moisture damage in asphalt pavements, in which air voids in pavements are saturated with water, and under traffic the trapped water repeatedly exerts pore pressure on the HMA, which leads to a loss of adhesion between aggregate and binder and a loss of cohesive bond within asphalt binder (Chen et al. 2008; Mallick et al. 2003; Pinkham et al. 2013). The effect of pore water pressure and saturation on debonding of asphalt paving mixes was investigated by Jimenez (1974) and, Kiggundu et al. (1988), while the effect of permeability and vehicle speed on pore water pressure in pavements has been investigated by a number of researchers (including, Novak et al. 2002; Mallick et al. 2003; Buchanan et al. 2004; Mallick et al. 2005; Birgisson et al. 2007; Pinkham et al. 2013). In general, the need for equipment for generating cyclic pore pressure in HMA has been suggested by most of the authors, to identify mixes with potential of moisture damage to allow the evaluation of mixes within reasonable amount of time and help in avoiding the other complicating effects of moisture damage.

Figure 1: MiST Device

The MiST equipment has shown good potential for identification of moisture susceptible mixes. Preconditioned values for bulk specific gravity and indirect tensile strength (ITS) of compacted specimens as well as visual inspection of the specimens can be compared with post conditioned values to determine the susceptibility of the HMA mix. A study by Chen and Huang (*2008*) used the previous version of the MiST to condition laboratory compacted specimens with and without anti-strip additives and with various gradations. They compared results from the MiST with those from traditional freeze-thaw conditioning, and determined that the MiST is effective to determine the moisture-susceptibility of HMA mixes in the laboratory. The specimens could be tested for mechanical properties before and after the conditioning process with the MiST. The test equipment is relatively inexpensive, and the conditioning could be completed within reasonable time period (< 24 hours), which alleviates a major limitation of the previously discussed ECS method. Also, a range of conditions (pressure, temperature, number of cycles) are available, and finally there is a growing body of literature on this equipment and an ASTM standard has also been developed for this method (ASTM D7870).

2.2.4 Multiple Cycle Freeze-Thaw

Asphalt mixtures in colder and wet climates such as that of the New England region experiences a substantial number of repeated freezing and thawing cycles in partial and fully saturated states (Jackson and Puccinelli 2006). In a study of roadways in Quebec, the average number of freeze-thaw cycles experienced by surface asphalt mixtures have been reported to be in a range of 40-50 per year (Fortin 2010). Research by Baker (2012) and Dave and Baker (2013) proposed the use of repeated freeze-thaw conditioning, shown in Figure 2, of asphalt mixtures using temperatures that are representative of the conditions experienced by roadways. Their results showed comparable moisture susceptibility between lab conditioned mixtures and those conditioned in field. Recently, Lamothe et al. (2015) evaluated contraction and expansions of partially saturated asphalt mixture

specimens to freeze-thaw cycles. The study demonstrated the effects of using brine at different salt concentrations and its effects on material expansion as well as extent of damage. Manning et al. (2014) tested asphalt mixture from New Hampshire with a wide range of conditioning approaches including multiple freeze-thaw cycles (3, 6 and 12). The specimens conditioned with freeze-thaw cycles were further divided into two groups, the first group represented dry freeze-thaw (no moisture inundation prior to start of cycling) and second group represented wet freeze-thaw (12 hour moisture inundation prior to cycling and each thaw phase was simulated by submerging specimens in water). The results for these specimens showed a continued decrease in compressive strength with increasing number of freeze-thaw cycles.

Figure 2: Multi-Cycle Freeze-Thaw Conditioning Set Up

2.3 Tests for Characterization of Moisture Conditioned Specimens

In order to evaluate the moisture susceptibility of an asphalt mixture, the mechanical capacity and integrity of the material needs to be evaluated pre- and post-moisture conditioning (such as, AASHTO T-283 modified Lottman process) or in a simultaneous manner while conditioning (such as, Hamburg Wheel Tracker). This section reports on commonly used tests as well as new tests that have been recently developed or are under development. The test procedures can be broadly classified as destructive versus non-destructive. The destructive test procedures are discussed first.

2.3.1 Hamburg Wheel Tracking Device

The Hamburg Wheel Tracking (HWT) device was originally developed in the 1970's by Esso A.G. of Hamburg, Germany to measure rutting susceptibility, based on a similar British device that utilized a rubber tire. Later, the City of Hamburg began testing specimens in temperature controlled water instead of an environmental chamber and discovered that some mixtures began to deteriorate from moisture damage, especially when subjected to a higher number of passes with the steel wheel (WSDOT 2012). Since its introduction to the United States in the early 1990's, the Hamburg Wheel Tracking (HWT) device (AASHTO T-324) has gained popularity as a moisture sensitivity test (Aschenbrener 1995). The test was recommended by Cooley et al. (2000) as suitable "go / no-go" test that can be used by agencies on a routine basis. Koktan and Dave (2012) reported that three US state transportation agencies require use of HWT for moisture susceptibility testing as well as several others that were actively evaluating some form of wheel tracking test as an alternative to their current procedures. The device was initially developed for evaluating rutting potential of asphalt mixtures and was further refined to determine the moisture damage potential. HWT is a simulative test procedure that imposes repeated load of 158 lb. onto asphalt mixture through steel wheels of 1.9 inch width and 8 inch diameter. The typical testing condition for moisture susceptibility submerges compacted asphalt specimens in water at a temperature of 50ºC. The device allows for use of either compacted slabs or two gyratory compacted specimens with flat faces placed against each other.

During the course of testing, the rut depths from repeated loading of steel wheels is measured and reported against number of passes. A typical testing requirement is 20,000 passes. Using the measured rut depth a number of properties can be inferred from the test, these include: creep slope, stripping inflection point, stripping slope and number of passes to failure. The HWT equipment and typical results are shown in Figure 3. Creep slope is the inverse of the initial rutting slope that observed in the initial portion of loading. The secondary slope indicative of the moisture-induced damage is referred to as the stripping slope. The inflection point between these slopes is indicative of the initiation point of the moisture damage. This stripping inflection point is often times used as an index parameter to compare different mixtures and to compare performance of the mixture

to the field. The number of passes to failure represents the required number of wheel passes at which the amount of rutting approaches a pre-set allowable level.

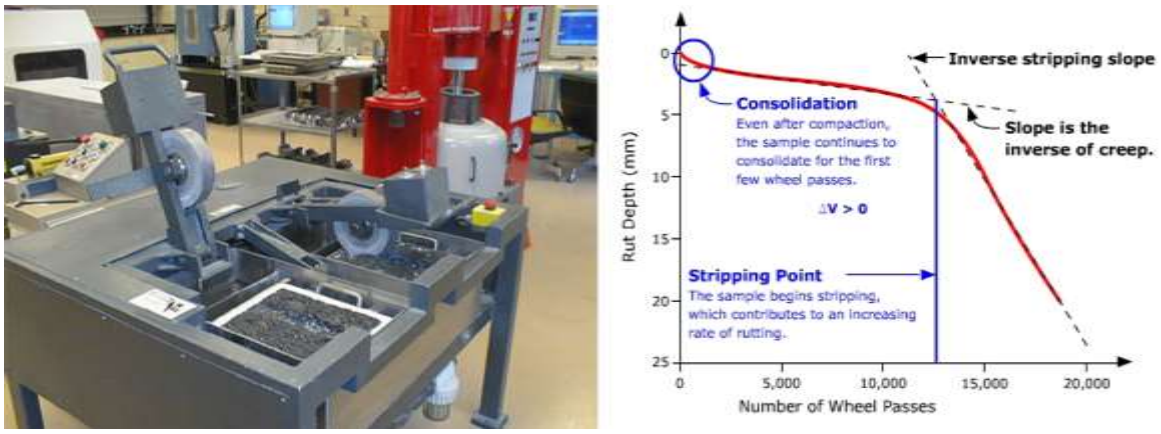

Figure 3: Hamburg Wheel Tracking Device and Typical Test Results (Pavement Interactive, 2015)

An extensive amount of research has been conducted to compare results from HWT with moisture susceptibility of asphalt mixtures and to refine the HWT procedures as well as data analysis. For example, Izzo and Tahmoressi (1999) compared six asphalt mixtures with and without anti-stripping additives and showed that the test is able to distinguish between the mixtures with and without additives. A study by Romero et al. (2008) proposed increasing test temperature for HWT to 54ºC when using asphalt binders with PG 70-XX grades (and higher) to be able to fully capture the rutting and moisture susceptibility of asphalt mixtures. Evaluation of asphalt mixtures from 16 field projects and their evaluation through a range of moisture susceptibility tests were conducted by Schram and Williams (2012). The results from that study showed HWT measured parameters to have good correlation with stripping performance in the field. Recently, the NCHRP 9-48 study employed the HWT for assessing moisture susceptibility of various warm-mix technologies (Martin et al. 2014). The study recommended use of HWT (as an alternative to AASHTO T-283) for moisture susceptibility testing and provided thresholds for stripping inflection point and stripping slope that can be used in the quality assurance (QA) process. Rahman and Hossain (2014) used HWT to evaluate moisture susceptibility and rutting of asphalt mixtures with RAP and concluded that moisture susceptibility increased with increasing RAP amounts.

2.3.2 Environmental Conditioning System with Dynamic Modulus (ECS/E)*

The NCHRP Project 9-34 (Solaimanian et al. 2007) focused on utilizing and improving a laboratory testing system for reliable prediction of moisture damage in HMA. For this purpose, the test procedure developed for the dynamic modulus (E*) proposed by NCHRP Projects 9-19 and 9-29 was applied to specimens conditioned with the environmental conditioning system (ECS) discussed earlier in this proposal. Mixes with known field performance were procured and tested with this system. For comparison, the indirect tensile strengths of conditioned and unconditioned specimens were also determined according to modified Lottman procedure (also known as,

Tunnicliff-Root procedure) specified by ASTM D4867. All mixes were also tested with the HWT device. For seven of the eight mixes researched in that project, the ECS/E* system was able to correctly estimate the moisture damage, which was better than ASTM D4867 and HWT procedures. It was also shown that the change in asphalt concrete modulus as a result of moisture damage can be used with the mechanistic empirical design for performance prediction purposes. Although ECS/E* is a better procedure, the long testing duration makes it less desirable or routine usage. However, the use of E* as a material parameter for assessment of extent of damage has great potential and could be used in conjunction with a quicker moisture conditioning system such as MiST.

2.3.3 Indirect Tensile Strength (ITS)

The use of ITS, shown in Figure 4, for moisture susceptibility was proposed by Lottman (1978) through the NCHRP 246 study. There have been further refinements to the moisture conditioning aspect of the procedure, however the use of ITS as measure of moisture induced damage has stayed the same. The original proposal by Lottman included use of both ITS and resilient modulus (M_R) as properties of interest. Subsequent research by Tunnicliff and Root (1984) through NCHRP 274 simplified the procedure and proposed only use of ITS. The current AASHTO T-283 procedure utilizes the ratio of the ITS measured on conditioned and unconditioned specimens, commonly referred to as the tensile strength ratio (TSR). While certain agencies (such as, Arizona DOT) require a minimum TSR as well as a minimum ITS on conditioned specimens ("wet strength"), a majority of agencies utilize only TSR.

The use of ITS as a moisture susceptibility parameter has received some criticism. Solaimanian and Kennedy (2000) concluded that the empirical nature of test and high susceptibility in giving false positives or false negatives is a major concern. NCHRP 9-34 study reconfirmed these findings. Use of ITS test procedure at temperature of 25ºC often times leads to crushing and shear type failure in the specimens as opposed to preferred indirect tensile failure. This is even more prominent for mixtures with softer binder grades, such as ones used in the New England region. Nonetheless at present, no other test method is more widely adopted or has the simplicity associated with it as ITS. Thus, in this study ITS will be used to test various mixtures.

Figure 4: Indirect Tensile Strength Setup

2.3.4 Dynamic Modulus

The use of dynamic modulus (E*) as a damage assessment parameter has been explored by a number of researchers, including the NCHRP 9-34 study (Solaimanian et al. 2007). A widespread adoption of AMPT device and use of dynamic modulus as a primary input to the AASHTO Pavement ME Design guide makes it a suitable parameter. Study by Nadkarni et al. (2009) showed that the ratio of dynamic modulus, referred to as E* stiffness ratio (ESR), was able to successfully able to distinguish between good and poor performing asphalt mixtures in Arizona. The effects of moisture induced-damage on dynamic modulus is found to be pre-dominant at higher temperatures and/or lower frequencies (Williams and Breakah, 2010). The primary criticism for use of dynamic modulus on routine basis has been the time requirement associated with specimen fabrication and testing, however for purposes of using an index parameter such as ESR, the testing time can be reduced by limiting tests to one or few temperatures. For example, on basis of the work by Williams and Breakah (2010) a singular warmer test temperature can be used. Furthermore, dynamic modulus measurements in indirect tensile mode (diametric loading) allows for use of this parameter with field core samples.

Using dynamic modulus measurements, pavement life predictions can be reliably made using mechanistic-empirical pavement design system such as AASHTOWare Pavement ME. This type of approach can allow extending the laboratory measurement of properties from only screening mixtures to a more of risk-based assessment. Use of pavement performance predictions can allow an agency to develop a more informed plan for use of remedial treatments, such as anti-stripping additives or hydrated lime, through use of life-cycle cost analysis. Due to positive experiences of previous researchers in use of dynamic modulus to successfully screen moisture susceptible mixes,

with the added benefit of linking laboratory property with pavement life cycle, the dynamic modulus measurements are proposed in this study.

2.4 Other Promising Procedures

Due to the limitations associated with the current moisture susceptibility procedures and to better understand the actual mechanisms behind moisture induced damage to asphalt mixtures, a significant amount of research has been undertaken to the topic. A brief review of recent research on the topic is presented here with objective of selecting procedures to be evaluated during the proposed study.

2.4.1 Florida HMA Fracture Mechanics Model (Energy Ratio Approach)

Birgisson et al. (2007) conducted a comprehensive laboratory experimental study to relate asphalt mixture characteristics with the potential severity of moisture damage. Their results showed that no single mixture property (i.e., tensile strength or stiffness) can be used to consistently capture the effects of moisture damage in mixtures due to the fact that moisture damage often affects overall behavior of asphalt mixtures. Therefore, they developed a new theoretical framework based on the Florida HMA fracture model (Zhang et al. 2001), along with several fracture energy parameters like fracture energy limit (FE), dissipated creep strain energy limit (DCSE), and the energy ratio (the ratio of dissipated creep strain energy to the minimum dissipated creep strain energy adequate for cracking performance) (Jailiardo 2003), which account indirectly for the influence of strength, stiffness, strain to failure, and the viscoelastic characteristics of asphalt mixtures. In addition, a new moisture conditioning method was developed by modifying a triaxial chamber, which is capable of applying cyclic pore pressure and loading separately or at the same time. The new moisture conditioning procedure and the fracture mechanics-based evaluation method were verified by testing asphalt mixtures of varying aggregate types and gradations, and the results indicated the viability of the Florida HMA fracture mechanics method with highly consistent evaluation of the level of moisture damage. Their results also indicate the capability of the Florida HMA fracture mechanics method evaluating the effectiveness of antistripping agents in enhancing adhesion of asphalt binders to aggregate surfaces. Bahia et al. (2007) evaluated energy ratio approach against TSR for sixteen asphalt mixtures with different aggregate sources as well as with and without anti-stripping additives. The results showed that both methods successfully distinguished poor performers from good performers, however the energy ratio based method suffered high variability and required considerably higher testing time.

2.4.2 European Research

In recent years, there have been several studies in Europe to better understand the moisture damage mechanisms and propose experimental techniques. Apeagyei et al. (2014) developed experimental methods to determine adhesive and cohesive strength degradations in asphalt by testing aggregate-

asphalt mastic composite samples exposed to varying degrees of moisture. The results of that study demonstrate that the procedure has merit to be used in screening of aggregate sources. A new test methodology, proposed by Kringos et al. (2011), utilizes a direct tension test on dog-bone specimen made with asphalt mastics. The study evaluated the effects of moisture diffusion on mastic mechanical response and showed continued exposure to moisture substantially lowered cohesive strength of mastics. Poulikakos and Partl (2009) have proposed a test procedure to identify moisture sensitivity of porous asphalt concrete by evaluating effect of water, temperature and loading frequency on mechanical properties of porous asphalt concrete. The test method uses 150 mm diameter cylindrical specimens which are subjected to cyclic loading under confined state (coaxial shear test [CAST]) in dry as well as submerged conditions. The conditioning procedure requires 10 Hz frequency loading for 42 hours (including 2 hours of tempering and 4 temperature cycles between 25 and 30 °C). Moisture susceptibility results using CAST reflected the field inspections of surface degradation.

2.4.3 PATTI Device

Pneumatic adhesive tensile test instrument (PATTI) was originally developed to measure adhesive bond strength of paint and finishes. This test was first used by Youtcheff and Aurilio (1997) to evaluate moisture susceptibility of asphalt binders. A number of subsequent studies have used PATTI for characterization of moisture damage affinity of asphalt binder-aggregate combinations. Canestrari et al. (2010) modified PATTI for adhesive and cohesive property measurements using asphalt binder films on aggregate substrate. Moraes et al. (2011) further modified the test procedure and used it in conjunction with dynamic shear rheometer to propose bitumen bond strength test for moisture susceptibility measurement. Using this procedure the study showed that use of asphalt binders modified with polyphosphoric acid (PPA) can improve the moisture resistance of mixes made with granite aggregate.

2.4.4 Fracture Energy Tests

In recent years the use of fracture energy concepts have become popular in linking pavement cracking performance with asphalt mix's mechanical properties. Fracture tests can be conducted in single or mixed-mode conditions (tension or shear or combined); most of the current test procedures focus on the tensile model (Mode-I) where peak load is used to determine the fracture toughness of the material and the area under the load-displacement curve provides the fracture energy. The semi-circular bend (SCB) test was explored by Molenaar (2000) and extensively evaluated through the TPF-5(132) study (Marasteanu et al. 2012). The disk-shaped compact tension (DCT) test for measurement of mixture fracture energy was proposed by Wagoner et al. (2005). The DCT and SCB tests have been extensively used for evaluating thermal cracking performance of asphalt pavements (Marasteanu et al 2012; Dave et al. 2015). The work by Apeagyei et al. (2006) showed the applicability of DCT test for evaluating moisture damage in asphalt mixtures. DCT fracture energies were also used recently to compare use of multi-cycle freeze-thaw conditioning of asphalt mixtures with AASHTO T-283 and field conditioned samples

(Baker 2012; Dave and Baker 2013 and 2015). Summary results presented in Figure 5 show that the multi-cycle F-T conditioned specimens compare reasonably with field conditioning whereas AASHTO T-283 conditioning does not. Both DCT and SCB tests have been identified by on-going NCHRP 9-57 study as promising procedures for cracking performance evaluation.

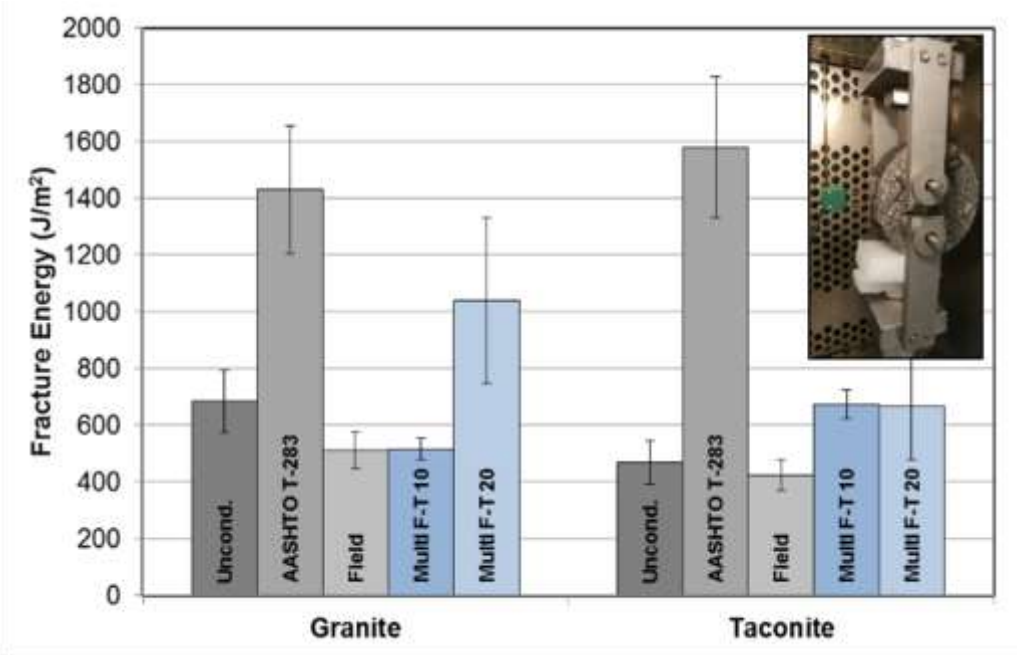

Figure 5: Comparison of Fracture Energy of Field and Lab Conditioned Specimens (Insert: DCT Test Setup)

2.4.5 Incremental Repeated Load Permanent Deformantion (iRLPD) Test

Azari and Mohseni (2011, 2012) proposed a cyclic test procedure at incrementally increasing stresses (or decreasing temperature) for evaluating rutting potential of asphalt mixtures. The procedure relies on similar fundamental principle as flow number (FN) test (AASHTO TP-79) and tries to identify a threshold at which asphalt mixture in compressive stress state transitions from secondary to tertiary creep. The test utilizes incrementally increasing stress to alleviate total test time associated with traditional flow number tests conducted using AMPT. The property measured from this test procedure is the minimum strain accumulation rate observed at end of 500 cycle loading for a given stress level. The loading is conducted in manner similar to resilient modulus and flow number test, i.e. 0.1 second load pulse followed by 0.9 second rest period. At present, a draft AASHTO specification for this method has been developed and is being balloted.

In 2013, the iRLPD testing methodology was explored for assessment of moisture-induced damage in asphalt mixes (Azari and Mohseni, 2013). The study proposed use of smaller sized (thinner) specimens as compared to traditional AASHTO T-283 citing previous NCHRP research that showed that the AASHTO T-283 sized specimens may not be uniformly conditioned due to their large size. Two specimen geometries were evaluated: ITS (6 inch diameter 1.5 inch thickness or 4 inch diameter 1.1 inch thickness) and semi-circular bend (SCB) specimens (6 inch diameter 1.5

inch thickness). It should be noted that unlike other on-going research on SCB that utilizes notched specimens, the iRLPD testing was conducted on un-notced or intact specimens. The loading sequence was modified for this procedure to 300 load cycles at each stress amplitude. Due to use of non-uniaxial geometry, the test control mode is also changed from stress-controlled to load controlled and the test is to be continued at increasing load increments until the minimum strain rate at 300 cycles drops to between 5 and 10. It should be noted that these thresholds and limits are ad hoc and may not be representative of conditions that might be experienced by asphalt mixes in field.

The proposal includes variations to current AASHTO T-283 moisture conditioning method using a two-step process to moisture and mechanically condition the specimens. Two alternatives are proposed for moisture conditioning: (1) use of MiST device without application of heat; or, (2) minimum 1 hour in the standard Rice test set-up (G_{mm} set up) with vacuum (15 mm mercury). The moisture conditioned samples are mechanically loaded for 300 cycles as per iRLPD protocol to induce moisture damage through generation of pore pressure. Finally, the conditioned samples are testing as per the iRLPD methodology at incrementally increasing stress amplitudes with 300 load repetitions at each stress level to determine minimum strain rate (MSR). The tested specimens are thereafter dried using the CoreDry device and tested again by following iRLPD methodology described earlier. The amount of moisture-induced damage is determined as ratio of the minimum strain rate for conditioned sample over dried sample.

The procedure has merit due to its use of both necessary conditions for moisture-induced damage: (1) presence of moisture; and, (2) stress caused by traffic loading. Fundamentally, the test meets the minimum requirements for reliable moisture susceptibility test. However, further evaluation of the test procedure is needed due to lack of comparison between test results and field performance as well as for determining the extent of variability associated with measurements.

2.5 Non Destructive Tests

2.5.1 Ultrasonic Pulse Velocity

The basic idea of UPV test is that the velocity of a pulse of compressional waves (P waves) passing through a medium depends on the elastic properties and density of the medium. The time of travel of the waves through the specimen is measured (tv), which, along with the bulk density (ρ), is used to calculate the bulk-constrained modulus of the material. Then, seismic (Es) and design (Ed) moduli of the material can be derived from the calculated bulk-constrained modulus.

The UPV test has been extensively used for evaluation of quality for Portland cement concrete mixes, and of lately, for HMA as well. More importantly, The UPV test has been shown to be a viable approach to detecting moisture susceptibility of HMA mixes because the measured seismic modulus (E_s) is sensitive to both of the deterioration effects of moisture: (1) due to the effect of pore pressure because of presence of water in the pores after moisture conditioning, and (2) due to the loss of integrity of the mix, as a result of loss in its cohesion or adhesion (Birgisson et al, 2003, Nazarian, 2005). Note that the pore water effect will be more significant and long lasting after moisture conditioning where a relatively greater amount of water is absorbed by aggregates (high absorption aggregates), and where the pore sizes are small and facilitate capillary action, which helps in retaining water (fine graded mixes). In mixes with higher voids or low absorption aggregates, the effect of pore water pressure may be reduced quickly after the moisture conditioning process (Birgisson et al, 2003) and hence a relatively quick test is more appropriate for the detection of the loss in integrity of the material due to pore water effects in such a case. This requirement makes the UPV test more appropriate for the evaluation of moisture susceptibility of HMA.

Note that while the loss in (as a measure of loss of integrity or deterioration of the mix) can be utilized to detect moisture susceptibility, the E_s values can also be transformed to design modulus (E_d) to estimate the loss in structural capacity or service life as a result of moisture damage, with the help of available data/relationships (for adjusting to frequency and strain levels see Aouad et al, 1993, and for temperature correction see Li and Nazarian, 1994) or with new data/relationships that could be developed on HMA that are used by the specific DOT. Good agreement between moduli measured by seismic methods and both laboratory and field methods have been reported in the literature (Saeed and Hall, 2002).

The UPV test is a promising procedure because of the following reasons: 1. This test is nondestructive and can be conducted in a very short period of time; 2. The test has been extensively evaluated, found to be sensitive to key properties of HMA and has been utilized to determine design moduli that could be used in M-E analysis; 3. Seismic modulus data have been previously

used successfully to detect moisture susceptible mixes (Birgisson et al. 2003; Nazarian et al. 2005; Maser et al. 2006); and 4. Well-established guidelines have been developed for regular use of this test by the Texas DOT (University of Texas, 2006).

2.5.2 Portable Seismic Property Analyzer

The Portable Seismic Property Analyzer (PSPA) is a small, relatively cheap, and rapid nondestructive testing device that provides the modulus of the top pavement layer in the field. The operating principle of PSPA is based on the propagation of stress waves in a medium, and the ultrasonic surface waves (USW) method, which is a simplified version of the spectral-analysis-of-surface-waves (SASW) method, is used to calculate modulus of the top pavement layer (Nazarian et al 1993). Briefly, this method utilizes the surface wave energy to determine the variation in modulus with wavelength (strictly speaking surface wave velocity with wavelength) because the modulus is proportional to the square of surface waves' velocity. A schematic of the variation in modulus with wavelength (often relabeled as depth), called a dispersion curve is shown in Figure 6 (Celaya et al 2009). For simplicity, the surface wave velocity, V_R, is converted to modulus, E, using:

$$E = 2\rho\left(1.13 - 0.16\nu\right)V_R^2\left(1+\nu\right)$$

Equation 1

Where:

ρ = mass density

ν = Poisson's ratio.

Up to a wavelength equal to the thickness of the top pavement layer, the moduli from the dispersion curve are equal to the actual moduli of the layer. As such, the modulus of the topmost layer can be directly estimated without a need of back calculation. In addition, the thickness of a top pavement layer can be estimated from the impact-echo method implemented in PSPA (Baker et al 1995).

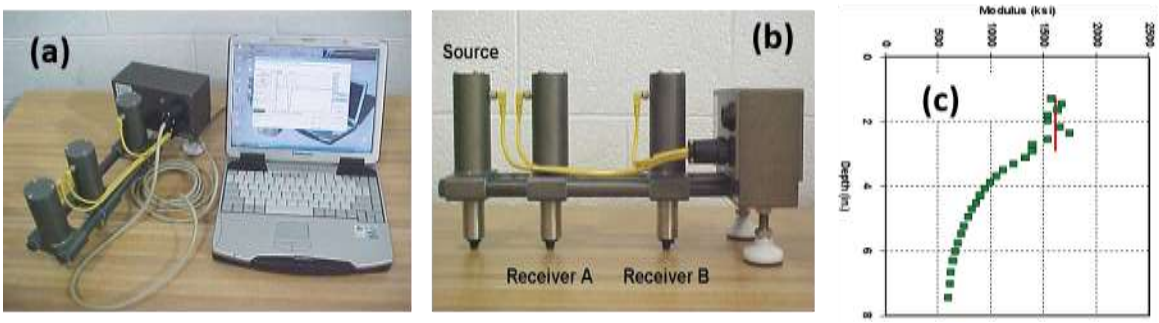

Figure 6: (a) and (b) Photos of the Portable Seismic Property Analyzer, and (c) a Typical Dispersion Curve Obtained from Time Domain Waveforms (Celaya et al. 2009)

Applications of PSPA include site characterization, evaluation of geotechnical and transportation systems, detection of defects in various structures, quality control, as well as estimation of subsurface stabilized base layers (Mallick et al, 2005).

2.6 Review of Moisture Susceptibility Requirements of New England and Other Transportation Agencies

Use of moisture susceptibility requirements by State agencies has been widespread. A 2003 survey showed that over 80% of agencies around the country required precautions to prevent the moisture susceptibility as reported by Hand (2012). With a wide range of moisture sources combined with application of different additives and RAP/RAS materials into the asphalt mixtures, agencies have tried to address this issue through use of different test procedures. While the most commonly used method, the modified Lottman procedure (AASHTO T-283), follows the requirements of AASHTO R-35 (Superpave) design method, some agencies require AASHTO T-324 (Hamburg Wheel Tracking Test) or other locally modified standards.

In developing this proposal, researchers conducted a preliminary review of agency specifications. Emphasis was given to New England region, although specifications from all US state transportation agencies and Canadian provinces were also reviewed. A synopsis of this review is presented in Figure 7. The review presented here reaffirms that a majority of agencies require a form of moisture susceptibility testing and AASHTO T-283 is most widely adopted in the United States. Out of all US states, 47 out of 50 require some form of moisture susceptibility testing. Of those 47, 40 use AASHTO T-283 or a minor variant of the test. Four out of the 47 state agencies use the Hamburg wheel tracker as a moisture susceptibility test. It is important to understand that that Figure 7 represents what procedure each agency specifies in their standard specification. In reality, different tests and procedures may be performed compared to what is written in the specification.

Figure 7: Review of State Transportation Agency Specifications for Moisture Susceptibility

Focusing on the New England region, a similar trend can be found. Per each states standard specifications, five out of the six states require some form of moisture testing and four of those five specify that AASHTO T-283 be used. Interestingly, the reality is slightly different. From technical meetings and surveys sent to the six New England agencies, it was reported that only three use T-283 and two use the Hamburg Wheel Tracker. This information is summarized in Table 1.

Table 1: New England Agency Moisture Susceptibility Requirements

State	Requirements for moisture susceptibility testing	Required Procedure	Reported Procedure
Connecticut	Yes	AASHTO T-283	AASHTO T-283
Maine	Yes	AASHTO R-35/AASHTO T283	AASHTO T-324/Hamburg (On a case by case basis)
Massachusetts	Yes	Stripping Test (MassDOT M03.10-11)	AASHTO T-324/Hamburg (On a case by case basis)
New Hampshire	Yes	AASHTO T-283	AASHTO T-283
Rhode Island	No	N.A.	N.A.
Vermont	Yes	AASHTO T-283	AASHTO T-283

The review of current agency practices indicates that there is a clear concern for moisture susceptibility across the country and at present, the modified Lottman procedure (AASHTO T-283) is most widely adopted with Hamburg Wheel Tracking tests as the second most popular choice for moisture susceptibility testing.

2.7 Treatments and Preventative Measures for Moisture Susceptibility

While moisture susceptibility has been identified as a significant problem to be considered when designing asphalt mixtures, there are a number of preventative measures available to alleviate some of the effects of moisture damage. These typically can be broken into two groups. The first is where certain properties of the component materials are selected prior to the mixture being designed. For example, when selecting the aggregates to be used in the design, emphasizing properties such as low porosity and absorption, rough and clean surfaces, and minerals that bonds strongly with most asphalt binders (limestones, for example) would all be expected to improve the moisture resistance of the mixture. Unfortunately, options like this are not always possible as asphalt production plants often have limited sources of aggregates to choose from, making alternative aggregate selections expensive and impractical for routine usage.

The other group of preventative measures is treating the asphalt mixture with materials designed to strengthen the internal bonds of the component materials. These materials typically come in two forms. The first is what is known as liquid anti-strip additives. These additives, which are usually added to the asphalt binder before the mixture is produced, aim to both reduce the surface tension of the binder, promoting increased coating of aggregates with binder, as well as changing the electrical charge of the binder so that it becomes opposite of that of the aggregate surface (which is typically negative). This change in electric charge is achieved by the inclusion of amines in the anti-strip additive.

The second common preventative additive is hydrated lime. In concept, hydrated lime works similar to amine-based anti-strip additives in that the primary goal is to modify the electric charge of the component materials. The difference is that hydrated lime aims to alter the surface charge of aggregates from negative to positive, allowing better bonding with asphalt binders (which tend to be negative). Lime is usually added as a slurry or directly to moist aggregates as it requires moisture to activate. The use of lime has been validated by many agencies, and has been included as part of specifications by many of them. The additional benefit of lime is that it acts as a (multifunctional) “active” filler that stiffens the binder and helps improve resistance against rutting especially under hot and wet conditions.

These preventative measures can be extremely useful in improving the moisture resistance of an asphalt mixture without excessively increasing costs or making the mixture impractical to produce. With this in mind, it should also be understood that these treatments do not guarantee good performance in terms of moisture susceptibility. While they typically will improve the performance, how much improvement is generally unknown and challenging to quantify. Because of this, methods are needed to assess the moisture susceptibility of asphalt mixtures in a reliable and repeatable manner.

2.8 Summary of Review

Through review of literature and agency practices, data from previous and on-going studies as well as relevant experience of the research team following can be summarized regarding the moisture susceptibility testing and analysis:

- Conditioning: For reliable moisture conditioning, it is critical that the process correctly captures conditions experienced by asphalt mixes in the field. Use of MiST based conditioning process allows for capturing the effects of traffic loading and climate relevant conditioning temperature. Use of multi-cycle freeze-thaw conditioning process that uses location specific freezing and thawing temperatures ensures that wintertime moisture damage is captured.

- Testing:
    - AASHTO T-283 (modified Lottman) procedure is prone to erroneous results due to high variability and non-fundamental nature of test in capturing moisture induced damage or measurement of damage.

    - AASHTO T-324 (Hamburg wheel tracking test) has been shown through numerous studies to be effective in screening good and poor performing mixes. The device is already available to at least three NETC agencies (Maine DOT and MassDOT use device on a case-by-case basis, Vermont AOT has a device).

    - Modulus measurements have shown promising results in previous studies, including those by the research team. These measurements can be made in-situ using Portable Pavement Seismic Analyzer (PSPA) as well as in lab using Asphalt Mixture Performance Tester (AMPT) or through Ultra-sonic Pulse Velocity (UPV) test. Since the dynamic modulus test using AMPT as well as PSPA and UPV are non-destructive, the same specimens can be tested before and after moisture conditioning. This approach allows for pinpointing moisture-induced damage as opposed to the AASHTO T-283 like approach where it is not possible to de-couple property degradation from specimen to specimen variability.

    - Fracture based measurements using either the Florida Fracture Mechanics approach (also referred to as, HMA Fracture Mechanics model) or through use of fracture-based cracking tests have also shown potential in previous studies due to their ability to better capture the fundamental mechanisms behind failure of asphalt mixes.

- Analysis: Use of combined lab testing and analysis framework can link lab measurements to actual pavement performance impacts and service life reduction. These are useful in

developing risk-based specification limits as well as allow for incorporating life-cycle cost analysis into decision processes, such as, whether to require anti-stripping additives or not.

- Dynamic modulus from the AMPT and/or fracture measurements can be used in conjunction with pavement analysis procedures (such as, AASHTO Pavement ME Design software) to predict pavement performance.

2.9 Summary of Survey

As part of the development of the material sampling and laboratory testing plans for this project, a comprehensive survey was created and distributed to the six New England transportation agencies. The focus of the survey was on the New England agencies experience with moisture damage in asphalt pavements, how material choices affect moisture susceptibility, and standard practices to address concerns with moisture susceptible materials. The following list details the key findings from the survey.\

- Out of the six New England states, four of the agencies indicated that they had historically had problems with moisture-induced damage in their asphalt pavements. Among these four, the primary distress in which the moisture-induced damage was discovered was surface stripping and raveling, particularly in the wheel path. This was most often manifest in the field as the development of a rough texture/loss of fines leading to raveling and erosion of the surface material. In general, most agency representatives believe the moisture-induced damage problems seen in their state are an asphalt material problem, mostly tied to aggregate source, binder properties and additives, and the volumetric design of the mixture.

- With regards to requirements states have in place to address moisture susceptibility in asphalt mixtures, all of the New England States (except Rhode Island) perform some form of a moisture susceptibility test for asphalt mixtures. Out of the five, three (CT, NH, and VT) require the use of AASHTO T-283, the standard superpave test, while two (MA and ME) perform AASHTO T-324/Hamburg Wheel Tracker using the stripping inflection point as the evaluated parameter for high value and specific projects of interest. While the requirements (such as frequency of test for mixes) for each state varied, all of the five agencies performed their moisture susceptibility test as part of the mixture design process. No states require a moisture susceptibility test as part of any QA processes. While many states do not currently require the test, many (such as CT and VT) indicated their interest in replacing their current testing requirements with the Hamburg.

- Out of the agencies that specify the AASTO T283 procedure, all of the agencies use the standard vacuum conditioning procedure without the use of the freeze-thaw cycle. In general, most agencies have low confidence in the connection between results from AASHTO T-283 and field performance. While no states currently use the procedure, both MA and ME indicated their interest in the use of alternative conditioning procedures, such as MiST.

- With respect to moisture treatments and preventative measures for asphalt mixtures, most of the New England agencies had experience using various types of chemical treatments in

their asphalt mixtures. Most of their experience was related to the use of liquid anti stripping agents added to the binder to improve the moisture susceptibility of the mixture. The states had various requirements that triggered the use of additives, such as failure of AASHTO T-283 requirements. The responses from the survey suggest that there has been mixed amount of success with the use of anti-strip additives in the region. There were some concerns expressed over the long-term performance of the various additives used.

3. Task 2: Identify and Inspect Moisture Susceptible Mixes and Develop Testing Plan

The following section details the two main aspects of this task. The first of these was the selection of asphalt mixtures to be used in this project. To elaborate on this, the criteria for selecting the materials as well as the spread of various material properties (such as additive use, geology, binder properties, etc.) for the mixtures is discussed in detail. The second main aspect of this task is focused on the development of the testing plan for this project. This includes discussion concerning the criteria for selecting each test and conditioning method as well as detailed descriptions of the theory and methodology behind each test and conditioning method used in this project. Lastly, a summary table is presented to show the breakdown of testing and conditioning combinations used for this project.

3.1 Study Mixture Information

To fulfill the objectives of this project, a series of asphalt mixtures produced and constructed in the New England region were selected for evaluation. These mixtures were chosen based off feedback from the survey discussed previously. The focus of this survey was for the agencies to identify mixtures that had been constructed in their state that had either performed well or poorly in the past with respect to moisture susceptibility. In addition to this, a secondary goal was to capture a wide range of properties within the selected mixtures. The wide variety of mixture properties was intended to reflect the diverse range of asphalt mixtures produced in the New England region during any given construction season.

On the basis of responses and recommendation from the surveys, a total of ten mixtures were chosen for evaluation. Of these ten mixtures, three were identified as being historically good performing, two were considered poor to moderate, and five were considered to have poor historic performance. While most of the region was represented, as mixtures were selected from four of the six New England states, the majority of the mixtures came from the northern states of the region. Out of the ten total mixtures, five were selected from Maine, three from Vermont, one from New Hampshire, and one from Connecticut. Figure 8 shows the locations of the plants from which the mixtures were selected, where blue points represent good mixtures and red points represent both moderately poor and poor mixtures.

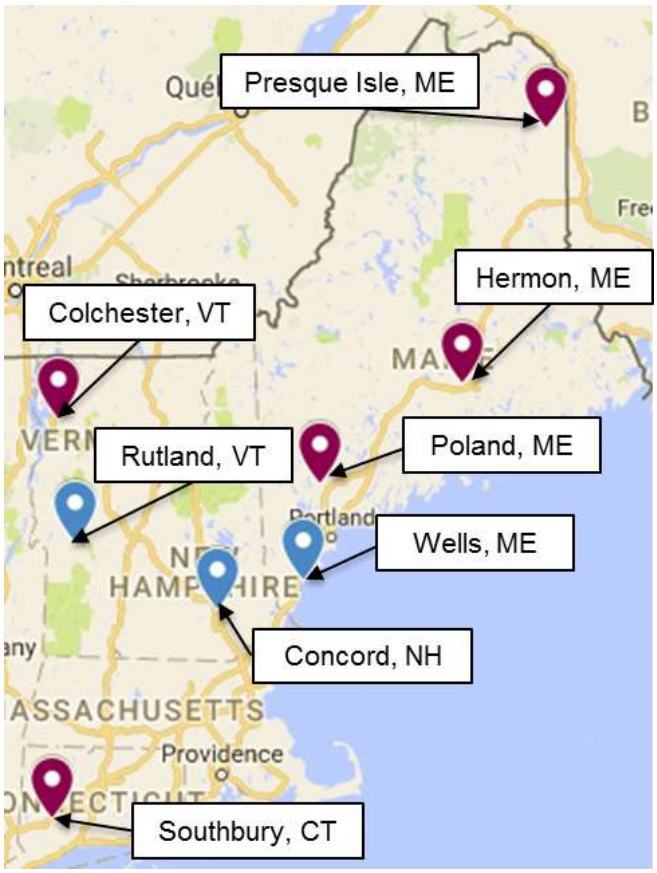

Figure 8: Study Mixture Production Locations (blue: good performers; red: poor performers

Table 2 shows an overview of select properties of the ten selected mixtures. As can be seen in the table, the mixtures selected have a wide variety of properties such as aggregate type, asphalt binder grades, additive usage, etc. The table also includes the historic performance, as reported by representatives of the state agencies, of the mixture as well as where it was produced.

Table 2: General Properties of Study Mixtures

Mix Name	Location	Performance	Aggregate Type	Binder Grade	Additive	NMAS (mm)
MEP1[1]	Presque Isle, ME	Poor	Limestone	64-28	No additive	12.5
MEP2[1]	Presque Isle, ME	Poor-Moderate	Limestone	64-28	Amine-based Anti-Strip Additive	12.5
MEP3	Poland, ME	Poor	Granite	64-28	No additive	12.5
MEP4	Hermon, ME	Poor	Sandstone/Limestone	64-28	No additive	12.5
MEG1	Wells, ME	Good	Diorite	64-28	No additive	12.5
VTP1[2]	Colchester, VT	Poor	Quartzite	58-28	WMA/Anti-Strip Additive	9.5
VTP2[2]	Colchester, VT	Poor	Quartzite	58-28	No Additive	9.5
VTG1	Rutland, VT	Good	Dolomite	70-28	WMA Additive	12.5
CTP1	Southbury, CT	Moderate[3]	Granite	64-22	Amine-based Anti-Strip Additive	12.5
NHG1	Concord, NH	Good	Granite	64-28	No Additive	12.5

[1,2] Indicates that mixtures are produced at the same plant, have the same volumetric properties, and the same gradations.

[3] This material was selected as part of this project as it had a history of failing moisture requirements, requiring remedial treatments to be used. The specific mixture used in this project has not seen significant amounts of moisture damage in the field like many Connecticut materials. Therefore, this material was classified as a moderate performer.

While the goal of selecting these mixtures was to have a wide variety of properties, a few were kept constant for all of the mixtures. The first is that all of the selected mixtures were produced and constructed as surface layers. The primary reason for this is all of the materials that the New England agencies had recent moisture failures with were surface mixtures. In addition, surface mixtures are more prone to moisture-induced damage due to greater exposure to precipitation, inundation, and traffic-induced stresses. Since the issues with these mixtures directly led to this study, focus was placed on this group of mixtures. Another commonality of the ten mixtures was that they were all produced as hot mix asphalt. While some of the mixtures used warm mix additives, these were only used as compaction aides as production and compaction temperatures were within normal ranges for hot mixtures. Table 3 contains general production information for the ten mixtures.

Table 3: General Mixture Production Information

Mix Name	Location	Production Date	Production Plant Type	Mixing Temperature (°C)	Compaction Temperature (°C)
MEP1	Presque Isle, ME	7/24/2017	Batch	154 +/- 10	144 +/- 5
MEP2	Presque Isle, ME	9/9/2017	Batch	154 +/- 10	144 +/- 5
MEP3	Poland, ME	6/8/2017	Drum	155 +/- 10	145 +/- 5
MEP4	Hermon, ME	6/21/2017	Batch	154 +/- 10	144 +/- 5
MEG1	Wells, ME	6/26/2017	Drum	155 +/- 10	145 +/- 5
VTP1	Colchester, VT	5/24/2017	Drum	140 +/- 20	120 +/- 5
VTP2	Colchester, VT	5/24/2017	Drum	140 +/- 20	120 +/- 5
VTG1	Rutland, VT	5/24/2017	Batch	171 +/- 11	152 +/- 5
CTP1	Southbury, CT	7/20/2017	Batch	155 +/- 10	145 +/- 5
NHG1	Concord, NH	10/3/2017	Drum	Not Available	Not Available

One of the common and accepted reasons for moisture-induced damage in asphalt mixtures is a loss of adhesion between the binder/mastic and the aggregate phases of the material. Naturally, it can be expected that the properties of the two phases and how they bond together will have an effect on moisture susceptibility. As can be seen in Table 2, the selected mixtures have a mix of these two properties. In terms of aggregate types, most of the study mixtures primarily contain granitic aggregates while a few others contain dolomite, limestones, diorites, and quartzites. The abundance of granitic mixtures is not surprising considering the widespread availability of it in the New England region. Ideally, a more even distribution of aggregate types would have been used, but practical limitations prevented this. Regardless, the chosen mixtures contain good and poor performers with aggregates that are typically considered good (limestone and dolomites) and poor aggregates (granite) for moisture susceptibility.

Similar to aggregates, the mixtures chosen for this project show a reasonable range of asphalt binder properties. In terms of Superpave performance grade, a majority of the mixtures in the study use PG 64-28 binders. In addition, two of the mixtures use PG 58-28 binders, one contains a PG 70-28 (the 70 high PG grade is intended to improve performance under heavy traffic, not for climate conditions), and one mixture from southern New England contains a PG 64-22 binder. This distribution of binder grades is relatively typical for New England as it is rare to see high grades warmer than 64 or colder than 58 and low grades colder than -28 or warmer than -22.

Table 4 shows some of the design properties for the project mixtures. Most of the volumetric properties are similar for all of the mixtures as all of these are surface mixtures. The only significant difference between the mixtures in terms of mix design is the design gyration level,

which is mostly a function of expected traffic levels. The gradations of the mixes are also similar to each other, and individual mix designs containing percent passing values as well as a 0.45 power chart can be found in the appendix.

Table 4: Study Mixture Design Data

Mix Name	Asphalt Binder Content (Percent by Weight)	Voids in Mineral Aggregates (VMA, %)	Voids Filled with Asphalt (VFA, %)	Maximum Theoretical Specific Gravity (G_{mm})	Bulk Specific Gravity (G_{mb})	Design Compaction Level (N_{des} gyrations)
MEP1	5.9	16.0	75	2.485	2.386	50
MEP2	5.9	16.0	75	2.485	2.386	50
MEP3	5.7	15.0	75	2.465	2.366	75
MEP4	5.6	16.0	75	2.475	2.376	50
MEG1	5.8	16.0	75	2.460	2.362	50
VTP1	6.0	16.5	76	2.452	2.354	50
VTP2	6.0	16.5	76	2.452	2.354	50
VTG1	4.9	15.5	74	2.553	2.451	80
CTP1	5.0	15.5	72	2.628	2.515	75
NHG1	5.7	Not Available	Not Available	2.465	2.366	75

A common practice to improve an asphalt mixture's resistance to moisture damage is to add treatments or chemical anti-strip additives. In the survey conducted for this project, most of the New England Agencies indicated that their specifications allow the use of both hydrated lime and liquid anti-strip additives, although their experience suggests that most producers choose to use the liquid additives. As can be seen in Table 2, three different mixtures containing anti-strip additives were chosen for the project. Two of these mixtures, MEP2 and VTP1, were produced both with and without anti-strip additives, allowing the effect of those additives to be directly analyzed. Out of the three mixtures with anti-strip additives, two of them use a traditional amine-based anti-strip additive while one uses a hybrid warm mix/anti-strip additive. This information can be seen in Table 5.

Table 5: Mixture Anti-Strip Additive Information

Mix Name	Additive Used?	Trade Name	Description	Dosage
MEP1[1]	No	-	-	-
MEP2[1]	Yes	Novagrip® 1212	Amine-Based Anti-Strip Additive	0.5% by Weight of Binder
MEP3	No	-	-	-
MEP4	No	-	-	-
MEG1	No	-	-	-
VTP1[2]	Yes	Rediset®	Hybrid Warm Mix/Anti-Strip Additive	0.5% by Weight of Binder
VTP2[2]	No	-	-	-
VTG1	No	-	-	-
CTP1	Yes	AD-here® 62-40	Amine-Based Anti-Strip Additive	1% by Weight of Binder
NHG1	No	-	-	-

[1,2] Indicates that mixtures are produced at the same plant, have the same volumetric properties, and the same gradations.

3.2 Development of Testing Plan and Methodology

3.2.1 Specimen Production

All of the materials from this project were sampled as loose mix from the production plants. The loose mix was placed in metal buckets where it was cooled and brought back to the laboratory for testing. To produce testing specimens, the loose mixture buckets were re-heated following a protocol originally developed by North Carolina State University. This protocol, which lowers the amount of aging the material experiences compared to conventional reheating methods, begins by heating the mixture bucket to a temperature of 10°C below the mixing temperature. After one hour at this temperature, the bucket lid is removed. After an additional hour, the mixture is removed from the oven and sorted into pans. The weight placed in each pan depends on what type of specimen is being produced, but it is typically around 7000g. Once separated, the mixture pans are placed back into the oven that is set to the mixture's compaction temperature. After an hour at this temperature, the mixture has been sufficiently heated and is ready for compaction.

Once the material is ready for compaction, the pans are removed from the oven and placed into preheated 150mm diameter steel molds. The amount placed into the mold depends on the density of the material and the specimens being produced, but the goal is to compact a specimen with 7 +/- 0.5% air voids. The mixture-filled molds are then placed into a Superpave gyratory compactor, seen in Figure 9, and compacted to a specific height (which depends on the specimens being

produced). Once compacted and sufficiently cooled so they do not break apart, the specimens are removed from the mold and allowed to cool for at least 12 hours.

Figure 9: Superpave Gyratory Compactor

After the compacted specimens have been cooled, the air voids of each specimen are measured. In this study, the aim was to have all of the specimens at 7 +/- 0.5% air voids in their final testing geometry. For some of the tests, the compacted specimen is already in the correct test geometry, so the voids are measured directly after cooling. For others, the compacted specimen is not the correct testing geometry so various saws and core drills are used to modify the specimen to the correct geometry. Once the correct geometry is achieved, the air voids are measured using an InstroTek Corelok device, pictured in Figure 10 and specified by ASTM D6752. Specimens that measure within the specified air void range are kept and sealed in plastic wrap until ready for testing, while specimens measuring outside the range are disposed.

Figure 10: InstroTek CoreLok Device

3.2.2 Moisture Susceptibility Methodology

Laboratory asphalt mixture moisture susceptibility evaluation methods typically combine some form of moisture conditioning with a mechanical test method. The concept is to measure the mechanical properties of the material before and after the moisture conditioning to observe the changes conditioning brings about. The first subsection of this section will describe the various mechanical test methods used in this project. The second subsection will describe the conditioning methods used, and the last subsection will detail which conditioning and testing combinations were used in the project.

3.2.2.1 Mechanical Testing

Indirect Tensile Strength

The indirect tensile strength test (ITS) is a quick and simple method that can be used to measure the tensile strength of a material. Due to the challenges associated with conducting a direct tension test on asphalt materials, it is far easier to measure tensile strength in an indirect manner. This is done by diametrically loading a cylindrical specimen (150 mm in diameter, 95 mm in height) placed on its side at a rate of 50 mm per minute at room temperature. This compressive loading causes tensile stresses along the diameter of the specimen due to Poisson's effect, eventually leading to tensile splitting failure perpendicular to the loading direction. The peak load withstood by the specimen is recorded, and the strength of the material can be calculated using Equation 2.

$$S_t = \frac{2P}{\pi DL}$$

Equation 2

Where:

S_t = Indirect Tensile Strength

P = Maximum Recorded Force

D = Specimen Diameter

L = Specimen Height

ITS was first proposed as a moisture susceptibility test by Lottman. Since then, ITS has been used extensively as a moisture susceptibility evaluation tool as it is a part of AASHTO T-283, which a majority of US state transportation agencies use as their standard test for evaluating moisture susceptibility. Similar to most moisture susceptibility methods, the material strength is measured before and after conditioning, resulting in a tensile strength ratio (TSR) as seen in Equation 3. TSR is usually used as a pass/fail parameter (for example, a TSR above 0.80 passes while a TSR below this is rejected) where high values of TSR are considered good and lower values are considered poor in terms of moisture susceptibility.

$$TSR = \frac{Average\ Conditioned\ Strength}{Average\ Unconditioned\ Strength}$$

Equation 3

ITS testing for this study was carried on an Instron servo-hydraulic load frame. The fixture used to conduct the test is shown in Figure 11.

Figure 11: Indirect Tensile Strength Test Fixture

Dynamic Modulus

Dynamic modulus testing is used to characterize the linear viscoelastic properties of a material. In simple terms, dynamic modulus is the ratio of stress to strain under oscillatory loading conditions. This represents the stiffness of the material and is a fundamental property that can be used to predict stresses and strains under any loading condition.

Dynamic modulus testing was conducted on an Asphalt Mixture Performance Tester (AMPT) manufactured by IPC Global. The AMPT, seen in Figure 12, is a self-contained servo-hydraulic load frame designed to test asphalt mixtures at different temperatures and loading frequencies. The dynamic modulus test was performed in accordance with AASHTO T-342.

Figure 12: Dynamic Modulus Specimen (Left), AMPT Device (Right)

The dynamic modulus test on the AMPT is conducted on 150mm tall cylindrical asphalt specimens with a diameter of 100mm. Before testing, three sets of brackets are attached (using epoxy) to the specimen length wise, separated by 120 degrees. These brackets are used to mount linear variable differential transformers (LVDTs) which are used to measure the on specimen strain. A dynamic modulus specimen with brackets can be seen in Figure 12. Once properly prepared, the specimen is placed into the AMPT's conditioning chamber where sufficient time is allowed to pass until the temperature of the specimen comes to equilibrium with that of the chamber. On the AMPT, dynamic modulus tests are conducted at temperatures of 37.8, 21.1, and 4.4 °C (100, 70, and 40 °F). The specimen is then sinusoidally loaded in compression at loading frequencies of 25, 10, 5, 1, 0.5, and 0.1 Hz. The specimen is then tested at additional temperatures until all of the desired temperatures have been completed.

Typical dynamic modulus raw data from the AMPT can be seen in Figure 13.

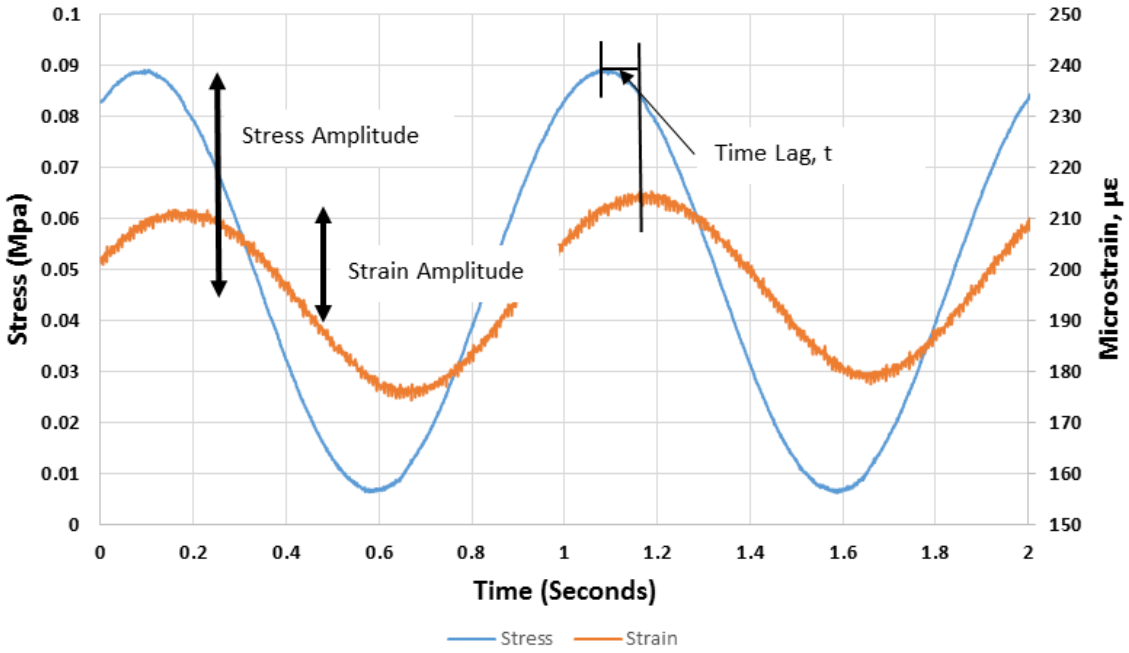

Figure 13: Raw Data from a Dynamic Modulus Test

To calculate dynamic modulus, both the stress and strain signals are fit with a sinusoidal function. Once fit, the dynamic modulus can be calculated by finding the ratio between the amplitude of the two fitted curves as seen in Equation 4.

$$|E^*| = \frac{Stress\ Amplitude}{Strain\ Amplutide}$$

Equation 4

Another property calculated from dynamic modulus results is the phase angle. Phase angle represents the time lag between applied stress and the resulting strain response. A phase angle of 0° would occur when there is zero phase lag (stress and strain occur simultaneously), meaning the material is behaving purely elastic. On the other hand, a phase angle of 90° occurs when the stress and strain are out of phase, meaning the material is behaving purely viscous. The phase angle can be calculated from raw dynamic modulus data using Equation 5.

$$\delta = 360 * t * \omega$$

Equation 5

Where

δ = Phase Angle

t = Time Lag between Stress and Strain Peaks

ω = Loading Frequency in Hz

Dynamic modulus and phase angle values are calculated at each temperature and frequency (for a total of 18 points for each specimen) using a curve fitting-based data analysis code. Using the calculated points, dynamic modulus and phase angle master curves can be constructed for each material. Master curves are built on the concept that asphalt mixtures are a thermorheologically simple material, meaning that the time-temperature superposition principle is valid. The time-temperature superposition principle relates the effects of time and temperature on the mechanical properties of viscoelastic materials. In simple terms, this means that the effects of time and temperature can be approximately equated, allowing all of the test data to be shifted to one time or temperature (known as a reference time or temperature). This allows asphalt material's linear viscoelastic properties to be predicted for time and temperatures far outside of the capabilities of conventional testing equipment (such as extremely high testing frequencies). For asphalt materials, master curves are usually constructed by shifting all of the test data to a reference temperature of 21.1 °C. A simplified version of master curve construction, which acts as a visual aid of the application of time-temperature superposition principle, can be seen in Figure 14. Master curves allow material properties to be directly compared in a clean, simple manner.

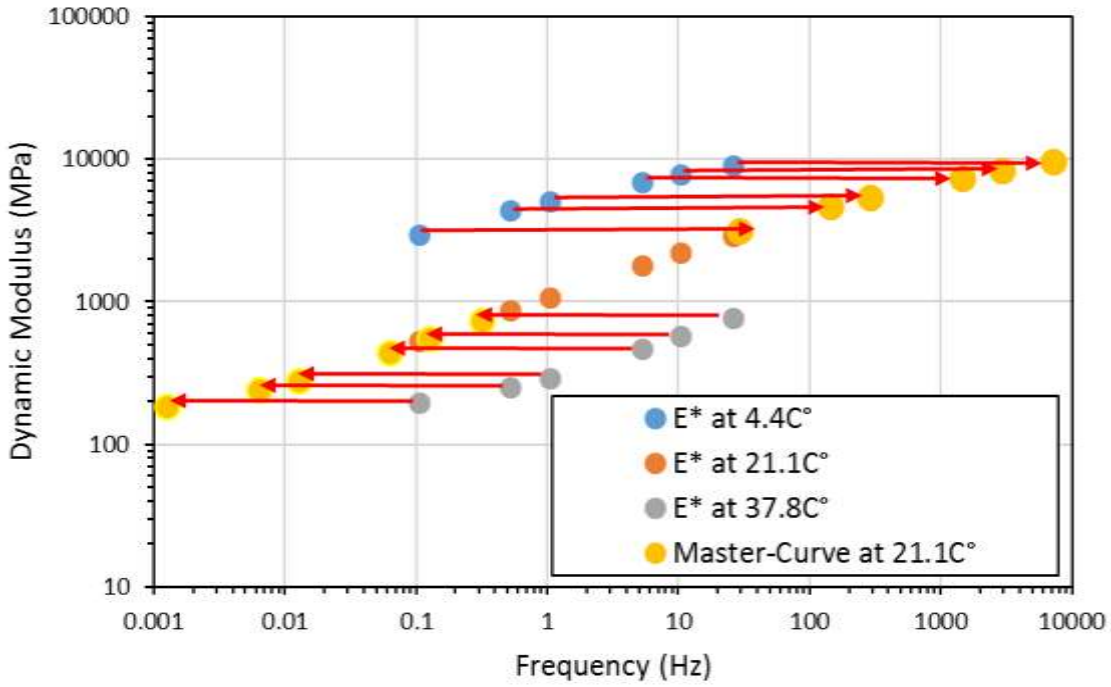

Figure 14: Dynamic Modulus Master Curve Construction Using the Time-Temperature Superposition Principle

In general, dynamic modulus has not been a common method to assess the moisture susceptibility of asphalt mixtures. Some reasons for this are that producing specimens for the test can be equipment intensive and time consuming, AMPTs are more expensive and more complicated than traditional load frames, and the test requires a certain degree of technical knowledge to run and analyze the results. In the few instances where dynamic modulus has been used as a moisture

susceptibility test method, the focus has been in the reduction in dynamic modulus when comparing conditioned specimens to unconditioned specimens, referred to as an E* stiffness ratio. The main advantage of measuring dynamic modulus is that while a simple index based ratio approach can be used to evaluate moisture susceptibility, it is also a fundamental property, which can be applied in a pavement analysis system to predict distress formation and long term performance.

One of the more popular pavement analysis systems, AASHTO PavementME, allows dynamic modulus data to be used as the primary material property input for the asphalt layers in the pavement. AASHTO PavementME is a mechanistic-empirical pavement analysis software that predicts distress levels in a pavement over its design life. These distresses include rutting, bottom up fatigue cracking, and thermal cracking. In addition to these distresses, PavementME also predicts the roughness of the road using the International Roughness Index (IRI). IRI is a value that quantifies and normalizes all of the degradation and deformations in a pavement over a standard length (typically a mile or kilometer). The advantage of using such an analysis system is that it allows the designer to predict the reduction in service of life and life cycle cost impacts of a pavement that has experienced moisture damage. These predictions, which are all calculated in a risk-based fashion, allow a quantitative analysis of the effects of using moisture susceptible materials compared to a simplistic pass/fail screening test.

In this project, dynamic modulus tests were performed on both moisture conditioned and unconditioned materials. The results of interest are the change in dynamic modulus and phase angle after a material has undergone moisture conditioning, allowing the consequent change in stiffness and material behavior to be quantified. Dynamic modulus and phase angle master curves were constructed as well as calculating dynamic modulus ratios and changes in phase angles to analyze the moisture conditioned materials. Dynamic modulus results were also used in conjunction with PavementME simulations to predict changes in pavement service life due to moisture damage for a wide range of materials.

Disk-Shaped Compact Tension Test

The disk-shaped compact tension test (DCT), specified in ASTM D7313, is one of many laboratory tests recently developed which focus on the evaluation of the cracking resistance of asphalt mixtures. The DCT test is a fracture mechanics-based test focused on the evaluation of low temperature cracking. The test is performed on a 150mm diameter, 50mm tall asphalt specimen as shown in Figure 15 in a controlled, low temperature environment. Tensile forces are applied to the two pre-drilled loading holes so that the crack mouth opens at a constant rate of 1mm/min until the specimen fully fractures. During the test, both the load and crack mouth opening displacement (CMOD) are monitored and recorded. These two values can be plotted against each other to form a curve similar to that shown in Figure 16.

Figure 15: DCT Test Specimen

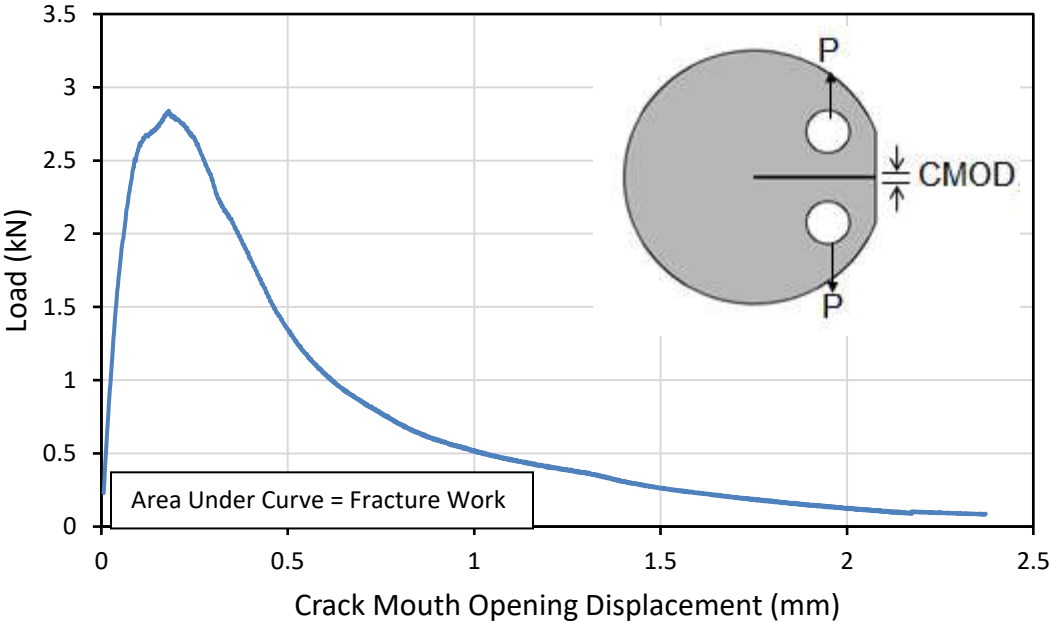

Figure 16: DCT Load vs CMOD Displacement Plot

The main property evaluated from DCT test data is fracture energy. Fracture energy is a measure of how much energy a material can withstand until experiencing a complete fracture over a unit area, which is typically expressed in J/m^2. Fracture energy is calculated by determining the area under the load-CMOD curve by integration of a fitted function or the trapezoid method. The area represents the work of fracture, W_f. The work of fracture is then divided by the area fracture surface of the specimen, which is the fracture ligament length multiplied by the height of the specimen, to calculate fracture energy. This can be seen in Equation 6.

$$G_f = \frac{W_f}{t * a}$$

Equation 6

Where

G_f = Fracture Energy

W_f = Work of Fracture

t = Specimen Thickness

a = Specimen ligament length

The focus of this project was looking at the change in fracture energy after the material had undergone moisture conditioning. One of the advantages of using fracture tests to evaluate moisture susceptibility is their ability to better capture the fundamental mechanisms of moisture-induced damage compared to test methods that include non-tensile stress loading.

In this study, DCT testing was completed using a fixture in an environmentally controlled MTS servo-hydraulic load frame as pictured in Figure 17. All testing was performed at a temperature of -18°C as all of the materials tested used PG XX-28 binder grades. Per ASTM D7313 specifications, the DCT test is performed at 10°C warmer than the PG low temperature of the binder in the mixture.

Figure 17: DCT Test Setup on Hydraulic Load Frame

Hamburg Wheel Tracker

The Hamburg wheel tracking device (HWTD) was originally developed in Germany as a tool to assess the rutting resistance of asphalt mixtures. Eventually, the test was conducted with the specimens submerged in water to control temperatures instead of an air controlled environmental chamber. This led to observations being made that certain mixtures began experiencing damage related to moisture rather than only rut deformation. Since then, the HWTD has gained popularity as a test to evaluate moisture susceptibility and remains common to this day.

The HWTD, per specifications in AASHTO T-324, is conducted by preparing four cylindrical asphalt specimens with a diameter of 150mm and height of 62.5mm and arranging them in a plastic mold as seen in Figure 18.

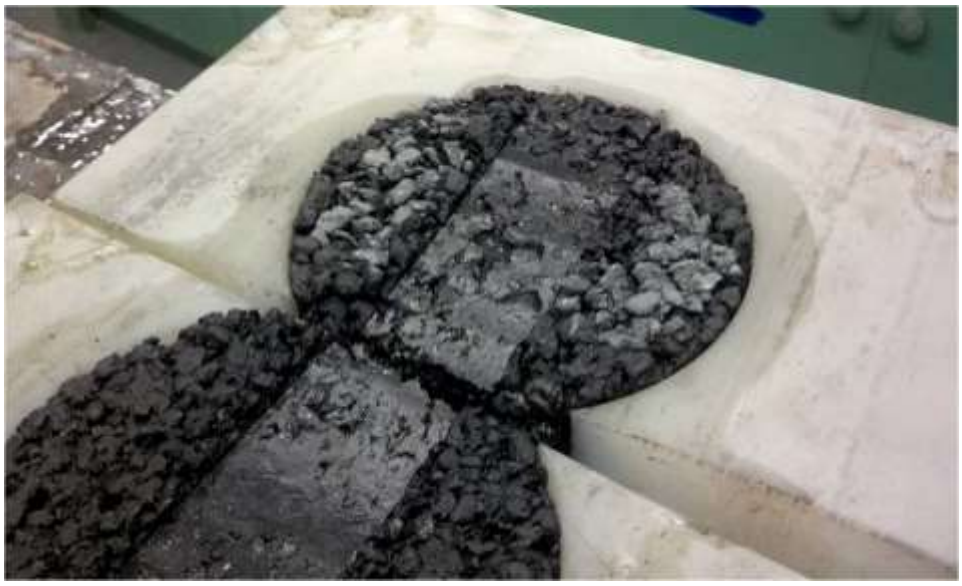

Figure 18: Hamburg Wheel Tracker Specimen Mold (Image from pavementinteractive.org)

The test, carried out in a device such as the one shown in Figure 19, is conducted by placing 158lb steel wheels onto the material surface. The wheels are then moved back and forth over the surface or a specified number of passes. A LVDT attached to the frame carrying the steel wheels is constantly recording the accumulated rut depth during the test. Once the test has been completed (typically 20,000 wheel passes), a curve showing the accumulated rut depth versus the number of passes is constructed. A typical curve, shown in Figure 19, will begin with a short consolidation phase where the material is still being compacted and consolidated. After this, the test transitions into a creep phase where the material experiences steady viscoplastic deformation. Eventually, the material will begin to experience moisture-induced damage, which results in a significant increase in the rate of rut depth accumulation. This section, the stripping phase, is what allows the moisture susceptibility of the material to be evaluated as it is assumed that the damage during this phase can be attributed to the presence of moisture. . It should be noted that a key assumption of using Hamburg results to assess moisture susceptibility is that this accelerated damage is primarily due to the internal breakdown of the material from the presence of moisture rather than traditional tertiary rutting and/or viscoplastic flow of the material

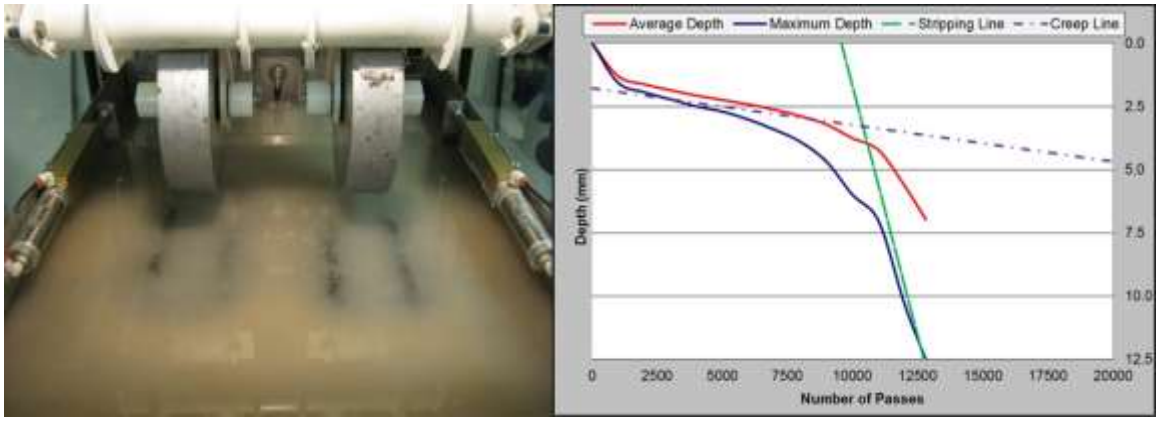

Figure 19: Hamburg Wheel Tracking Device (Left) with Typical Results (Right)

The two most common parameters measured from Hamburg results are the measured final rut depth and the stripping inflection point. The final rut depth is the measured rut depth after 20,000 wheel passes have occurred. Sometimes, this rut depth will occur earlier as the specimen will rut more than the device limits allow (such as 20.0mm), causing the test to end earlier than the typical 20,000 passes. Looking at Figure 19, the final rut depth value occurs at the end of the blue line.

The Stripping inflection point (SIP), shown as the intersection between the green and dashed line in Figure 19, is calculated by first finding the stripping slope and creep slope lines. These lines are both parallel and tangent to the creep (steady, controlled deformation) and stripping (increased deformation rate after creep) phases of the Hamburg test. SIP is calculated by finding the number of passes at which the creep slope and stripping slope lines intersect. The concept behind the SIP is that it takes into account both how quickly stripping damage begins to occur as well as how quickly the stripping damage accumulates once it has begun. Asphalt mixtures with higher SIP and lower final rut depth values are considered more resistant to moisture-induced damage as compared to mixtures with lower values.

Recently, more novel methods to analyze Hamburg results have been developed. One of them, developed by Yin et al. at the Texas Transportation Institute, aims to separately analyze the rutting and stripping damage of the Hamburg curve (2014). One of the issues this method attempts to address is how the calculation of SIP is heavily influenced by the algorithms used to find the creep slope and stripping slope lines. Minor deviations with these lines can have significant impacts on the calculated SIP and the implied performance of the material.

The method developed by Yin et al. (referred to as the TTI method) proposed two new parameters to evaluate moisture susceptibility from Hamburg results. The first of these parameters is the stripping number, LC_{SN}. LC_{SN}, shown on a Hamburg data curve in Figure 20, is calculated by first fitting Equation 7 to the raw Hamburg data.

$$RD = p * \left[\ln\left(\frac{LC_{ult}}{LC}\right)\right]^{\frac{-1}{B}}$$

Equation 7

Where

RD = Rut Depth

LC = Load Cycles

B, p, LC_{ult} = Fitting Coefficients

The point of interest is the number of load cycles at which the accumulated rut depth begins to increase again after the creep phase of the test. This point is approximated by calculating the inflection point, or where the second derivative is equal to zero, of Equation 7. In its simplified form, this point can be directly calculated using Equation 8.

$$LC_{SN} = LC_{ult} * exp\left(-\frac{B+1}{B}\right)$$

Equation 8

Where

LC_{SN} = Stripping Number

B, LC_{ult} = Fitting Coefficients from Equation 7

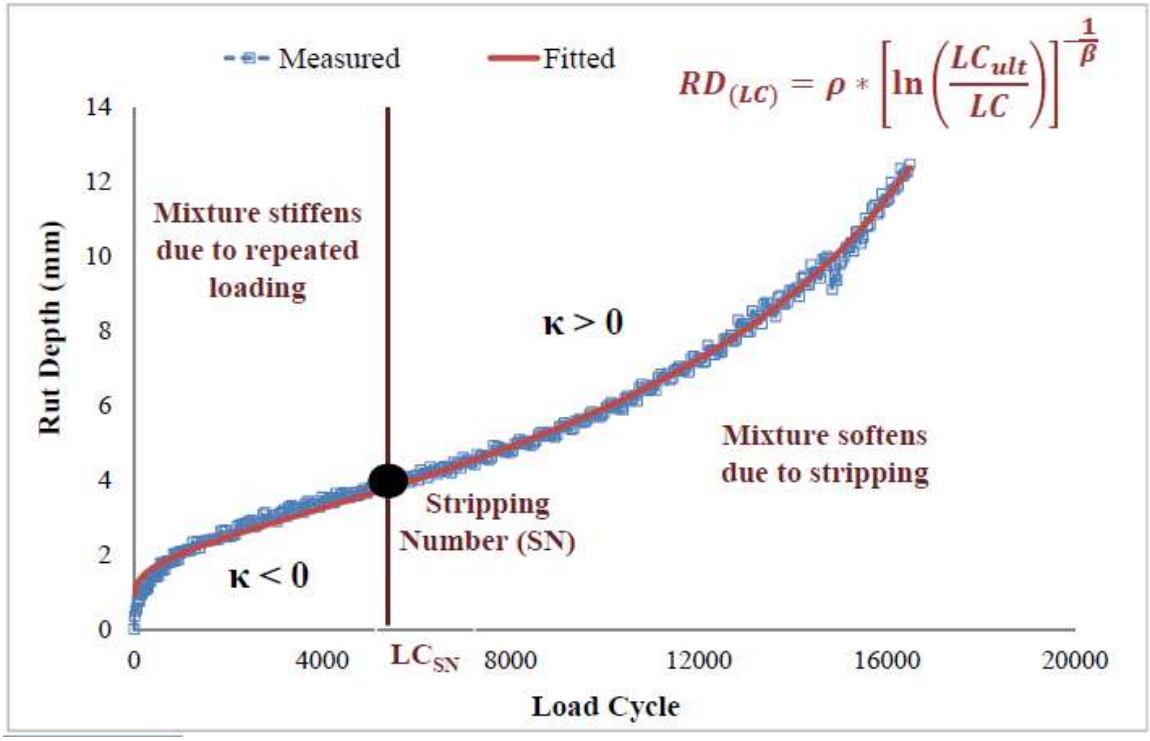

Figure 20: Hamburg Curve with LC_{SN} Calculation (Image from Yin et al. 2014)

The second parameter of the TTI method is known as the stripping life, LC_{ST}. LC_{ST} is calculated by first taking the LC_{SN} and zeroing the accumulated rut depth to that point. Next, Equation 9 is fit to the data points occulting after the LC_{SN}. It should be noted that this equation is written in terms of strain, not rut depth. The definition of strain in the TTI method is the rut depth divided by the original height of the specimen.

$$\varepsilon^{st} = \varepsilon_0^{st} * \left(e^{\theta(LC-LC_{SN})} - 1\right)$$

Equation 9

Where

ε^{st} = Stripping Strain

ε_0^{st} = Initial Stripping Strain

LC = Load Cycles

LC_{SN} = Stripping Number

θ = Fitting Coefficient

Once Equation 9 has been fit, the LC_{ST} is calculated by determining the number of load cycles after the stripping number are required to induce a certain amount of stripping strain in the material. The value proposed by the TTI method is 0.20, which corresponds to 12.5mm of deformation on

a standard 62.5mm height specimen. The LC_{ST} can be calculated directly using the Equation 10. An example of LC_{ST} on a Hamburg curve is shown in Figure 21.

$$LC_{st} = \frac{1}{\theta} * ln\left(\frac{12.5}{T * \varepsilon_0^{st}} + 1\right)$$

Equation 10

Where

LC_{ST} = Stripping Life

ε_0^{st} = Initial Stripping Strain

T = Specimen Thickness in mm

θ = Fitting Coefficient

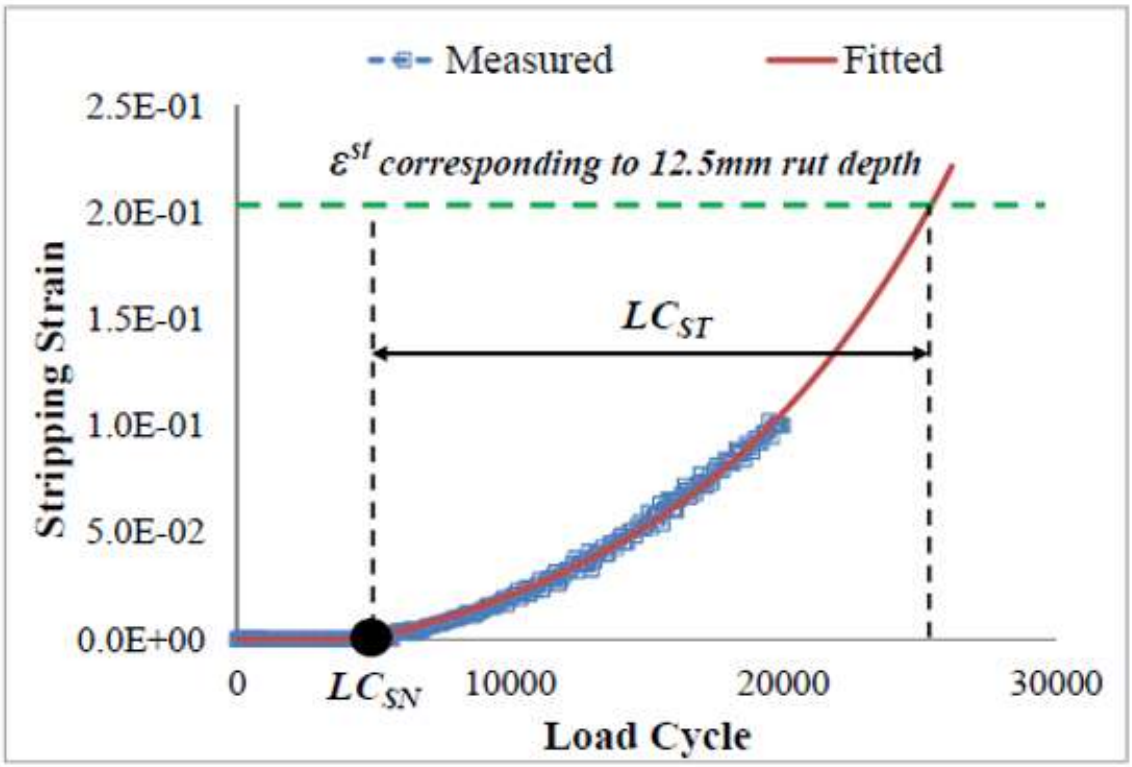

Figure 21: Hamburg Curve with LC_{ST} Calculation (Image from Yin et. al. 2014)

The advantage of the two parameters proposed in the TTI method is that they provide a more consistent means to evaluate moisture susceptibility compared to the relatively variable SIP. The stripping number captures how many load cycles are required for moisture to begin the process of penetrating into and breaking down the bond between the aggregates and mastic. All accumulated

rut depth before this is assumed to be caused by viscoplastic effects, while all rut depth increase after this point is assumed to be caused primarily by stripping damage, although the theoretical viscoplastic effects are not ignored. The stripping life, on the other hand, describes how quickly the stripping damage evolves once stripping damage first occurs. These two parameters describe unique, but equally important types of material behavior under moisture-induced stresses. To improve moisture resistance of a material, a high stripping number and stripping life are desired.

In this study, all Hamburg testing was performed on an InstroTek SmarTracker at a temperature of 45°C. To evaluate moisture susceptibility of the mixtures used in this study, both the traditional and TTI method analysis was performed.

3.2.3 Moisture Conditioning

Modified Lottman Conditioning

The modified Lottman conditioning procedure, first developed in the 1970s, is one of the most popular and common moisture conditioning procedures in the United States due to it being included in AASHTO T-283. Modified Lottman conditioning involves taking a subset of compacted asphalt specimens and submerging them in a vacuum chamber. Approximately 20 inch-Hg partial pressure is applied to the chamber for 5 to 10 minutes to saturate the specimens. The modified Lottman protocol specifies that the specimens should be between 70 and 80 percent saturated per Equation 11. If the specimen measures less than 70 percent after the 5 to 10 minutes of vacuum saturation, they are placed back into the vacuum until they are within the specification limits. On the other hand, specimens measuring above 80 percent saturation are considered to be damaged and must be discarded.

$$S = \frac{100 * J'}{V_a}$$

Equation 11

Where

S = Percent Saturation

J’ = Mass of Absorbed Water

V_a = Specimen Air Voids

Once saturated, the specimens are then wrapped in plastic film and placed inside a plastic bag and are subjected to a single freeze cycle. This cycle lasts 16 hours at a temperature of -18°C. After the freeze cycle, specimens are removed from the plastic and placed into a 60°C water bath for 24 hours. After this, the specimens are cooled to room temperature and are ready for testing. A Lottman water bath can be seen in Figure 22.

Figure 22: Lottman Temperature Controlled Water Bath (Image from pavementinteractive.org)

Modified Lottman conditioning is intended to simulate somewhere between 4 to 12 years of moisture-induced damage depending on location and climate. This procedure, typically combined with indirect tensile strength testing as is done in AASHTO T-283, has seen mixed success at predicting field performance historically. While it is generally acknowledged that the Lottman procedure is able to distinguish very poor performing and very good performing materials, the procedure has received fair amounts of criticism as a tool for routine usage such as mixture design. One of the reasons is that the Lottman method only simulates moisture-induced damage caused by static immersion in water. The conditioning procedure does not simulate the variations in pore water pressure from traffic loading, which can produce scouring in the material as well as very high internal stresses at aggregate and asphalt interfaces. This effect is well documented as a cause of moisture-induced damage for asphalt mixtures in field conditions (Chen et al. 2008; Mallick et al. 2003; Pinkham et al. 2013).

In this study, the Lottman procedure was used without modification as specified in AASHOT T-283.

Moisture-Induced Stress Tester

The moisture induced stress tester (MiST), specified by ASTM D7870, is a moisture conditioning procedure that was originally developed in the early 2000's as a simulative method for moisture-induced damage in asphalt mixtures. The MiST device, pictured in Figure 23, is a self-contained unit that is able to control temperature and pressures in a dynamic fashion.

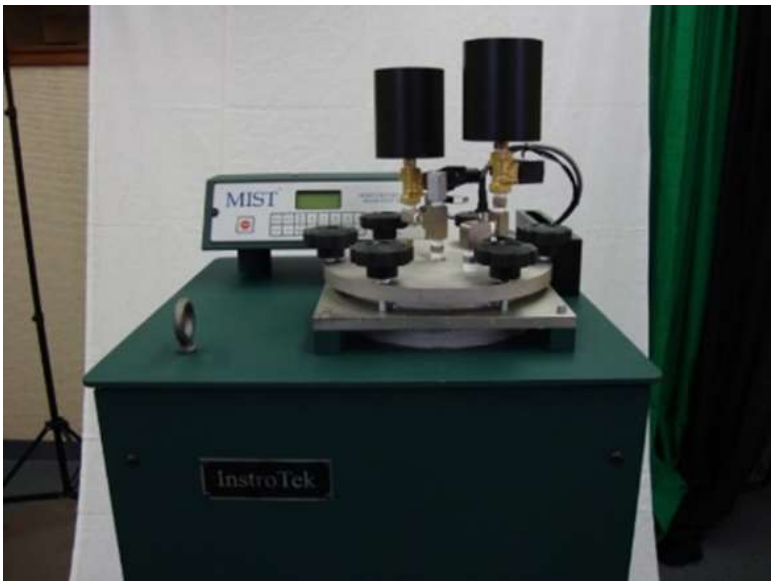

Figure 23: MiST Device

MiST conditioning begins with selecting a subset of specimens for conditioning. These specimens are placed into the MiST device. In the MiST, the specimens are first submerged for a period of 20 hours at 60°C, although the temperature can be adjusted for softer mixes to prevent excessive damage. Once this first phase of conditioning is finished, the MiST begins cycling the pressure inside the device. This is achieved by using an air bladder system, which is able to produce pressures up to 40 psi inside the device. Standard MiST procedure specifies that the specimens be subjected to 3500 cycles of 40 psi pressure for a period of 3.5 hours. Once the pressure cycles are completed, the specimens are cooled with water so that they are not damaged when being removed from the device.

The MiST process is intended to mimic the effect of hydraulic scouring, one of the most common forms of moisture damage in asphalt pavements, in which water trapped in the air voids (saturated) of the material repeatedly exerts pore pressure on the asphalt under the action of traffic, which can lead to a reduction of the adhesive strength between aggregate and binder and a loss of cohesive bond strength within asphalt binder. In general, the need for equipment for generating cyclic pore pressure in HMA has been widely suggested by researchers to identify mixes with potential of moisture damage to allow the evaluation of mixes within a reasonable amount of time and help in avoiding the other complicating effects of moisture damage. The MiST device is able to simulate both damage caused by static-immersion through the 20-hour saturation phase and traffic-induced damage through the 3.5-hour pressure cycling phase of the conditioning. Incorporating both of

these conditioning techniques into one procedure gives MiST a distinct advantage over other procedures that only incorporate one of these techniques. In addition to this, MiST equipment has shown good potential in identifying moisture susceptible mixtures (Chen and Huang 2008).

In this project, MiST conditioning was used in combination with various mechanical test procedures. The device was programmed to perform a 20-hour saturation period followed by 3500 cycles at 40psi pressure for a period of 3.5-hours as specified in ASTM D7870. The standard conditioning temperature of 60°C was used.

3.2.3.1 Multiple Cycle Freeze-Thaw Conditioning

Multiple cycle freeze-thaw is a conditioning scheme that is intended to simulate the substantial amount of freezing and thawing saturated asphalt mixtures in cold, wet climates experience during the late fall, winter, and early spring months. The concept behind this is that water trapped in the voids of an asphalt material will exert high internal pressures on the material as it expands while freezing. If the forces caused by the expansion are large enough, significant internal damage can occur causing a reduction in mechanical properties of the material on a large scale. This phenomenon is widely recognized and accepted in Portland cement concrete where durability is regularly quantified in terms of freeze-thaw resistance, such as ASTM D666.

The protocol used in this research involved estimating three components of typical freeze-thaw cycles in the New England region: average annual number of freeze-thaw cycles, average high temperature of freeze-thaw cycles, and average low temperature of freeze-thaw cycles. These three values were determined using data outputs from the Enhanced Integrated Climatic Model (EICM), which simulates asphalt pavement temperatures over time taking into account factors such as air temperature, air speed, presence of moisture, sunlight exposure, etc. Using EICM, 20 years of pavement temperature data were simulated for a typical New England pavement. A simple code was written to analyze the data. This code would first identify any freeze thaw cycles that occurred by looking for data where the local maximum temperature was greater than 0°C and the local minimum temperature was less than 0°C. Each cycle was counted and the maximum and minimum temperature of each cycle was recorded. From this, it was determined that a representative New England pavement will experience approximately 30 annual freeze-thaw cycles with an average high temperature of 6°C and an average low temperature of 4°C.

This protocol was then simulated in the lab by using an environmental chamber. Specimens were first saturated in a similar manner to the saturation used with modified Lottman conditioning, where the only difference was that the 20 inch-Hg partial pressure was applied to each specimen for 20 minutes. Saturation levels were not measured or considered. The saturated specimens were then sealed in plastic and submerged in an anti-freeze solution. The anti-freeze was used so that the liquid media the specimens are submerged did not impart any damage on the specimen through freezing itself. With the specimens in the anti-freeze placed into an environmental chamber, the freeze-thaw conditioning was started by conditioning the chamber at 6°C for two hours. Afterwards, the temperature cycling began by varying the temperature in a triangular waveform

where the chamber would cool to the low temperature of 4°C and raise back to 6°C over a period of 8 hours. The freeze-thaw setup used in this study can be seen in Figure 24.

Figure 24: Laboratory Freeze-Thaw Conditioning Chamber

3.2.4 Test and Conditioning Combinations used in this Research

As mentioned previously, moisture susceptibility test methods typically combine a form of moisture conditioning and mechanical testing into one procedure. The goal is to evaluate the change in material properties before and after moisture conditioning, and determine if that change is significant enough to define the material as being moisture susceptible. In this project, a testing matrix was developed using combinations of the methods described in the previous sections, which can be seen in Table 6. The specific procedure selection was based off both research and local transportation agency interests.

Table 6: Test and Conditioning Method Combinations used in Project

Mechanical Test Method	Modified Lottman Conditioning	MiST Conditioning	Multi-Cycle Freeze-Thaw
Indirect Tensile Strength	Yes	Yes	No
Hamburg Wheel Tracker	No pre-conditioning used. Traditional and TTI (Yin et al 2014) analysis used		
Dynamic Modulus	No	Yes	No
Semi-Circular Bend (SCB)	No	Yes	No
Disk-Shaped Compact Tension (DCT)	No	No	Yes

4. Task 3: Laboratory Testing

The following section presents the laboratory testing results conducted during the project. This includes test results from indirect tensile strength, dynamic modulus, disk-shaped compact tension, semi-circular bend, Hamburg wheel tracker, and ultrasonic pulse velocity tests on the ten mixtures chosen for this project. All results are analyzed and general trends within the data are discussed. The ability of each test result to distinguish between good and poor performers is also highlighted, where emphasis is placed on the tests ability to show clear and consistent separation between the different materials. Additionally, discussion concerning the potential of each procedure as a replacement moisture susceptibility test is included in each section of results.

4.1 Indirect Tensile Strength (ITS) and Tensile Strength Ratio (TSR)

Results from ITS testing are shown in following section. The plots shown display both the measured strength values as bars which correspond to the left Y axis, and the TSR values as points corresponding to the right Y axis. All strength values are the average of three replicates while the TSR value is a ratio of those averages. The error bars on each strength value represents one standard deviation. The color of the bars and points are tied to the historic performance of the material where red represents poor mixtures, orange represents poor-moderate, and blue represents good.

Figure 25 shows the results from ITS paired with modified Lottman conditioning as is specified by AASHTO T-283. Looking at the strength results alone, the good performing mixtures are generally stronger in both an unconditioned and moisture conditioned state. The average strength values reflect this as the average unconditioned and conditioned strengths are 107.8 psi and 97.7 psi for the good, 90.8 psi and 65.8 psi for the poor-moderate, and 75.6 psi and 67.7 psi for the poor mixtures. These values are shown in Table 8. While these strength values show distinction between the good, poor-moderate, and poor mixtures, it is worth noting that the mixtures all have different binder grades. Binder grade has a significant impact on measured strength values as ITS is conducted at room temperature. Stiffer binders, which the good mixtures mostly use, will generally give higher strength values than mixtures with relatively soft binders, which most of the poor mixtures use.

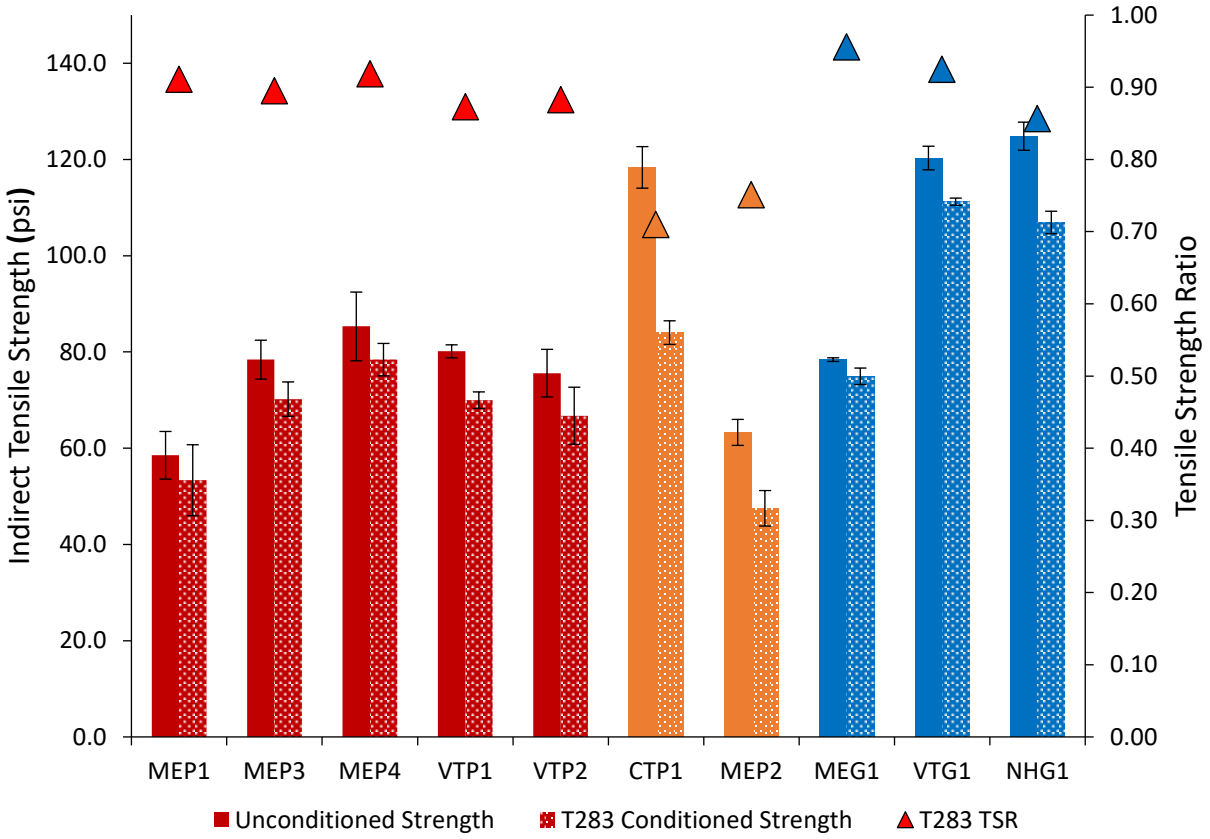

Figure 25: Indirect Tensile Strength with Lottman Conditioning Results (red: poor performing mixes; orange: poor-moderate performing mixes; blue: good performing mixes)

When considering the TSR values from Lottman conditioning, the results become less clear. Comparing the good and poor materials, there is little differentiation in TSR values both visually in Table 7 and in average values shown in Table 8. Both sets of mixtures have TSR values ranging from 0.85 to 0.95 with their averages being within 0.01 of each other. The results suggest that these two groups of mixtures would both perform well in the field as they have retained more than 80 percent of their strength, the pass/fail threshold set in AASHTO T-283, after moisture conditioning. While this is known to be inaccurate considering the mixtures historic field performance, this is not particularly surprising as all of the mixes were designed using Superpave mix design specifications, which require the mixture to pass AASHTO T-283 requirements. Interestingly, the poor-moderate mixtures had the lowest TSR values which were in the 70 percent range.

Table 7: Indirect Tensile Strength Results with Rankings

Mix	Performance Descriptor	Unconditioned Strength (psi)	Lottman Conditioned Strength (psi)	Mist Conditioned Strength (psi)	Lottman TSR	Rank	MiST TSR	Rank
MEP1	Poor	58.5	53.3	48.2	0.91	4	0.82	8
MEP3	Poor	78.4	70.2	73.4	0.89	5	0.94	2
MEP4	Poor	85.3	78.4	84.7	0.91	3	0.99	1
VTP1	Poor	80.1	70.0	66.7	0.87	7	0.83	7
VTP2	Poor	75.6	66.7	70.0	0.88	6	0.93	3
CTP1	Moderate	118.4	84.0	91.6	0.71	10	0.77	9
MEP2	Poor-Moderate	63.3	47.5	43.2	0.75	9	0.68	10
MEG1	Good	78.4	74.9	72.1	0.95	1	0.92	4
VTG1	Good	120.3	111.2	108.6	0.92	2	0.90	5
NHG1	Good	124.8	106.9	105.0	0.85	8	0.84	6

Table 8: Average Indirect Tensile Strength Results

Mix Performance	Average Unconditioned Strength (psi)	Average Lottman Conditioned Strength (psi)	Average MiST Conditioned Strength (psi)	Average Lottman TSR	Average MiST TSR
Poor	75.6	67.7	68.6	0.90	0.90
Poor/Moderate	90.8	65.8	67.4	0.73	0.73
Good	107.8	97.7	95.2	0.91	0.89

The results from ITS testing paired with MiST conditioning are shown in Figure 26. Interestingly, the results in this plot look similar to those in Figure 25. A similar trend of the good mixtures being stronger than both the poor-moderate and poor mixtures is shown, as well as little distinction among the TSR values can be seen. A slightly wider range of 0.82 to 0.99 for TSR values among the good and poor performers exists, but the average TSR values for the two mixtures groups is again only separated by 0.01. This suggests that MiST conditioning is relatively similar, in terms of its effect on ITS and TSR, as Lottman conditioning and that neither methods are able to clearly distinguish good and poor performing mixtures when paired with ITS testing. The same trend where the poor-moderate mixtures have the lowest TSR values (between 0.70 and 0.80 in this case) was observed with MiST conditioning.

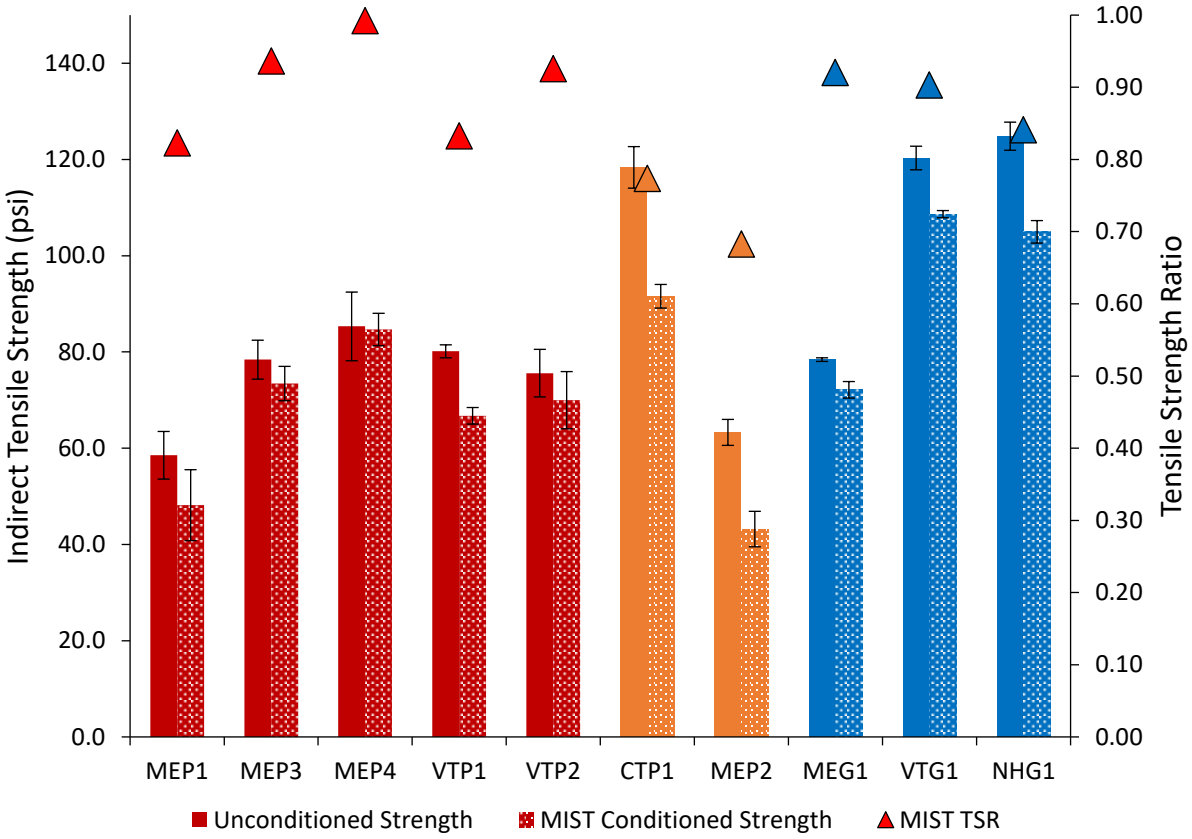

Figure 26: Indirect Tensile Strength with MiST Conditioning Results

Lastly, the TSR rankings for all ten materials are shown in Table 7. Comparing the rankings of good and poor performing mixtures, there are no obvious differences between the two sets of mixtures. For the Lottman conditioning, the good generally rank better than the poor mixtures, but the opposite is true for MiST conditioning. The only consistent trend in the rankings is that the poor-moderate mixtures consistently were the worst performing materials.

Considering that both Lottman and MiST conditioning strengths were measured on ITS specimens, limited comparisons can be made between the two conditioning methods. Figure 27 shows this comparison in terms of indirect tensile strength with respect to a unity line. Interestingly, the results suggest that there is little difference between the two methods with respect to their effect on indirect tensile strength as all of the points fall near the line of equality. This is surprising as it is generally assumed that MiST is a more aggressive, damaging conditioning procedure as it includes both the effects of pore pressure and moisture inundation.

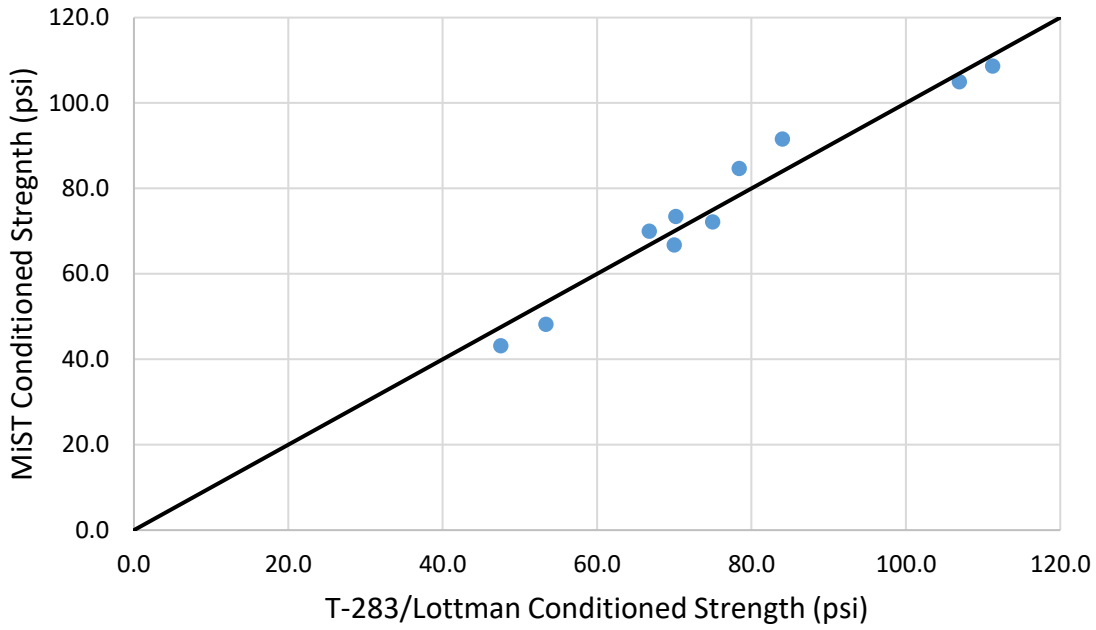

Figure 27: Comparison between Lottman and MiST Conditioned Strength

One potential explanation for this observation of little difference between the two methods, as well as why neither method is able to show clear distinctions between the good and poor materials, is that ITS results may not capture the effects of moisture damage for typical New England mixtures. Since ITS is conducted at room temperature (typically 25°C), many New England mixtures are too soft to exhibit a pure tensile failure during the ITS test. Instead, there is a substantial amount of creep and shear failure in the material close to the loading heads. The concept behind using ITS as a moisture susceptibility evaluation tests is that it is directly stressing the internal adhesive and cohesive bonds within the material through splitting tensile stresses. The mechanisms behind the creep and shear failures, on the other hand, are not directly stressing the areas which are expected to be most sensitive to moisture-induced damage. Because soft New England materials are experiencing substantial amounts of shear and creep damage, it is likely that ITS will not be able to reliably capture the effects of moisture damage for these materials.

4.2 Dynamic Modulus

The following section shows results from dynamic modulus testing paired with MiST conditioning. Dynamic modulus tests were conducted to measure the change in linear viscoelastic properties of the material due to moisture conditioning. The results are presented for the three mixtures from Vermont and three mixtures from Maine. Unfortunately, not all of the mixtures survived the MiST conditioning (such as MEP3) where the specimens crumbled apart during the conditioning, making the specimens untestable. While the reason this happened is not clear, a general trend of the poor materials with soft unconditioned dynamic modulus results was correlated to crumbling during conditioning. Regardless, these mixes are not included in this result section. Some general information about the tested mixtures is shown in Table 9.

Table 9: Mixes Tested with Dynamic Modulus and MiST Conditioning

Mix Name	Location	Performance	Aggregate Type	Binder Grade	Additive	NMAS (mm)
MEP1	Presque Isle, ME	Poor	Limestone	64-28	No additive	12.5
MEP4	Hermon, ME	Poor	Sandstone/Limestone	64-28	No additive	12.5
MEG1	Wells, ME	Good	Diorite	64-28	No additive	12.5
VTP1[1]	Colchester, VT	Poor	Quartzite	58-28	WMA/Anti-Strip Additive	9.5
VTP2[1]	Colchester, VT	Poor	Quartzite	58-28	No Additive	9.5
VTG1	Rutland, VT	Good	Dolomite	70-28	WMA Additive	12.5

[1] *Indicates that mixtures are produced at the same plant, have the same volumetric properties, and the same gradations.*

Figure 28 shows the dynamic modulus master curves for the three Vermont mixtures while Figure 29 shows the master curves for the Maine materials. This plot includes master curves for the mixtures in both an unconditioned (solid point) and MiST conditioned (hollow point) state. All of the master curves presented in this section are plotted on a log-log scale and were shifted to a reference temperature of 21.1°C.

Looking at the master curves in Figure 28 and Figure 29, it is apparent that all mixtures experience a reduction in stiffness after MiST conditioning. This is most evident at lower frequencies, which represent slow traffic speeds or high pavement temperatures. The reduction in stiffness at high frequencies is less evident due to the log-log scale the data is being plotted on and the proximity of the points, but it is still noticeable for the two poor performing mixtures. Comparing the good and poor performing materials, the reduction of stiffness appears to be less for the good material as compared to both of the poor performing materials.

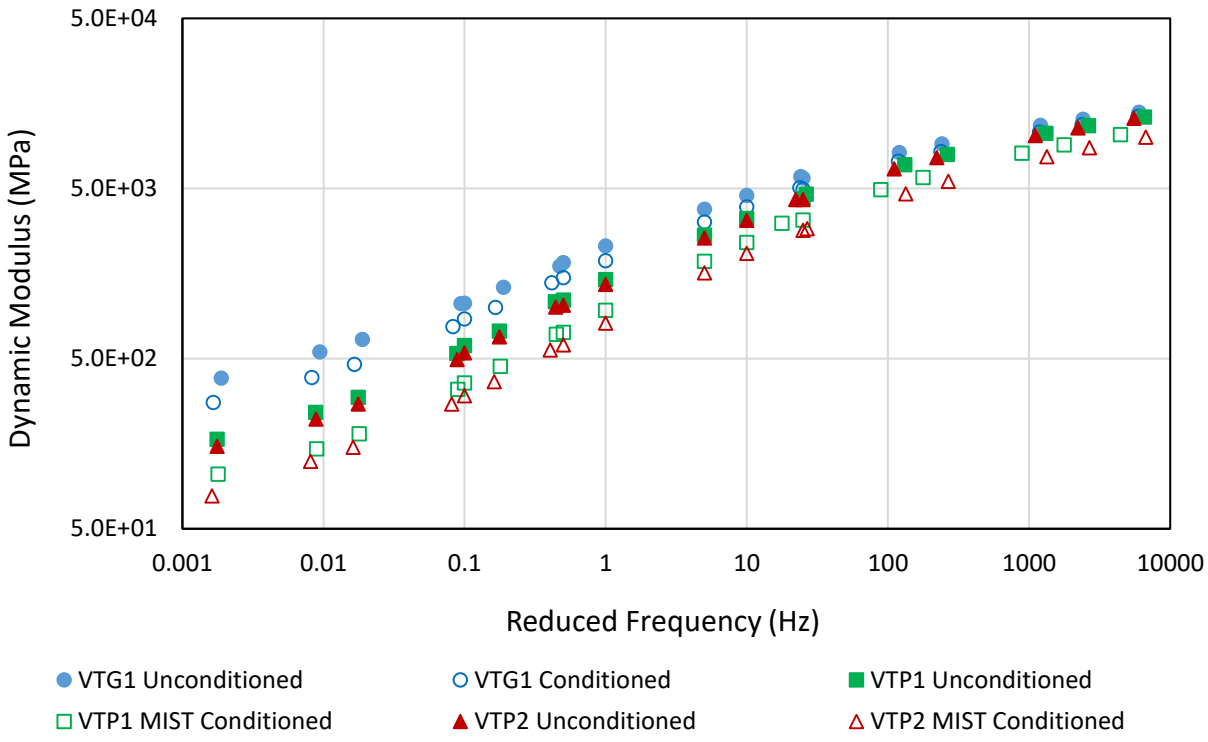

Figure 28: Vermont Dynamic Modulus Results

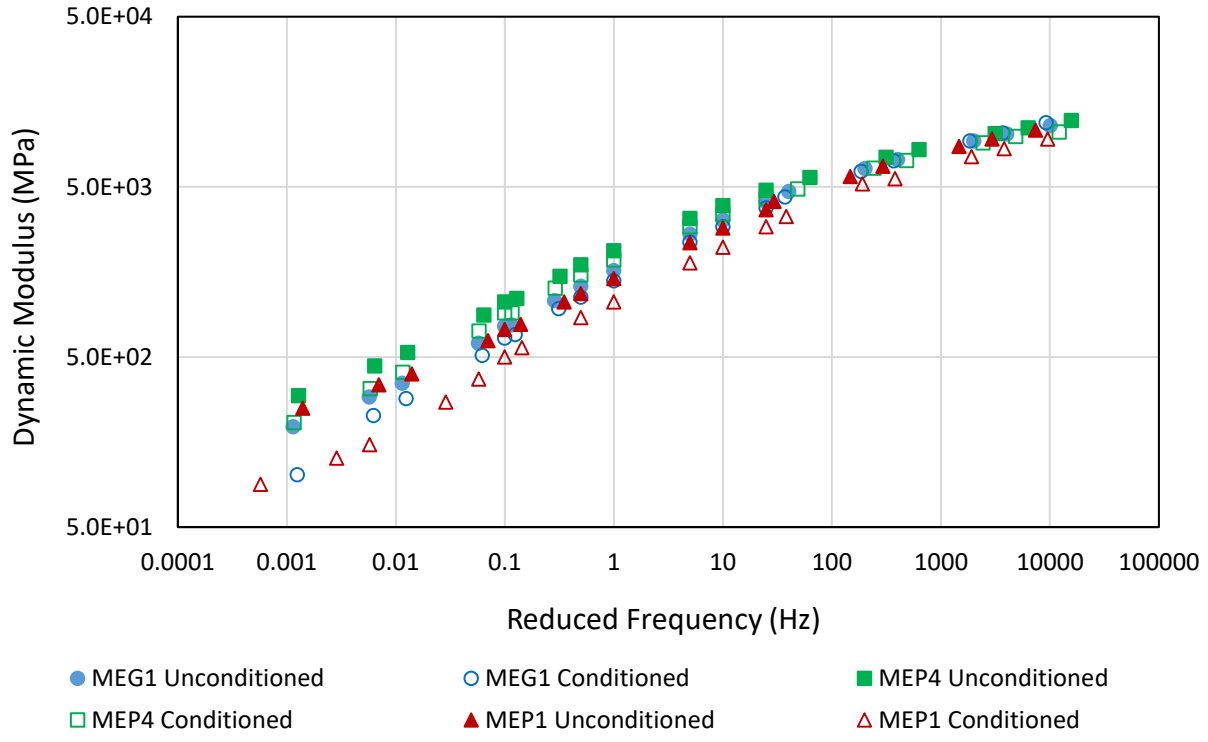

Figure 29: Maine Mixture Dynamic Modulus Results

Since visual observations on log scales can be misleading, the dynamic modulus ratio (moisture-conditioned modulus divided by unconditioned modulus), values at various frequencies along the master curve are shown in Figure 30 and Figure 31 . The results in this plot support the visual observations made from Figure 28 and Figure 29. Looking at the ratios, it can be seen that the materials experience a drop in stiffness across all frequencies after conditioning. This reduction in stiffness is much more pronounced at lower frequencies where the dynamic modulus ratio for the Vermont materials is as low as 0.71 for the good performer and 0.53 for the poor performer without the anti-strip additive. Looking at the Maine materials at the low frequencies, the dynamic modulus ratio is as high as 0.79 for the good performer and as low as 0.37 for the poor performer. As the frequency increases, the dynamic modulus ratio steadily increases to values around 0.95 for the good performer and approximately 0.80 for both poor performers for the Vermont materials, while the Maine materials experience similar increases to 1.03 for the good performer and approximately 0.87 for both poor performers. These results suggest that asphalt mixtures are more affected by moisture conditioning at slower traffic speeds and higher temperatures.

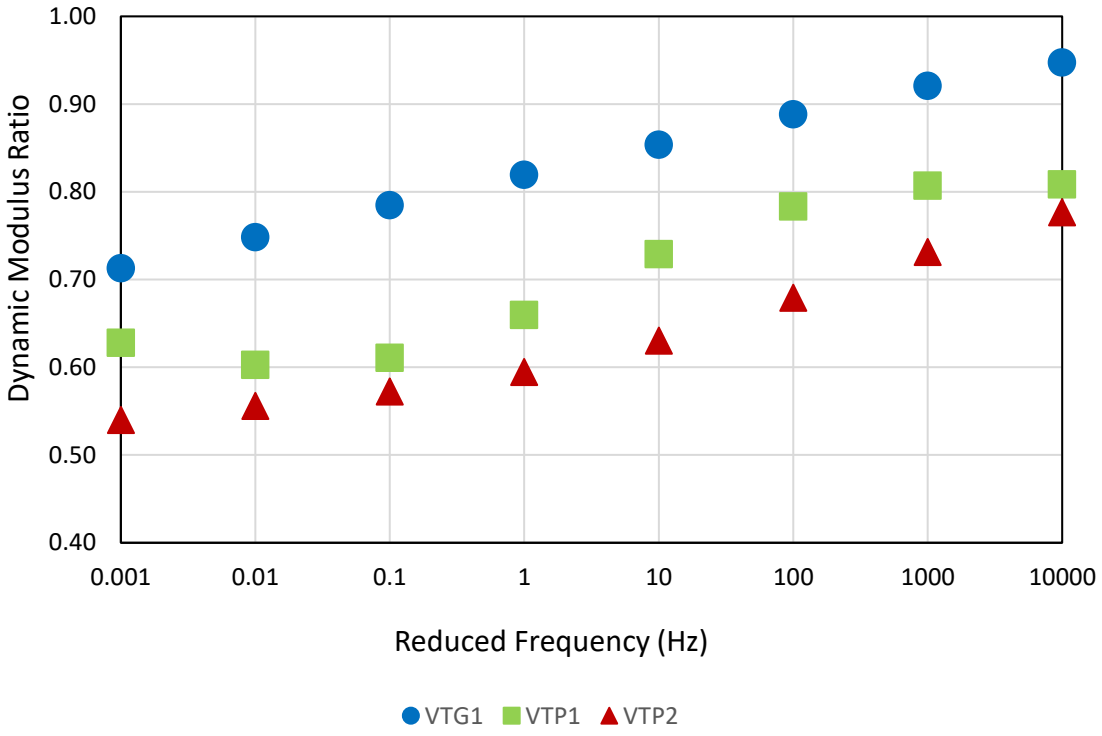

Figure 30: Vermont Dynamic Modulus Ratio Results

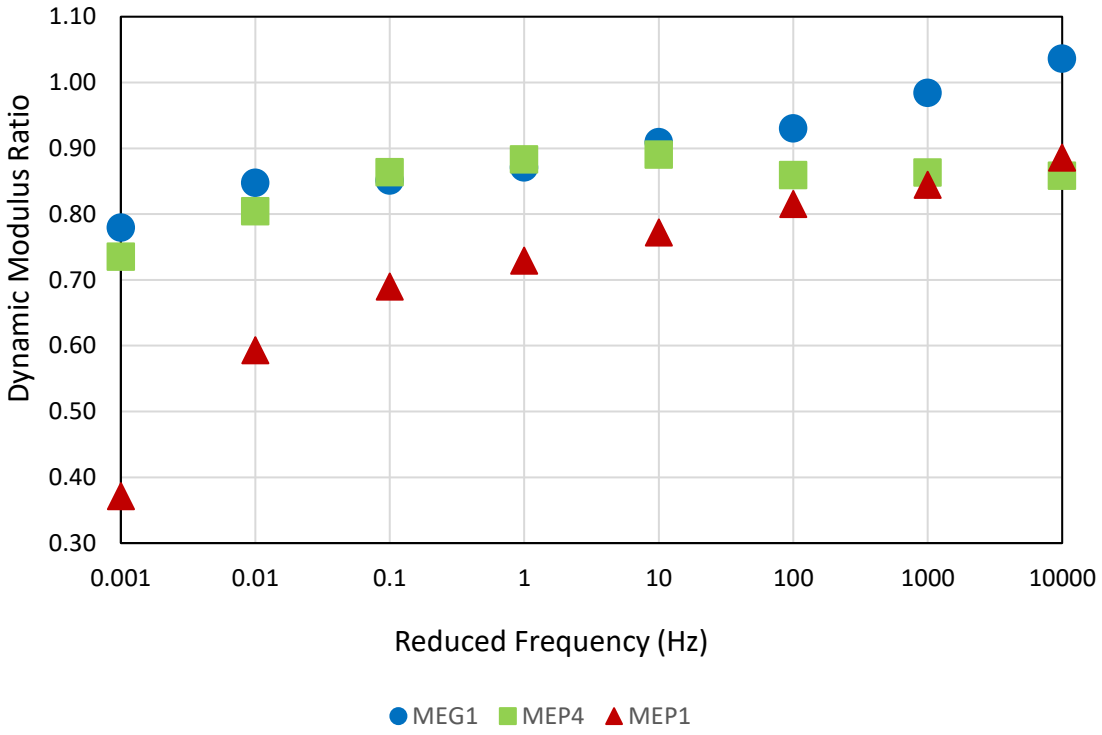

Figure 31: Maine Dynamic Modulus Ratio Results

It can also be seen in Figure 30 and Figure 31 that the good performers generally experience a substantially less reduction in stiffness compared to the two poor performers. For the Vermont materials, the good performing mixture dynamic modulus ratio ranges from 0.71 to 0.95 compared to the poor performing mixtures where the dynamic modulus ratio ranges from around 0.60 to 0.80. For the Maine materials, the good performing mixture dynamic modulus ratio ranges from 0.79 to 1.03 while the poor performing mixtures dynamic modulus ratio ranges from around 0.37 to 0.88. Although the magnitude varies from mixture to mixture, the good performer's modulus ratio is consistently between 0.15 and 0.20 higher than the poor performing mixtures throughout the master curves. This result is promising as it indicated that dynamic modulus is able to distinguish good and poor performing mixtures when paired with MiST conditioning, unlike the testing previously presented.

Another promising result in Figure 30 is that it appears that dynamic modulus is able to distinguish the effect of an anti-strip additive as well. This is most evident at the lowest frequency of 0.001 Hz and frequencies between 1 Hz and 1000 Hz where the dynamic modulus ratio of the poor performer with the anti-strip additive (VTP1) is between 0.05 and 0.1 larger than the poor performer without the anti-strip additive (VTP2). This difference is much clearer than those shown for ITS testing where the effect of anti-strip additives could not be observed.

In addition to dynamic modulus, the change in phase angle after conditioning was also observed. The results from this, shown as a master curve in the same manner as dynamic modulus, are plotted in Figure 32 and Figure 33. Looking at the results for the Vermont materials, it is apparent that all three mixtures experience an increase in phase angle after MiST conditioning. The amount of increase in phase angle is much more pronounced after the peak of the curves around 0.50 Hz, where the mixture transitions into binder dominated behavior. This increase in phase angle can be as low as 0.5 degrees at lower frequencies, to as much as an increase of 5 degrees at some of the intermediate frequencies. The increase in phase angle shows that after moisture conditioning, the mixtures are exhibiting a more viscous response under loading.

Looking at the phase angle results for the Maine materials shows somewhat different trends as compared to the Vermont materials. In general, the larger increase in phase angle when comparing the good performer and poor performer can be seen. However, this is only if the good performer is compared to MEP1, which is considered an extremely poor performing material by field experience. When comparing phase angle changes between the good performer and MEP4, the opposite is observed where the good material experiences more substantial changes in this case.

Similar to the dynamic modulus changes, the increase in phase angle is generally more substantial for the poor performing mixtures compared to the good performing mixtures. Across all frequencies for the Vermont materials, the good performing mixture experiences an increase of phase angle of no more than two degrees. Compared to the two poor performing mixtures, which can increase up to five degrees at intermediate frequencies, the good performer is undergoing significantly less change in material behavior. These differences are less apparent in the Maine

materials, but the general trend can still be observed when comparing the good material to the well-known poor performer, MEP1.

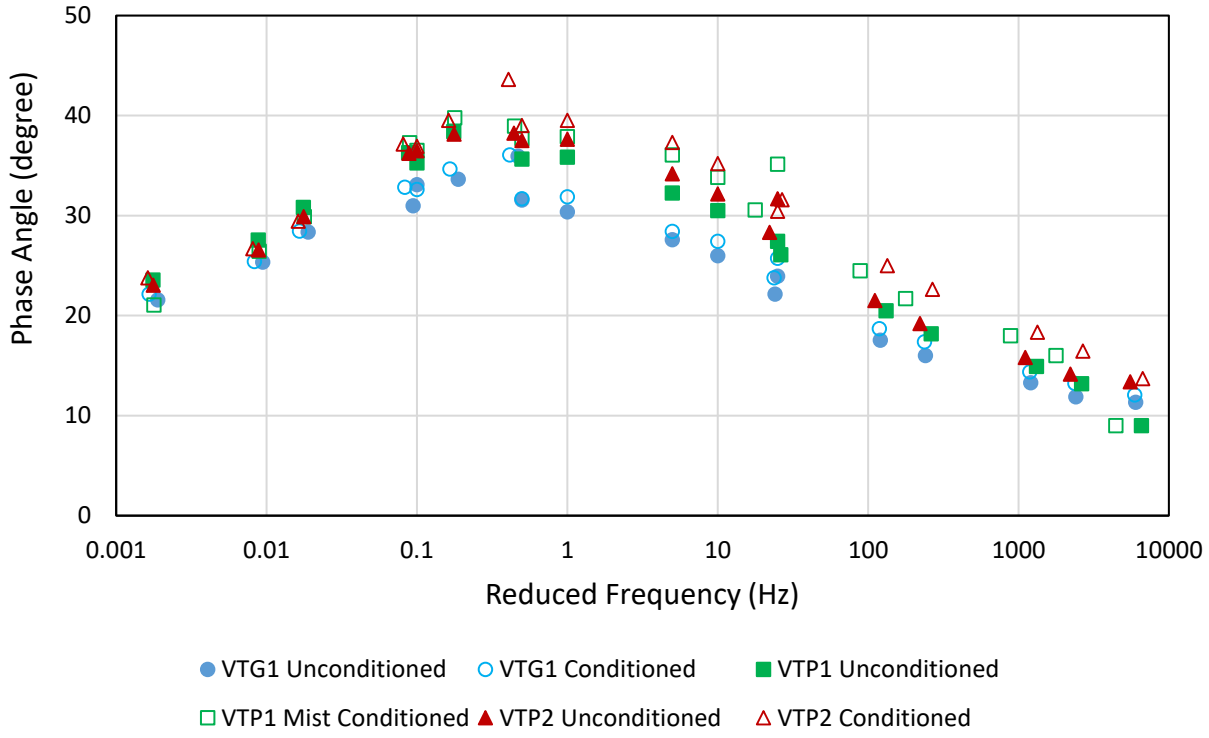

Figure 32: Vermont Phase Angle Results

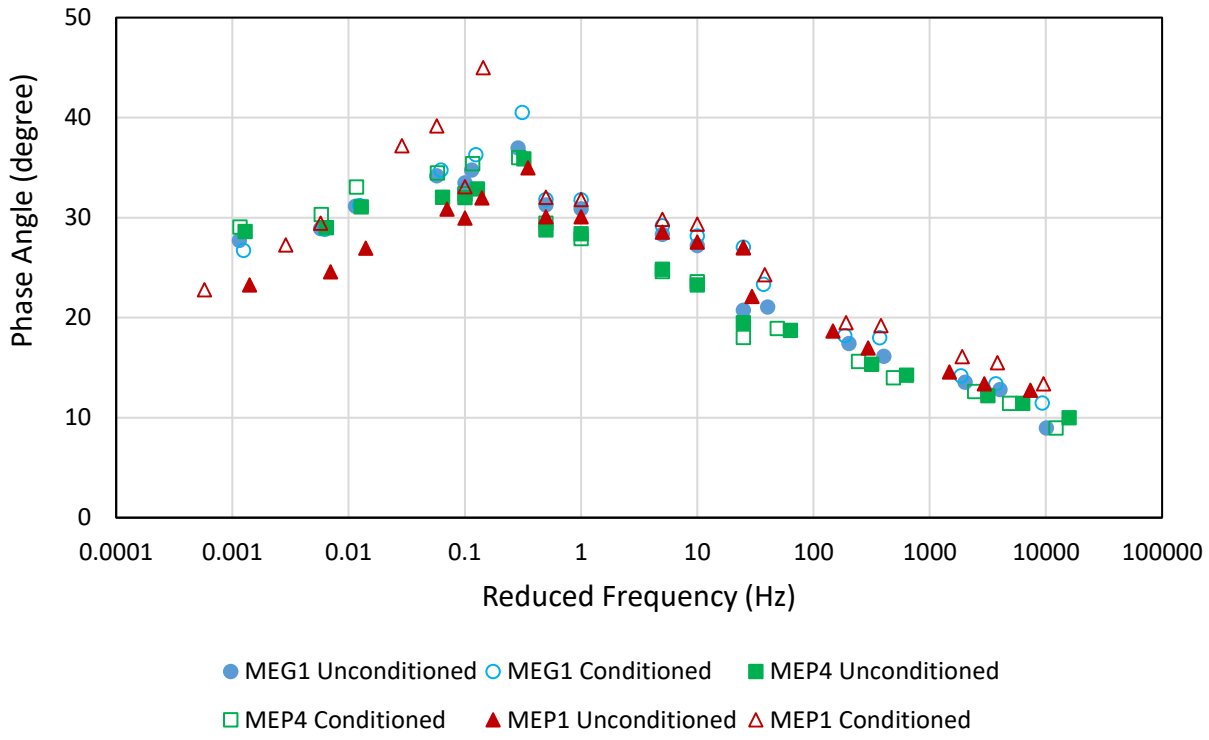

Figure 33: Maine Phase Angle Results

Overall, the results from dynamic modulus are promising considering the objectives set forth in this study. Both dynamic modulus and phase angle results were able to clearly distinguish the good and poor performing mixtures, while dynamic modulus was able to somewhat distinguish the performance of the mixture using an anti-strip additive compared to the same mix without an anti-strip additive. Results from dynamic modulus testing showed that asphalt mixtures experience both a reduction in modulus and an increase in phase angle after moisture conditioning, meaning that the materials are both softer and behaving in a more viscous manner.

One reason dynamic modulus results may be more promising as compared to strength measures for moisture susceptibility is that dynamic modulus is able to capture a larger amount of damage as compared to strength measurements. This is because dynamic modulus is a property measured on an entire specimen, allowing all of the damage due to small defects within the specimen to be captured at the test level regardless of their locations within the material. Strength measurements, on the other hand, typically focus on failure within one region of the material. This is especially apparent with strength tests that involve fracture, such as ITS or DCT, where the region of failure is highly controlled by the test geometry. In this case, it is likely that many regions of local damage (especially near the surface of the material) will not be fully captured by strength measurements as they are not along the failure plane.

Another advantage of using a modulus measure, which captures the overall response of the whole specimen and corresponding softening mechanisms from moisture-induced damage, is ability to use this measure in mechanistic pavement analysis.

4.3 AASHTOWare PavementME

One of the advantages of measuring dynamic modulus is that it is a fundamental material property allowing it to be used with pavement analysis models to calculate stresses and strains in a pavement structure, which can be tied to distress predictions. As mentioned in the methodology section, AASHTO PavementME (version 2.3.1 at the time of the project) was chosen as the pavement analysis tool for this project as it uses dynamic modulus as the primary material input for asphalt layers. The results from this section show two different pavement structures simulated using PavementME. Both pavement structures were simulated using dynamic modulus values measured on unconditioned and MiST conditioned mixtures. All other properties of the pavement structure were held constant so that the potential effects of moisture conditioning could be isolated. The dynamic modulus data from the three Vermont mixtures was used for the PavementME simulations.

Figure 34 shows the cross sections of the pavements used in this analysis. A relatively representative thick and thin pavement structure for the New England region were chosen. Table 62 in the appendix shows some of the parameters used to perform the PavementME analysis such as traffic counts, material properties, etc. It is worth noting that the simulations with the moisture conditioned material properties were conducted in a "worst case" scenario where those properties were assumed to be present at the time of construction. In reality, this is unlikely to occur as moisture damage occurs over time. This choice was made for the sake of simplicity and practicality as it should give a reasonable estimate of the potential implications on pavement performance of using materials with moisture-induced damage.

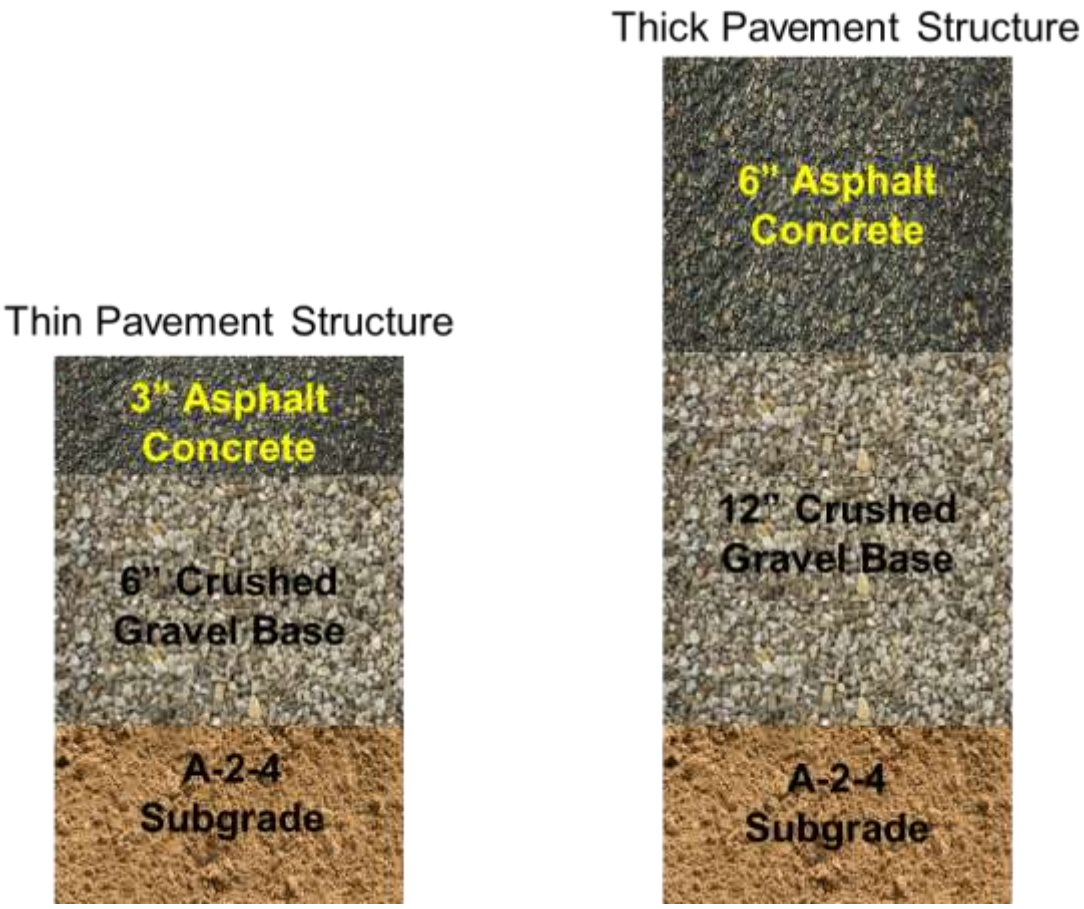

Figure 34: Pavement ME Thin and Thick Pavement Structures

The following plots show the results from the thin pavement simulation. All results are plotted in terms of predicted distress and roughness amounts with respect to the amount of time the pavement has been in service. Both distresses and roughness predictions are compared to a Pavement ME failure threshold, shown on the plots with a dashed black line.

Figure 35 shows the predicted rut depth of the thin pavement structure. Looking at Figure 35, it can be seen that all three mixtures are predicted to have higher rut depths with conditioned properties, which is not surprising considering their reduction in stiffness. This increase is more pronounced for the two poor performing mixtures, especially as the service life of the pavement increases. In the first few months of service, there is little distinction between any of the mixtures. The two poor performers are predicted to accumulate an additional 0.2 inches of rut depth compared to the baseline condition. This is much larger compared to the good performing mixture, which only experiences and additional 0.08 inches of rutting.

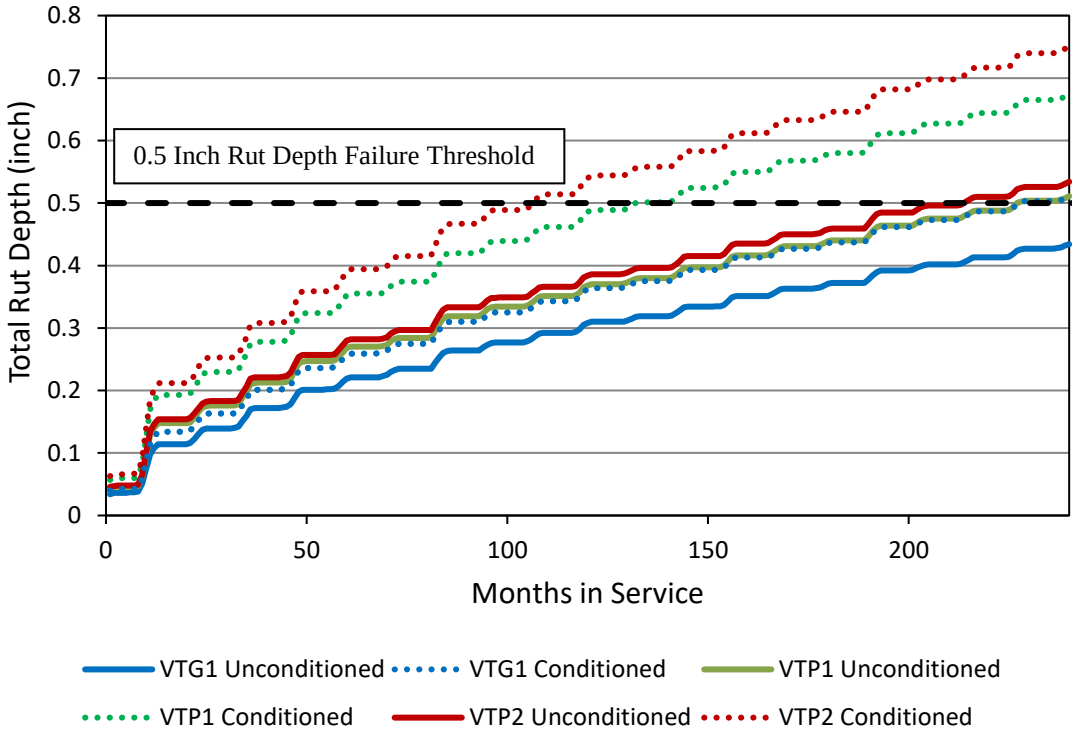

Figure 35: Pavement ME Predicted Rut Depth Results for Thin Pavement Structure

A common failure threshold, which is the default threshold in Pavement ME, of 0.5 inches of rut depth is also shown on the plot. Pavement life in terms of rutting can be defined as when the predicted rutting crosses this threshold. Looking at Figure 35, it is apparent that all of the moisture conditioned materials reach the failure point earlier than their unconditioned counterparts. When comparing the two poor performing mixtures to the good, significant differences in loss of pavement life can be seen. For example, VTP2 passes the rutting threshold at 214 and 107 months in the unconditioned and conditioned state respectively. This difference represents a significant loss of life of 107 months, almost 11 years, compared to the 20 year design life of this pavement section. Compared to the good performing mixture VTG1, which loses approximately half as much life at a loss of 50 months, this is a substantial difference in expected pavement life. Loss of life values can be seen in Table 10.

Looking at the bottom up fatigue cracking results in Figure 36, similar trends are observed. At the beginning of the life of the pavement, there is very little distinction between any of the mixtures. As time progresses, the conditioned materials begin to experience significantly increased amounts of cracking. This effect is more pronounced for the poor performing materials that see an additional five percent fatigue cracking compared to the good mixture, which only increases about two percent. In terms of life, all of the mixtures fail during the same general timeframe. When comparing the poor and good performing materials, relatively little difference is seen in the predicted loss of life. Both of the poor materials lose approximately 1 year of life due to moisture

conditioning compared to the good material, which loses 8 months of life. Considering to the design life of 20 years, this loss of life is minor.

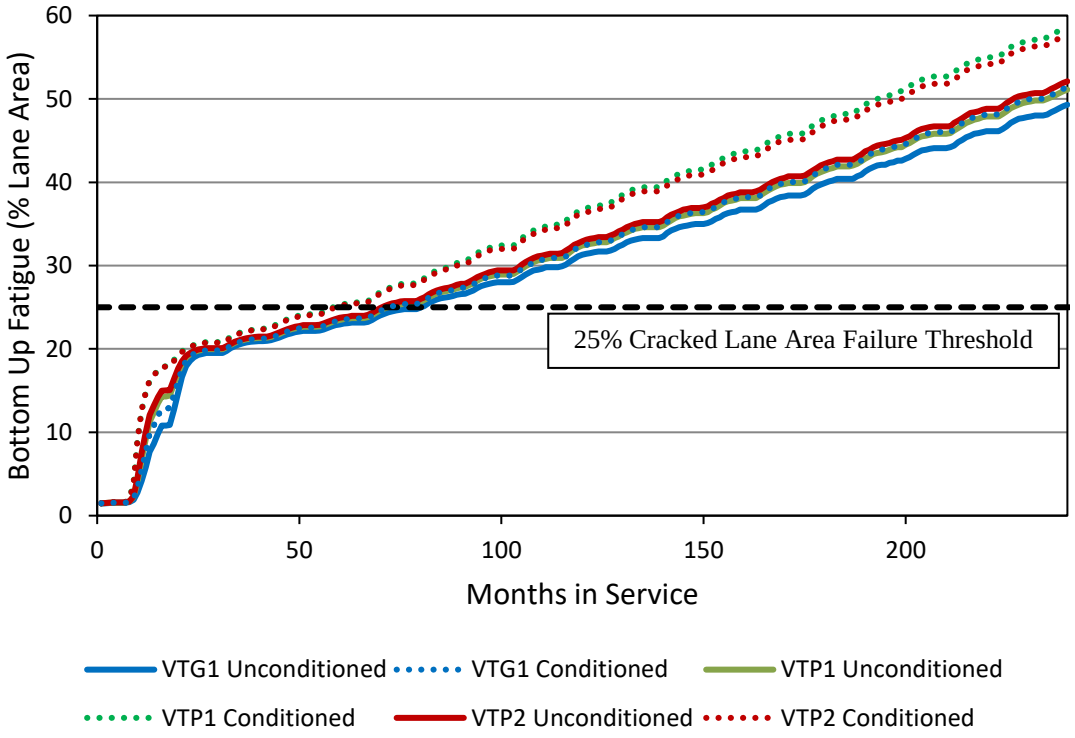

Figure 36: PavementME Predicted Fatigue Cracking Results for Thin Pavement Structure

Figure 37 shows the predicted international roughness index, which quantifies the surface roughness of the pavement, for the thin pavement simulations. In general, the increase in roughness for the conditioned materials is first noticed after about one year of service, and then continues to increase at a rate similar to the unconditioned materials throughout the pavement life. Similar to the two previous plots, this effect is more pronounced for the poor materials compared to the good performer, which has relatively little difference throughout its life. Comparing loss of life, the two poor materials lose 21 and 28 months of life compared to the good material which only loses 11 months of life after moisture conditioning.

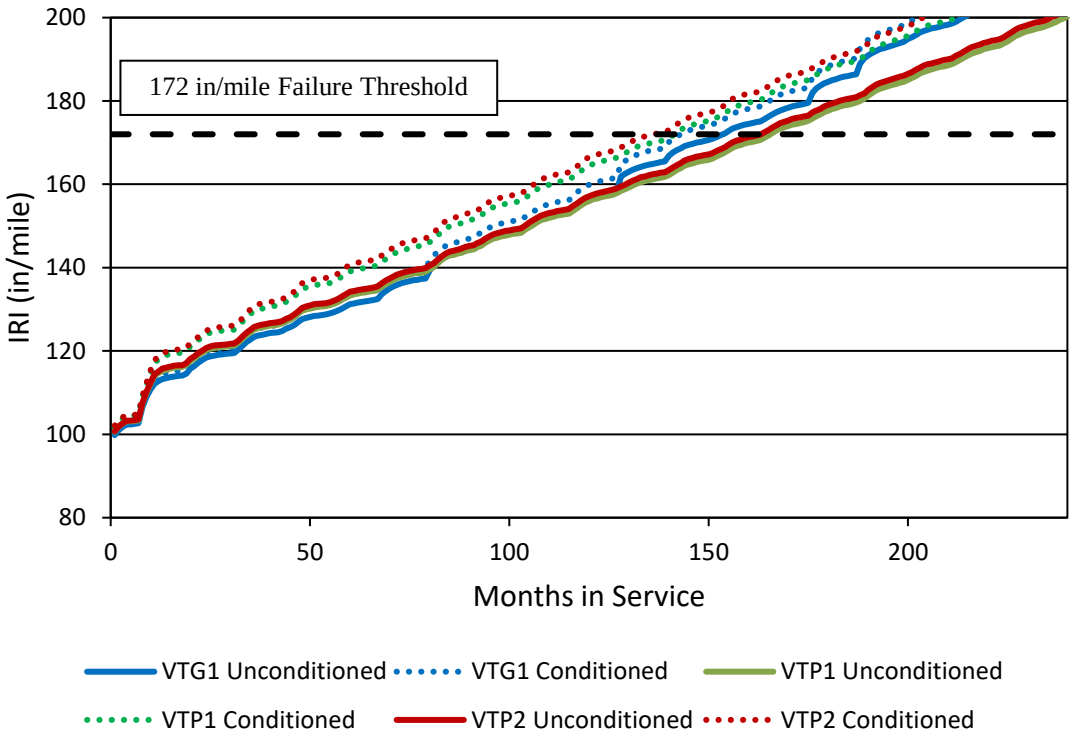

Figure 37: PavementME Predicted Roughness for Thin Pavement Structure

Table 10 and Figure 38 show the summarized predicted life and loss of life for each material and distress type. For the thin pavement section, it can be seen that the most substantial differences in life are observed when comparing to the rutting failure threshold. While both roughness and fatigue cracking both show reductions in life, the loss is relatively minor compared to the design life of 20 years for these pavements.

Table 10: Predicted Pavement Life for Thin Pavement Section

Mixture	State	Months to Failure/Pavement Life		
		IRI (172 inch/mile)	Rutting (0.5 inch)	Fatigue Cracking (25% Cracked Lane Area)
VTG1	Unconditioned	154	≈ 270	81
	Conditioned	143	228	73
	Loss of Life	11	≈ 50	8
VTP1	Unconditioned	166	227	72
	Conditioned	145	135	59
	Loss of Life	21	92	13
VTP2	Unconditioned	164	214	71
	Conditioned	136	107	59
	Loss of Life	28	107	12

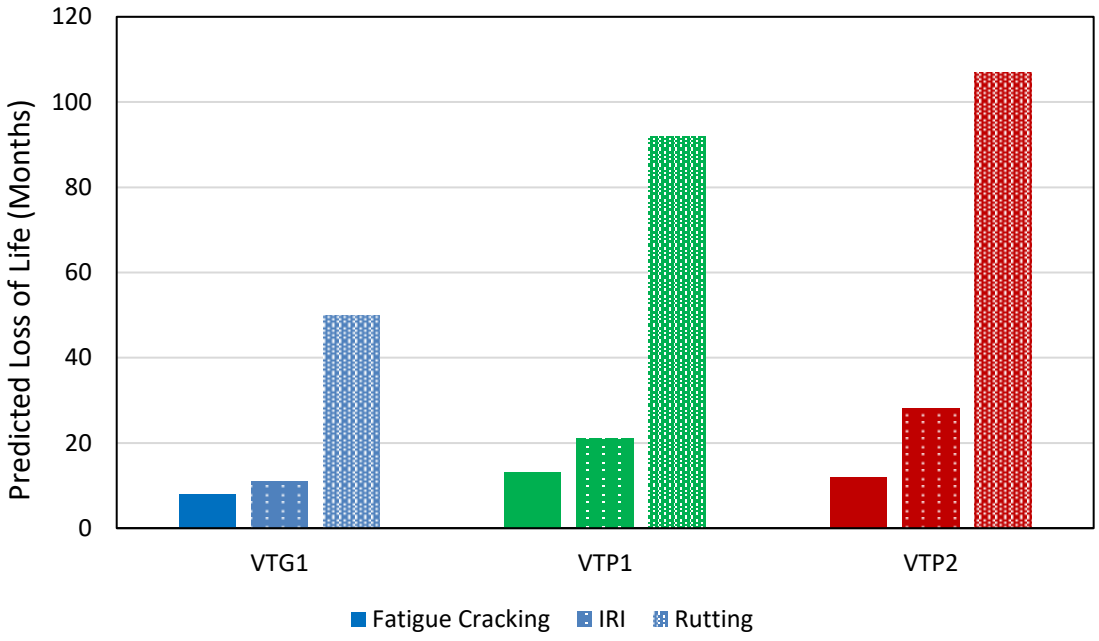

Figure 38: Predicted Loss of Life for Thin Pavement Section

The next three plots show the predicted rutting, fatigue cracking, and roughness for the thick pavement sections. Generally, the trends seen in the thin pavement are reflected in the thick pavement for rutting and roughness. The predicted fatigue cracking trend is somewhat different, however.

Figure 39 shows the predicted rut depths for the thick pavement section. Similar to the thin pavement section, the conditioned materials are predicted to experience substantially more rut depth throughout their service life. This effect is most pronounced for the poor materials towards the end of their service lives. When comparing the loss of life due to moisture conditioning. In this case, the two poor materials lose between 60 to 63 months of life due to conditioning, where the good material only loses 37 months of life. This difference, while less magnitude than the thin pavement, is a significant difference as the poor materials lose almost twice as much life as the good material.

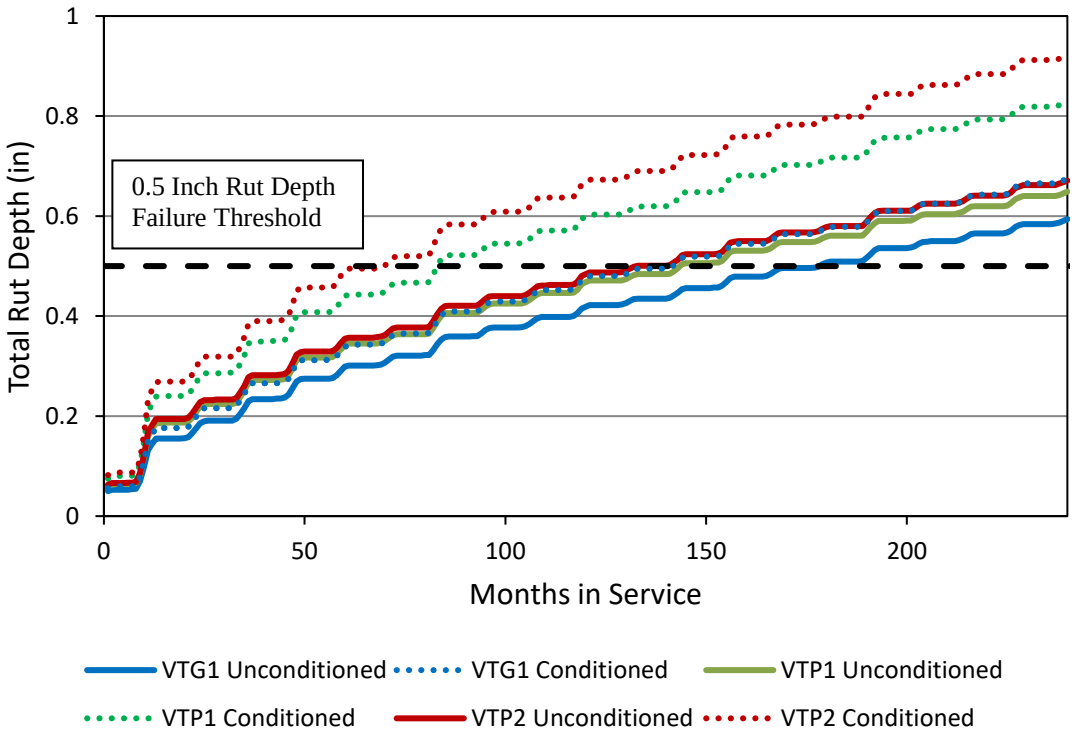

Figure 39: PavementME Predicted Rutting for Thick Pavement Structure

Figure 40 shows the predicted fatigue cracking for the thick pavement section. Compared to the thin section, the predicted cracking amount is substantially less in the thick pavement. Unlike the thin pavement, the moisture conditioned materials begin to distinguish themselves early in the pavement life. This can be most clearly seen with the poor materials where between 40 and 60 months, there is predicted to be an additional 10-15 percent lane area of fatigue cracking due to

the effects of moisture conditioning. After 60-70 months of service, the difference between conditioned and unconditioned materials becomes much smaller at around 5 percent.

Comparing loss of life between the poor and good materials shows significant differences when comparing the poor and good materials. The two poor materials are predicted to lose between 49 and 51 months of life from moisture conditioning whereas the good material is only predicted to lose 25 months. Similar to the rut depth predictions, the good material loses half as much life as compared to the poor materials.

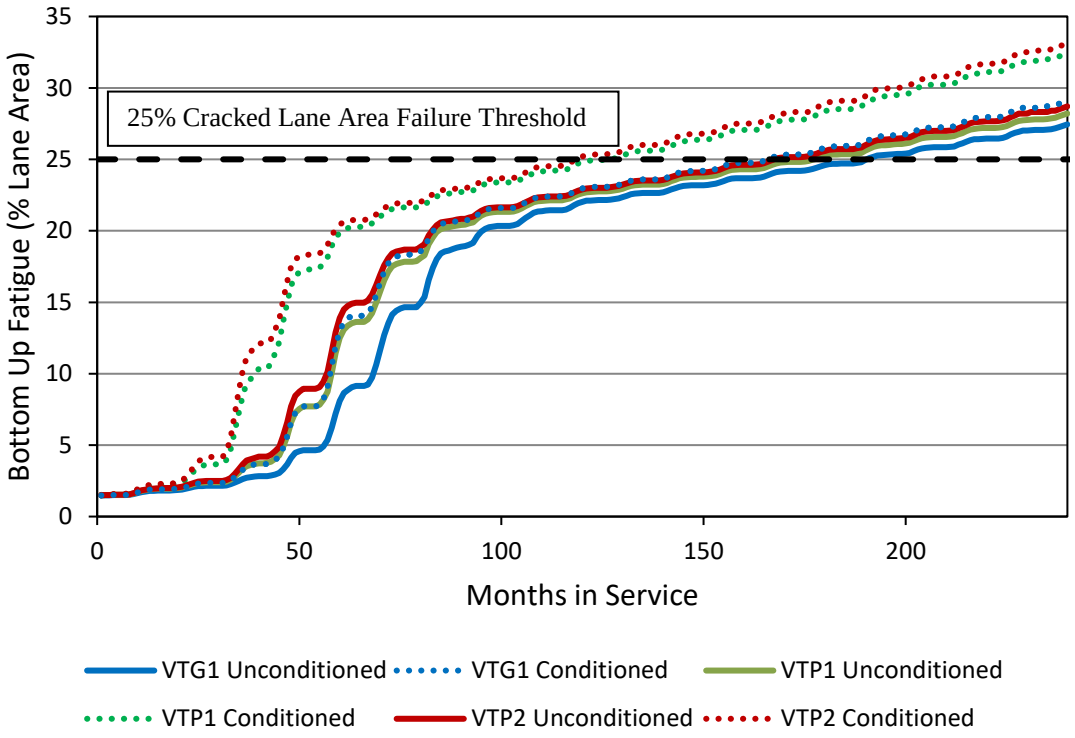

Figure 40: PavementME Predicted Fatigue Cracking for Thick Pavement Structure

Predicted IRI values for the thick pavement sections are shown in Figure 41. Similar to the thin pavement section, the increase in IRI due to moisture conditioning is most apparent during the middle and late portions of the pavement life. For the conditioned materials, the rate of increase in IRI is slightly faster than that for the unconditioned materials.

When comparing the loss of life between the poor and good materials, the poor materials lose substantially more life. The poor materials, which lose between 29 and 35 months of life, are expected to lose almost three times as much life as the good material, which only loses 8 months due to moisture conditioning.

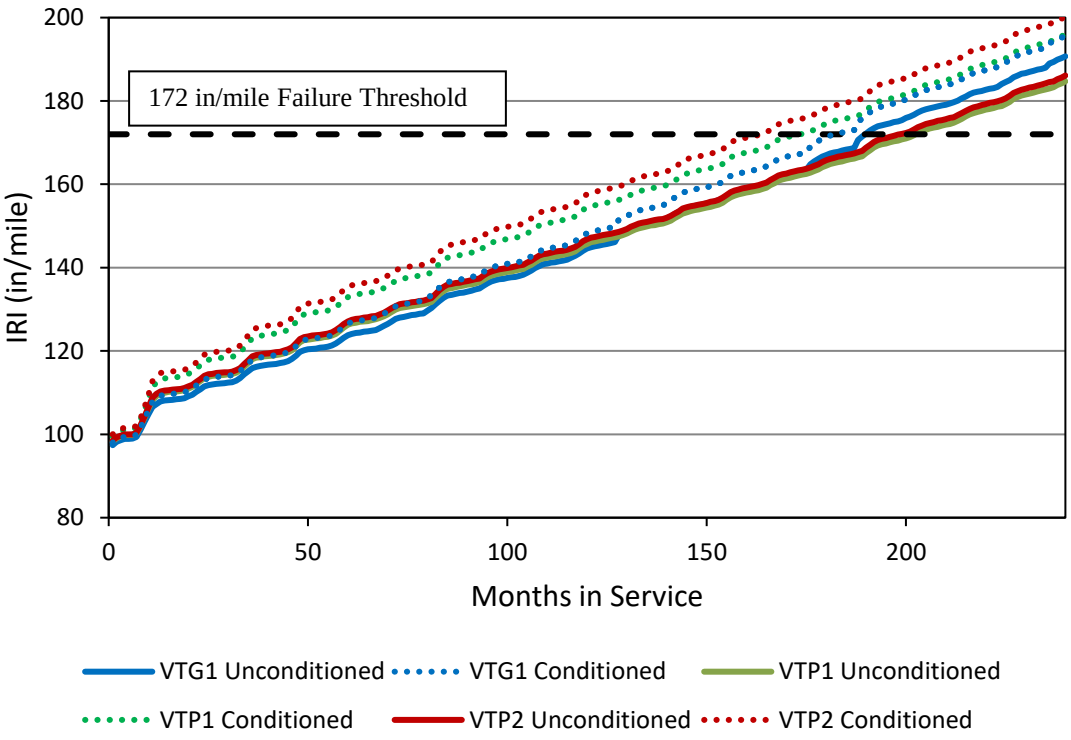

Figure 41: PavementME Predicted Roughness for Thick Pavement Structure

Similar to the thin pavement section, Table 11 and Figure 42 show the predicted life and loss of life for each material and distress type. For the thick pavement, all three failure modes show significant losses in life with the use of moisture conditioned properties.

Table 11: Predicted Pavement Life for Thick Pavement Section

		Months to Failure/Pavement Life		
Mixture	State	IRI (172 inch/mile)	Rutting (0.5 inch)	Fatigue Cracking (25% Cracked Lane Area)
VTG1	Unconditioned	190	179	191
	Conditioned	182	142	166
	Loss of Life	8	37	25
VTP1	Unconditioned	203	144	178
	Conditioned	174	84	127
	Loss of Life	29	60	51
VTP2	Unconditioned	199	133	168
	Conditioned	164	70	119
	Loss of Life	35	63	49

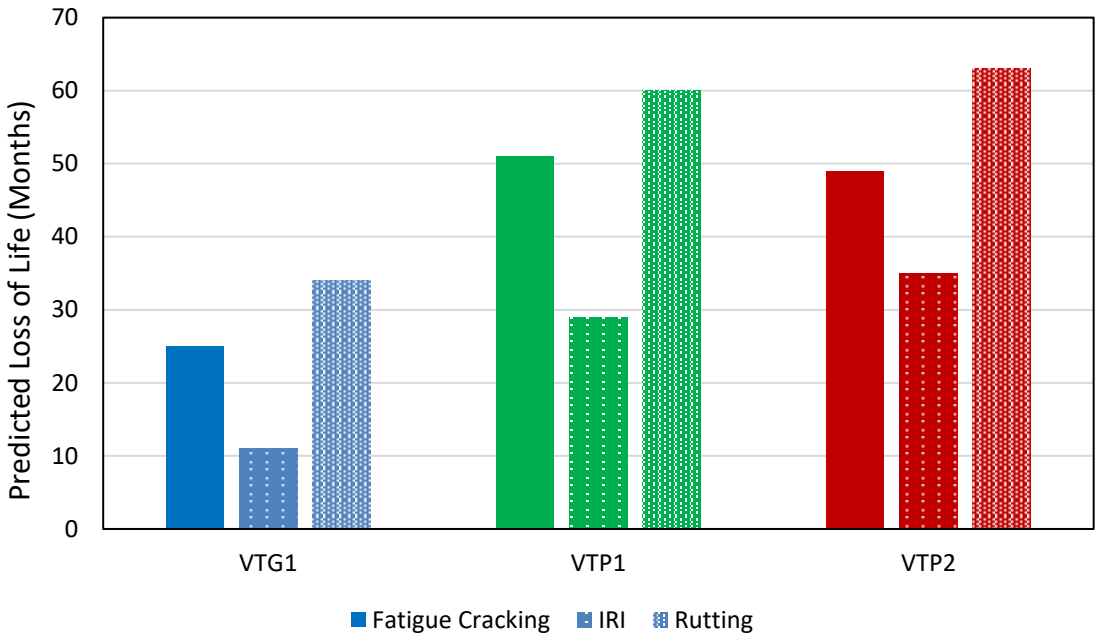

Figure 42: Predicted Loss of Life for Thick Pavement Section

Overall, the results from the Pavement ME simulations suggest that using moisture conditioned material properties has a significant impact on pavement performance. This impact on performance is heavily dependent on the definition of failure as the predicted loss of life ranged from as little as 8 months to up to 107 months depending on the material, failure definition, and pavement structure. Out of the three failure modes shown in this section, rutting is the most affected by moisture conditioning. When looking at loss of life, moisture conditioning brought about anywhere between 37 and 107 months of reduced life whereas fatigue cracking and IRI thresholds typically reduced life between 8 and 50 months.

When comparing poor and good materials in terms of loss of life, the differences are substantial. While the difference in magnitude in loss of life varies for each pavement and failure threshold, the good material always experiences less loss of life due to moisture conditioning. In most cases, the loss of life of the poor materials is between 2 and 3 times as much as that of the good material. These results emphasize the importance of material selection when moisture induced damage is a concern. It should be remembered that these simulations are performed in a worst case scenario, which may not accurately reflect what would occur in a real pavement. Regardless, these predictions provide a basis to understand the potential loss of pavement performance due to moisture conditioning for materials with varying amounts of moisture susceptibility.

4.4 Disk-Shaped Compact Tension (DCT)

Results from DCT fracture testing are shown in the following section. DCT testing was paired with a newly developed freeze-thaw conditioning procedure to investigate the implications of using mixtures with varying levels of moisture susceptibility on low temperature cracking performance. Five out of the ten mixtures were tested with DCT, which are shown with general descriptions in Table 12. The same color scheme as the ITS section is used in this section.

Table 12: Mixes Tested with DCT and Multi-Cycle Freeze-Thaw Conditioning

Mix Name	Location	Performance	Aggregate Type	Binder Grade	Additive	NMAS (mm)
MEP1[1]	Presque Isle, ME	Poor	Limestone	64-28	No additive	12.5
MEP2[1]	Presque Isle, ME	Poor-Moderate	Limestone	64-28	Amine Anti-Strip Additive	12.5
VTP1[2]	Colchester, VT	Poor	Quartzite	58-28	WMA/Anti-Strip Additive	9.5
VTP2[2]	Colchester, VT	Poor	Quartzite	58-28	No Additive	9.5
NHG1	Concord, NH	Good	Granite	64-28	No Additive	12.5

[1,2] Indicates that mixtures are produced at the same plant, have the same volumetric properties, and the same gradations.

Figure 43 shows the fracture energy results from DCT testing, where the bars represent the average fracture energy of three replicates and the error bars are one standard deviation. Looking at the results, the freeze-thaw conditioning appears to have little detrimental effects on the thermal cracking performance of the materials. In fact, the only material that experienced a significant change after conditioning was VTP1, which increased in fracture energy 120 J/m^2 after conditioning. The other mixtures experienced no significant changes in fracture energy after conditioning, ranging from a decrease of 15 J/m^2 with MEP2 to an increase of 20 J/m^2 with NHG. This results-based observation is also reflected in Figure 44, which shows representative load-CMOD curves of both unconditioned, and freeze-thaw conditioned specimens. As can be seen, the two sets of curves are very similar to each other, suggesting no significant changes to material properties are occurring due to freeze-thaw conditioning. It is also worth noting that every mixture, regardless of being in an unconditioned or conditioned state, exceeded the recommended threshold to resist thermal cracking of 400 J/m^2 established by MnDOT from laboratory and field results.

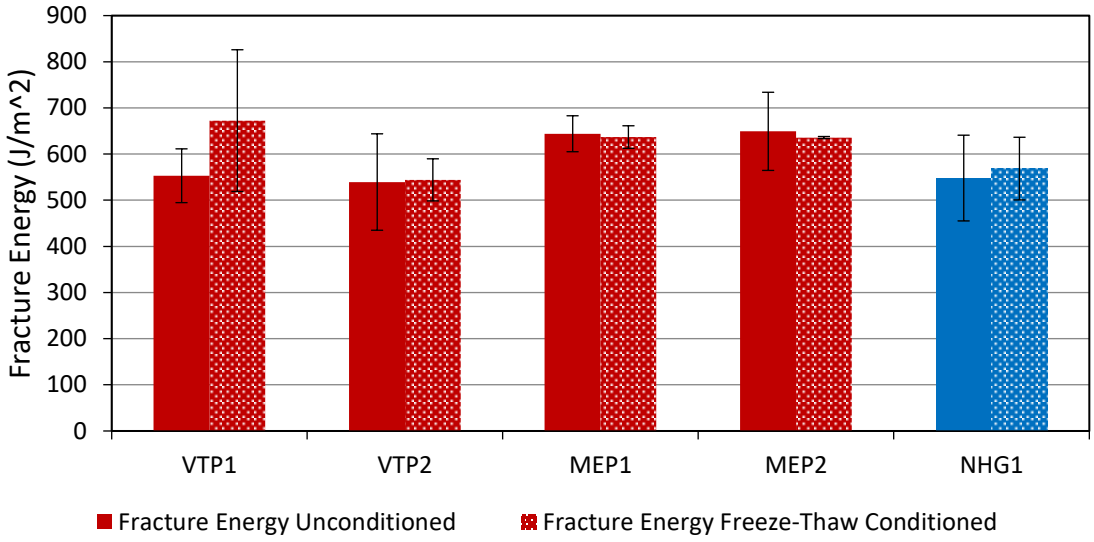

Figure 43: DCT Fracture Energy Results

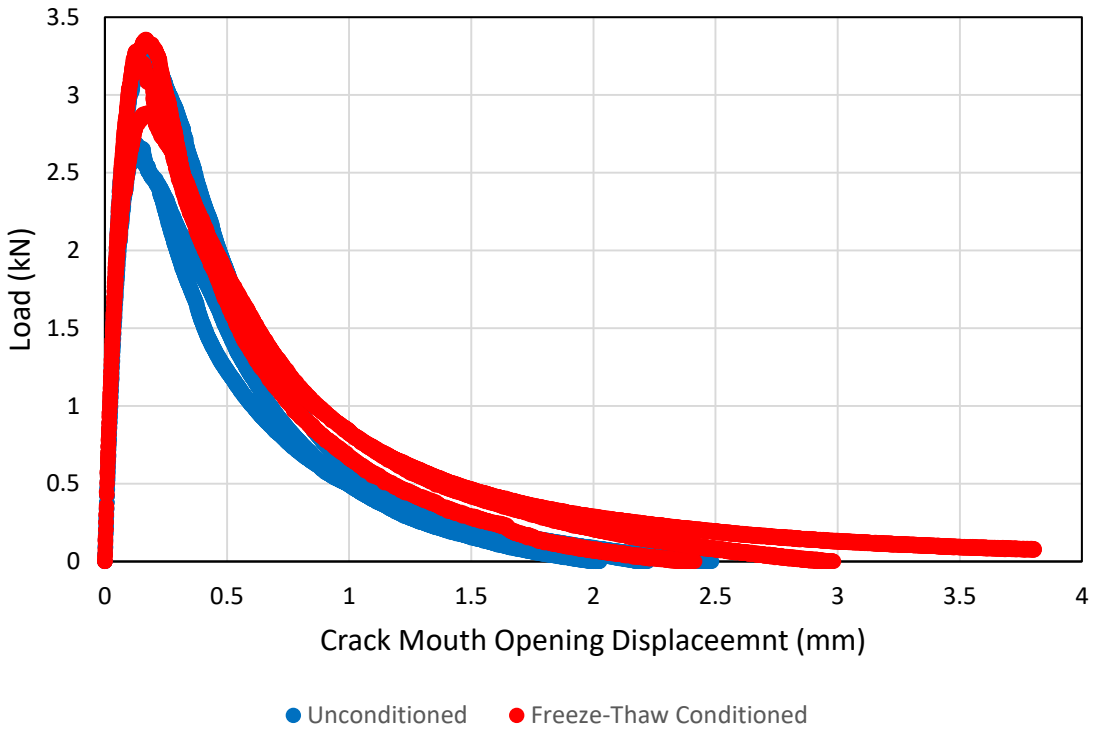

Figure 44: Representative Load-CMOD Curves for Unconditioned and Freeze-Thaw Conditioned DCT Specimens

When comparing good and poor performing mixtures, the fracture energy results are not able to distinguish the two mix groups. As can be seen in Table 13, the average change in fracture energy after conditioning of both groups of mixtures are an increase of 25.9 J/m^2 for the poor performers and 20.5 J/m^2 for the good performers. This minor increase in fracture energy (compared to the average values for each group) is insignificant suggests that freeze-thaw damage is not an effective moisture susceptibility predictor and that it does not affect low temperature cracking resistance for these mixtures.

In addition to not being able to distinguish between good and poor performing materials, the DCT results also showed no significant effects of anti-strip additives. When comparing either VTP1 to VTP2 or MEP1 to MEP2, there were no obvious trends occurring with the addition of anti-strip additives.

Table 13: Average Fracture Energy Results

Mix Performance	Average Unconditioned Fracture Energy (J/m^2)	Average Freeze-Thaw Conditioned Fracture Energy (J/m^2)	Average change in Fracture Energy (J/m^2)
Poor	596.4	622.3	25.9
Good	548.0	568.5	20.5

DCT was chosen to be evaluated in this study to investigate the effectiveness of a fracture mechanics based approach to moisture susceptibility evaluation. DCT, as well as most fracture based approaches, are able to capture the fundamental mechanisms of moisture-induced damage better than strength based measurements. The pure tensile failures associated with fracture failures directly stress the internal adhesive and cohesive bonds of asphalt materials where moisture-induced damage is expected to occur. Interestingly, the results from this project did not show any significant differences between historically good and poor performing mixtures. Considering fracture based tests ability to capture moisture damage and past success using DCT as a moisture susceptibility test method, it is likely the case that the freeze-thaw condition scheme is the limiting factor in this situation. This is supported as results before and after conditioning were very similar. If the conditioning protocol were having a significant effect on the materials, it would be expected that some differences in results would be observable.

4.5 Semi Circular Bend (SCB)

Results from SCB fracture testing are shown in the following section. SCB testing was conducted on materials in an unconditioned and MiST conditioned state to investigate the effectiveness of using a fracture test at intermediate temperatures to determine moisture susceptibility of asphalt mixtures. The results in this section are presented in the same manner and color coding as those in the ITS section.

Figure 45 shows the pre and post conditioning fracture energy results from SCB testing, where each solid bar represents the average fracture energy of the unconditioned material while the patterned bars represent the fracture energy of MiST conditioned materials. When examining the effect of conditioning, there is a consistent increase in fracture energy for all of the materials after conditioning. While the amount varies from material to material, this increase in generally between 30 and 100 percent. This increase in fracture energy after conditioning suggests that the materials cracking performance is improving after experiencing severe moisture damage from the MiST process, which is unexpected and nonsensical when considering real world field experience concerning moisture-induced damage. In addition to this observation, it can also be seen that there is no consistent differentiation between the poor and good mixtures in terms of fracture energy results. This includes both the magnitude and ratio of increase in fracture energies.

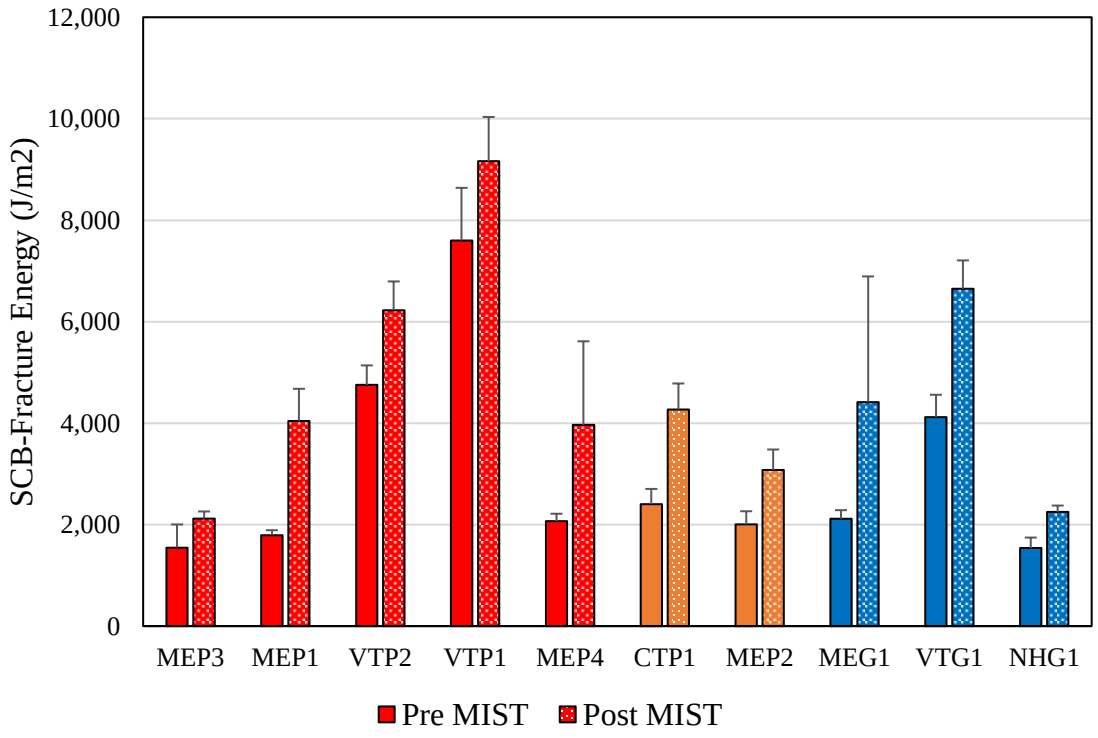

Figure 45: SCB Fracture Energy Results

Figure 46 shows the flexibility index results from the same series of SCB tests as shown in Figure 45. As can be seen in the results, the same general trends seen in the fracture energy results are

evident in the flexibility index results where there is a consistent increase in flexibility index after experiencing the moisture conditioning via the MiST. In this case, however, the increase is much more substantial where each mixture experiences an increase in flexibility index of almost 100 percent, with some even becoming five times larger than the unconditioned value. Similar to previous results, this suggests that the material would be expected to resist cracking significantly more than the unconditioned material. Another difference noticed with the flexibility index results is that there is some distinction between the good and poor performing materials. As is evident in Figure 46, all of the poor and poor-moderate materials, with the exception of VTP2), experience an increase in flexibility at least double of that of the unconditioned value. Compared to the good performing materials, their increase is substantially less where only one of the materials increases double relative to the original value while the other two increase between 1.5 and 1.8 times the original value. While this shows a distinct differentiation between the good and poor materials, using flexibility index is not a promising parameter as the implications with increases in performance after conditioning are troubling and challenging from an implementation perspective.

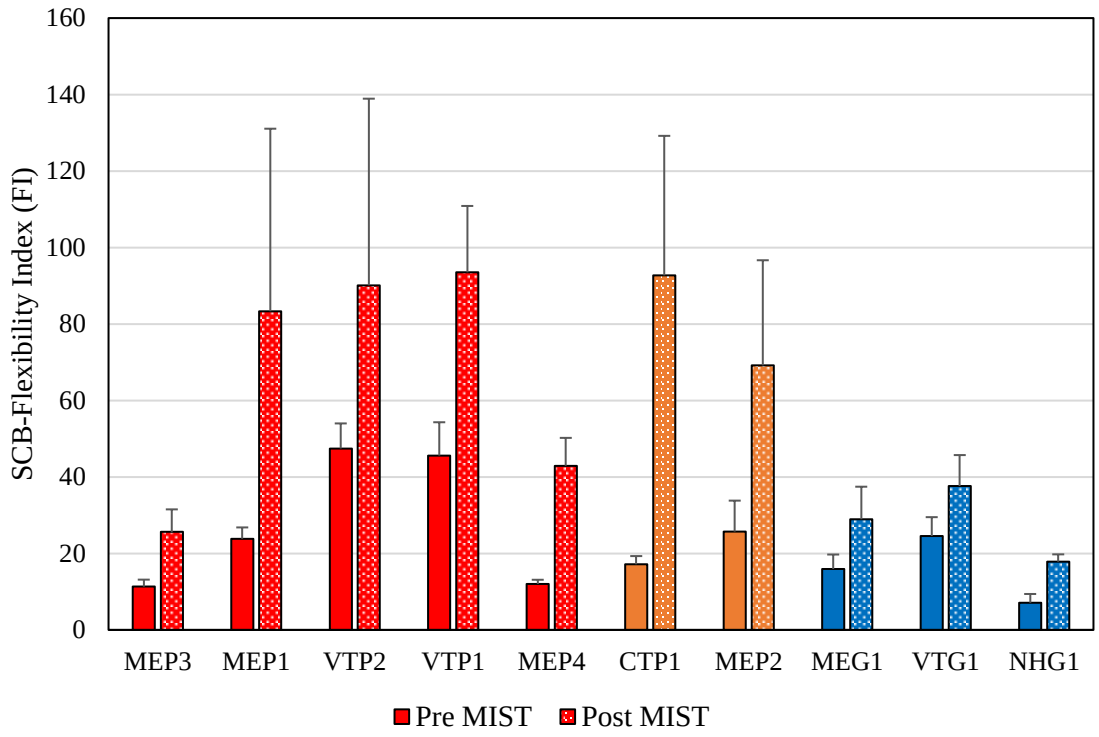

Figure 46: SCB Flexibility Index Results

One potential explanation for the unexpected increase in fracture energy and flexibility index after moisture-induced damage is similar in concept to the problem previously mentioned concerning ITS testing. SCB tests are conducted at room temperature where an assumption is made that the specimen will primarily fail/deform due to material fracture rather than creep or plastic deformation. Considering the materials used in this study (and most of those used in New England)

use relatively soft binder grades, this assumption may not be entirely valid as high amounts of creep were observed during the tests. While fracture energy can still be technically calculated from these results, a significant portion of the calculated fracture energy was not dissipated through actual fracture in this case (rather plastic deformation and creep), making the results unreliable in terms of fracture properties and cracking prediction In addition to this, it was previously seen in the dynamic modulus results that the MiST conditioning process generally makes materials behave both softer and more viscous. This behavior further complicates the previously mentioned problem as more creep and deformation is occurring during the test as compared to the stiffer, unconditioned materials. Due to these challenges associated with using SCB as a moisture susceptibility test as conducted in this project, the test is not a promising procedure for routine usage during mix design.

4.6 Hamburg Wheel Tracker

Results from Hamburg wheel tracker testing are shown in the following section. All ten of the study mixtures are presented in this section, and the same color convention as the ITS section is used where red represents poor, orange represents poor-moderate, and blue represents good mixtures. Results from both traditional Hamburg analysis and the TTI method are presented and analyzed. All of the results are calculated for individual Hamburg results, and then averaged together (rather than combining curves and calculating values off that). For reference, representative Hamburg curves for each mix are shown in Figure 47.

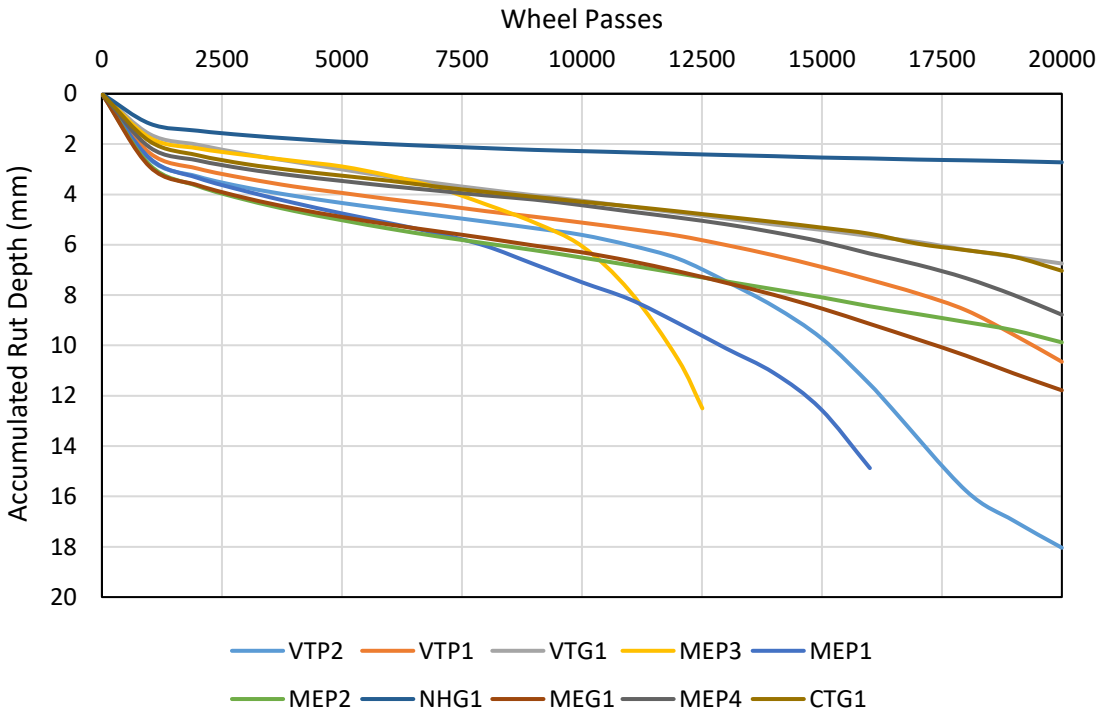

Figure 47: Hamburg Raw Data Curves

Figure 48 shows the results from traditional Hamburg analysis. This includes both the passes to failure, which corresponds to a rut depth of 12.5mm, and the calculated stripping inflection point (SIP). The plot includes error bars, which represent the maximum and minimum measured values. Looking at the passes to failure first, the results show that a majority of the poor mixtures failed within the standard 20,000 passes of the test. On the other hand, all of the poor-moderate and good performing mixtures did not exceed 12.5mm during the test. Considering this, the rut depth could be a promising parameter as it is able to distinguish good and poor performing materials. This is also reflected in Table 14 where the average values for each mixture performance category is compared. It should be noted that any mixture that did not fail was calculated as if the number of passes to failure was 20,000.

Although this parameter shows promise, it should be noted that the Hamburg wheel tracking test was conducted at a single temperature in this study. Rut depth can be somewhat misleading as a soft material could experience viscoplastic deformation at the high temperatures the Hamburg test is conducted at, but no moisture-induced rut damage. This can be seen in limited cases in the results. Looking at the raw data curves in Figure 47 for both MEG1 and NHG1, it can be seen that MEG1 experiences significantly more rut depth accumulation, although neither material shows significant accumulation of moisture-induced damage (which would be seen as a significant increase in rut depth accumulation). This is likely because MEG1 is a softer material as compared to NHG1. Although neither material reached the defined failure rut depth of 12.5mm, it is conceivable where a softer material would reach the failure rut depth without any signs of moisture-induced damage. This issue can be somewhat corrected by changing the temperature of the test, but this is an approximate correction as the temperature adjustments for current Hamburg specifications are solely based off of high temperature PG grades. While this is promising, there is no guarantee that two materials with the same high temperature PG grade will have equal rut resistance. In addition to this, there is no guarantee that materials with different PG grades are behaving similar at temperature ranges specified. Challenges like this support the use of parameters that ignore rut depth, such as stripping inflection point.

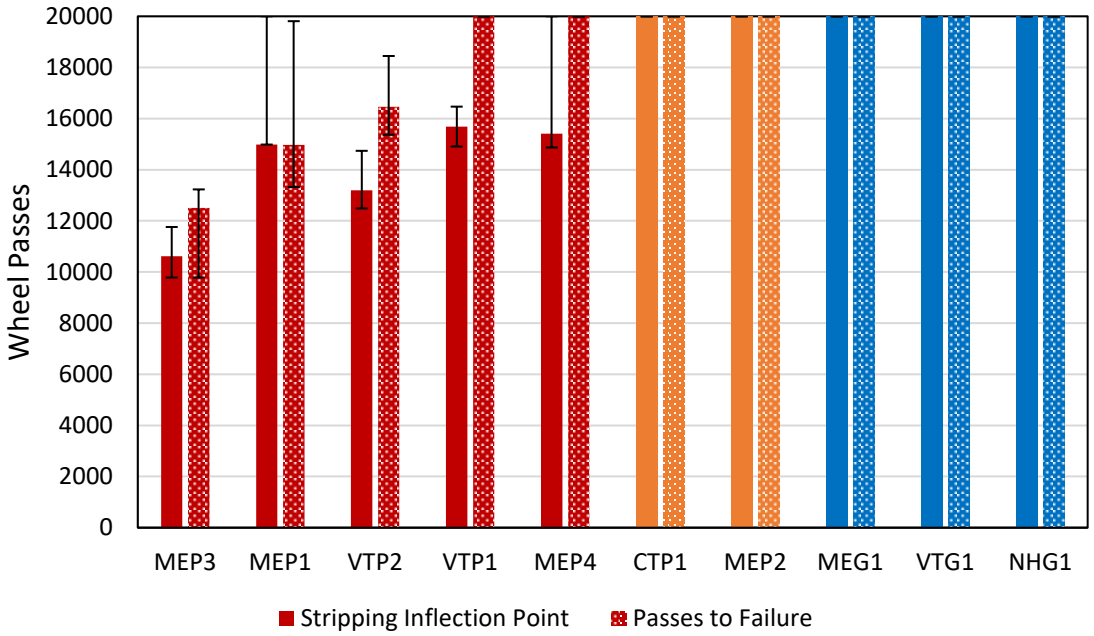

Figure 48: Traditional Hamburg Results

Looking at the SIP values, shown with solid bars in Figure 48, it is apparent that all of the poor performing mixtures experienced a SIP before the test concluded. As with the rut depth results, any bar shown as 20,000 passes for SIP means that no striping inflection point occurred during the test according to the algorithm used. Comparing the good and poor performing mixtures, it is

apparent that the stripping inflection point does an excellent job at distinguishing the two types of materials. The poor mixtures never exceed 16,000 passes before experiencing a SIP where none of the good mixtures experienced a SIP. The average values, shown in Table 14, also reflect this observation.

Table 14: Average Hamburg Results using Both Traditional and TTI Analysis

Mix Performance	Average Passes To Failure	Average Stripping Inflection Point	Average Stripping Number	Average Stripping Life
Poor	16788	13978	8349	16417
Poor-Moderate	20000	20000	20997	25000
Good	20000	20000	25472	26949

Another observation from the traditional Hamburg data is that the results are able to distinguish mixtures with and without anti-strip additives. Looking at the results from MEP1 (no anti-strip additive) and MEP2 (amine-based anti-strip additive), the effectiveness of the additive is clear. The presence of the additive took a mix that experienced a SIP and rutting failure around 15,000 passes to a mix that did not experience either of those. In the case of the two poor performing Vermont materials, VTP2 (no anti-strip additive) experienced a stripping inflection point and rutting failure 2,500 and 3,500 passes earlier respectively compared to VTP1 (hybrid WMA/anti-strip additive). While this difference is not as clear as the two Maine mixtures, it is still a clear, observable difference in material behavior. This results-based observation can also be seen in the raw data in Figure 47, where both mixtures without anti-strip additives show much clearer signs of stripping damage.

Figure 49 shows the Hamburg results from the TTI analysis. It should be noted that, similar to the traditional results, a value of 25,000 passes for either parameter means that they did not occur within the test, indicating excellent performance. The first parameter calculated is the stripping number, which represents how quickly a material begins experiencing moisture-induced damage. Looking at the results, there is a clear distinction between the poor and good performing mixtures. Most of the poor mixtures, with the exception of MEP4, began stripping before 8000 wheel passes. On the other hand, the good performing mixtures only had one mixture begin stripping (at 13,000 passes) while the other two had no measurable stripping point. The poor-moderate materials behaved, as one would expect, in the middle of the poor and good performing mixtures. These observations are reflected in the average calculated values in Table 14. Similar to the previous plot, this includes error bars, which represent the maximum and minimum measured values.

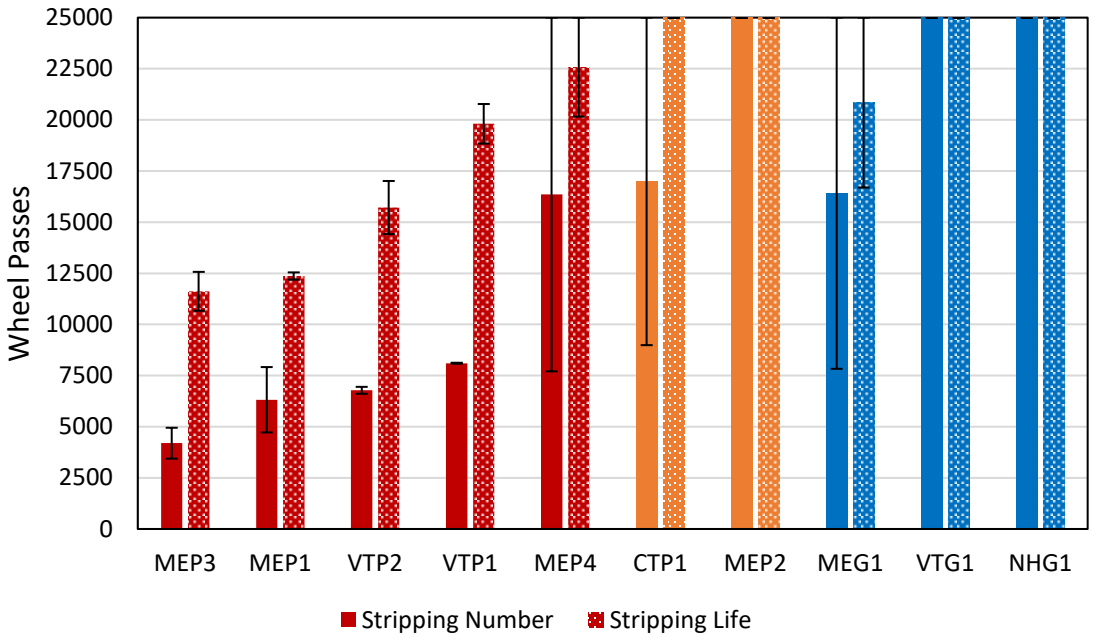

Figure 49: Hamburg Results with TTI Proposed Parameters

The calculated stripping life, which represents how quickly stripping damage progresses in the material, shows a similar trend where the poor materials consistently perform worse than both the poor-moderate and good materials. As shown in Table 14, the average stripping life of the poor materials is substantially lower than that of both of the other two material groups. The only exception to this general trend is MEG1, which has a lower stripping life than a few of the poor and poor-moderate mixtures.

Similar to the traditional results, the TTI analysis is able to distinguish the effect of the anti-strip additive. Considering MEP1 and MEP2, this difference is easily observable as MEP1 had a stripping point occur around 6,000 passes and a stripping life around 16,000 passes where MEP2 had neither of these occur. This difference is also apparent when looking at VTP2 and VTP1 where the mix without an anti-strip additive has stripping points and stripping lives that are a few thousand passes less than the mixture with the anti-strip additive.

Overall, the results from Hamburg testing are very promising considering the main goal of this research. All four of the parameters used in this section show clear distinction between good and poor performing materials, and some are even able to distinguish the poor-moderate materials as well. In addition, both methods are able to identify differences with and without anti-strip additives. Comparing the two analysis methods, it appears that the TTI method shows larger distinctions between the materials in terms of results for the materials used in this study. This can be seen in Table 14 where the difference in average stripping number and stripping life values between poor and good materials is larger compared to the differences in results calculated using traditional analysis.

One of the main advantages of using the Hamburg wheel tracking test, and potentially why it is showing the most promising results for this study, is that it is a simulative test. While other tests focus on use of engineering or fundamental mechanical property, Hamburg is an empirical measure with loading conditions that are simulative of traffic loads on saturated asphalt mixtures. While, from mechanistic analysis perspective this poses a challenge, from the perspective of capturing distress mechanisms that are not currently simulated in mechanistic analyses, such as raveling, the simulative nature of HWT gives it a distinct advantage. The Hamburg test is able to directly simulate the effects of both moisture inundation when the specimens are submerged in heated water as well as the effects of pore pressure damage from the action of the wheel. While the other tests may capture more useful properties from a mechanistic perspective, they are not able to capture these effects as closely to real life as the Hamburg test is able to.

4.7 Ultrasonic Pulse Velocity (UPV)

Results from UPV testing are shown in the following section. UPV is a non-destructive test that was used to approximate the change in modulus due to moisture conditioning from the MiST process. Results presented in this section were measured on the same specimens before and after MiST conditioning. The specimens used to obtain these results were disk shaped specimens similar to those used for ITS and SCB. The results in this section are presented in the same manner as the ITS, SCB, and Hamburg sections.

Figure 50 shows the seismic modulus results from UPV testing where the solid bars represent the modulus before conditioning and the patterned bars represent the modulus after MiST conditioning. As can be seen in the results, all of the materials except for the good Vermont mixture, experience a decrease in stiffness after conditioning. Three factors should also be considered – the effect of moisture, frequency and temperature. The tests on the post-conditioned samples were conducted after ensuring that no moisture was retained in the samples (by drying the samples under room temperature and weighing to a constant weight). Undetected minute traces of moisture in the samples could have affected the test results, particularly if the aggregates are absorptive. In this regard, a rigorous specification of ensuring the adequate drying time of samples with specific type (absorption) of aggregates could be helpful to further increase the accuracy of results from this test. Secondly, the transducers in this study were selected to ensure two full wavelengths, considering the thickness of the available samples. A better approach will be to standardize the thickness of the samples based on an optimum frequency of the transducer. Finally, only one temperature (25°C) was utilized for this test. Tests conducted at multiple temperatures could be more indicative of the change in modulus after the conditioning process.

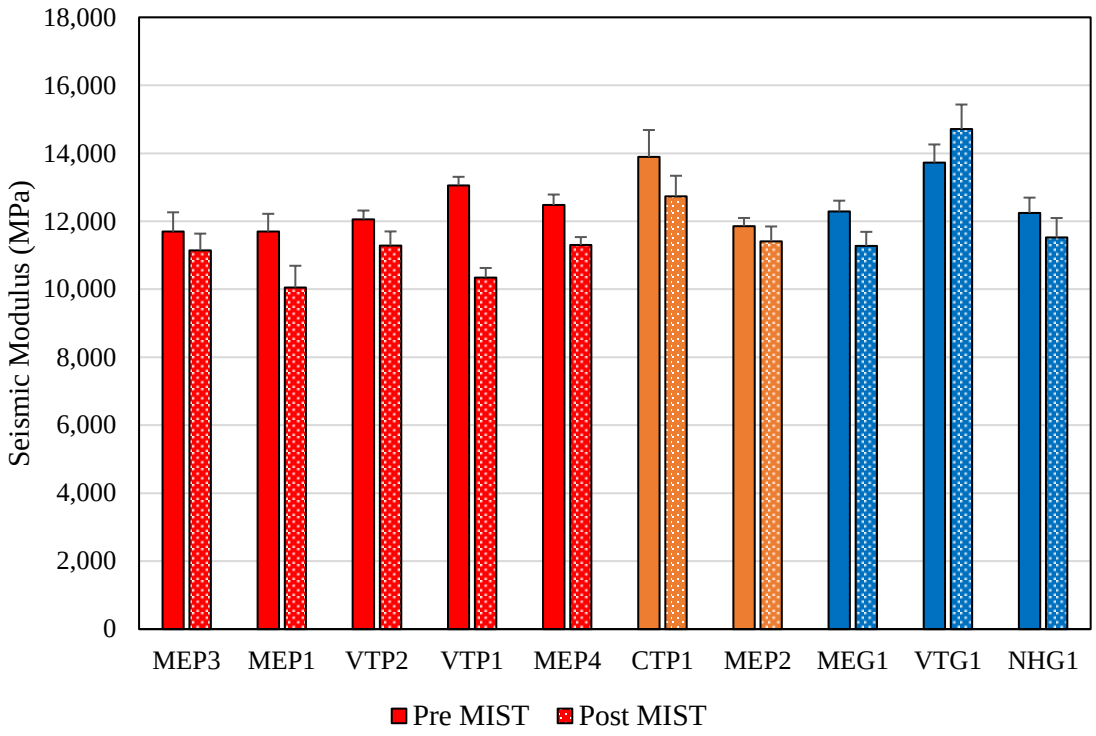

Figure 50: UPV Seismic Modulus Results

When considering the UPVs ability to distinguish good and poor performing mixtures, the results from this project are promising. While the differences seen in Figure 50 are not entirely clear, the ratios tell a different story. Table 15 shows the average seismic modulus ratios of the three material performance groups. When comparing the three material performance groups, it can be seen that there is consistent increase in average UPV ratio from the poor to poor-moderate to good materials of 0.89 to 0.94 to 0.98. While these increases are not statistically significant, they support the expected order of the materials when comparing them to historic field performance. The UPV results suggest that it holds promise as a regular screening tool for moisture susceptible mixes.

Table 15: Average UPV Results

Mix Performance	Average Unconditioned Seismic Modulus (kPa)	Average Conditioned Seismic Modulus (kPa)	Average Seismic Modulus Ratio
Poor	12196	10826	0.89
Poor-Moderate	12875	12071	0.94
Good	12754	12504	0.98

5. Task 4: Final Conclusions and Recommendations

The main goal of this project is to compare a series of asphalt mixture moisture susceptibility test methods in terms of their ability to be a reliable replacement for currently used test methods in the New England region. A number of moisture susceptibility test methods were identified through review of literature. Using methods that have shown promising results in previous studies and experience, a series of historically good and poor performing mixtures from the New England region were evaluated to achieve the project goals. Results were analyzed to determine which tests are able to distinguish historically good and poor performing mixtures on a consistent and reliable basis. The tests methods evaluated in this research included indirect tensile strength paired with modified Lottman and moisture induced stress tester conditioning, dynamic modulus paired with moisture induced stress tester conditioning, disk-shaped compact tension testing paired with a newly developed multi-cycle freeze-thaw conditioning scheme, semi-circular bend test paired with moisture induced stress tester conditioning, the Hamburg wheel tracking test using both traditional and novel analysis methods, and ultrasonic pulse velocity as a non-destructive test. As part of a secondary goal of this research, the previously mentioned methods were also evaluated for their ability to identify and distinguish the performance of mixtures treated with remedial measures to improve moisture resistance. Out of the ten mixtures selected for this research, two sets of identical mixtures were produced with the only variable being the presence of a moisture treatment. Comparing results from these sets of materials provided insight into effectiveness of tests to be able to distinguish the performance differences between mixtures with and without treatments.

Another goal of this project was to quantify the potential effects of moisture-induced damage on pavement performance and service life. This was accomplished using dynamic modulus results of mixtures in both an unconditioned and moisture conditioned state with AASHTO PavementME, a pavement analysis program. Two pavement structures were simulated using PavementME to predict the rutting, fatigue cracking, and international roughness index of the pavements when surfaced with both unconditioned and moisture conditioned materials. These results were compared to each other as well as established failure thresholds for each of the predicted distresses to determine the potential loss of pavement life due to moisture-induced damage on materials with varying levels of moisture susceptibility.

The following section summarizes the main findings, conclusions, and recommendations from this project. These are listed and explained in the following sections.

5.1 Conclusions

On the basis of the findings presented in this report, a number of conclusions can be drawn.

- Indirect tensile strength ratios, regardless of whether modified Lottman or moisture induced stress tester conditioning was used, were unable to distinguish the performance of good and poor performing mixtures. This result is not entirely a surprise as findings similar to this are what led to the research study.

- Indirect tensile strength values were able to distinguish good and poor performing mixtures. The results consistently showed that good materials were stronger in both unconditioned and moisture conditioned states as compared to their poor performing counterparts. While this finding is promising, it should be understood that this trend may be caused by stiffer binder grades in the good performing mixtures.

- Disk-shaped compact tension results did not show significant distinction between the good and poor materials used in this study. Minor differences were seen between the unconditioned and freeze-thaw conditioned specimen fracture energy results. Consequently, the change in performance after conditioning was minimal for both sets of materials. At this point, it is unclear whether this is due to the materials being unaffected by the conditioning scheme or that the low temperature failure mechanism is unable to capture the effects of freeze-thaw damage.

- Results from semi-circular bend testing, whether from fracture energy or flexibility index values, were not able to consistently and clearly differentiate good and poor performing materials. Interestingly and unexpectedly, both fracture energy and flexibility index increased after moisture conditioning, suggesting that the material is becoming more crack resistant after moisture-induced damage. While it is unclear exactly what mechanism is causing this, it appears that the moisture induced stress tester procedure can have a softening effect on materials.

- Results from ultrasonic pulse velocity tests showed consistent, although small differences between good and poor performing materials. When comparing the good and poor performing materials, test results showed that the poor materials consistently experienced a larger percentage in modulus decrease after conditioning when compared to the good materials. Since this is a nondestructive method and the equipment is relatively cheap (~$5K), this test can be used as a screening test during routine mix design. Use of a more appropriate drying time (after conditioning and before conducting the test) can improve the efficiency of this test method.

- Results obtained from dynamic modulus paired with moisture induced stress tester conditioning were promising considering the main goal of this research. The good performing material was clearly and consistently retaining more of its initial stiffness as measured by dynamic modulus compared to both poor performing materials. Similar differences were observed where the poor materials experienced substantially higher increases in phase angle after conditioning as compared to the good material.

- After conditioning, the materials consistently experienced a reduction in modulus and increase in phase angle from dynamic modulus testing. This suggests that the material is behaving in a softer, more viscous manner. This trend indicates that moisture susceptible materials may be particularly prone to rutting problems after being exposed to moisture-induced damage.

- Dynamic modulus results were somewhat able to distinguish the effect of treatments to improve moisture resistance in the materials. Dynamic modulus ratios from two mixtures with and without an anti-strip additive were compared across a wide range of frequencies. While the material with the anti-strip additive consistently retained more of its initial stiffness, the difference was similar to typical test variability. No significant differences were observed between the two mixtures when comparing the increase in phase angle.

- Hamburg wheel tracking test results were very promising considering the main goals of this study. Whether traditional or TTI analysis was used to determine suitable moisture stripping performance parameter, clear and consistent differences were observed between poor and good performing materials. In many cases, the good materials never reached failure during the entire Hamburg test while most, if not all, of the poor materials failed. The average results among the different material groups also support these conclusions. In addition to these observations, Hamburg results were also able to clearly identify the effect of both moisture treatments used in this study. When comparing the two sets of mixtures with and without anti-strip additives, the material with anti-strip additives performed better with respect to every measured result. When comparing traditional and TTI Hamburg analysis, both methods were able to distinguish good and poor materials. In general, the TTI analysis showed larger differences in results (in terms of magnitude) but this difference was not substantial. Both analysis methods can be conducted on the same test results.

- Overall, the results presented in this research suggest that dynamic modulus and the Hamburg wheel tracker hold promise as moisture susceptibility tests during mixture design for agencies in New England. When considering their ability to distinguish the effect of treatments and practical limitations, the Hamburg wheel tracker holds the most promise

out of these three tests. Results from the Hamburg consistently showed the clear distinction between good and poor materials as well as materials with and without moisture treatments. In addition to this, the equipment required to conduct the Hamburg test is cheaper, less complicated to understand and operate, and more readily available for agencies in New England.

- PavementME results emphasized the importance of moisture susceptibility on material selection choices when designing pavements. PavementME results showed that materials with high amounts of moisture susceptibility experienced significantly more reduction in life due to moisture-induced damage compared to good performing materials. In some cases, this reduction in life was more than three times larger than the good materials. These emphasize the importance of using moisture resistant materials in wet weather climates as moisture-induced damage can have a significant impact on the structural integrity and life cycle cost of pavements.

- Results from pavement analysis using PavementME showed that moisture-induced damage can have significant impacts on pavement life. For all three distresses measured, simulations with moisture-conditioned material properties were predicted to have consistently shorter lives. Out of the three distresses, rutting was the most sensitive to moisture-induced damage where some materials could experience a reduction in life of more than 50 percent after moisture conditioning.

5.2 Final Recommendations

On the basis of the testing and analysis performed for this project, several recommendations were developed. These recommendations seek to fulfill the main objective of this study: to recommend an evaluation framework consisting of appropriate test and analysis procedures that is reliable and suitable for moisture susceptibility testing of asphalt mixtures used in New England.

- Considering past experiences and the results presented in this report, it is recommended that New England agencies do not rely on data obtained from indirect tensile strength testing through specifications such as AASHOT T-283. Previous experience in the region has showed that materials which have passed specification requirements for tensile strength ratios have failed on multiple occasions in the field from moisture-induced damage. The results from this project supported these findings showing that tensile strength ratio is not able to identify and distinguish mixtures with known good and poor field performance. The indirect tensile strength procedure is prone to producing false positive results, which can (and has) caused agencies trouble when placing these materials in the field. Considering the results from other tests in this report, the use of indirect tensile strength-based moisture susceptibility tests for routine usage during mixture design is not recommended.

- This project also investigated two fracture mechanics-based test methods for use as moisture susceptibility tests: the disk shaped compact tension test was paired with a multi-cycle freeze-thaw conditioning procedure to capture low temperature thermal cracking performance and the semi-circular bend test was paired with MiST conditioning to capture intermediate temperature fatigue cracking performance. The concept behind using these test methods is that fracture failures are better able to capture the mechanisms behind moisture-induced damage when compared to indirect tensile strength (which includes substantial amounts of compressive and shear damage). However, neither approach was able to consistently distinguish between good and poor performing materials. While it is unclear whether the problem lies with the testing or conditioning for the two procedures used, it is clear that the challenges associated with the results from these fracture tests make them not suitable for recommendation as a routine test method during mix design.

- Dynamic modulus paired with MiST conditioning was identified as a promising procedure due to its ability to clearly distinguish good and poor performing materials and its ability to be used in conjunction with PavementME (and other performance evaluation tools) to predict the potential effects of moisture-induced damage on pavement performance. The dynamic modulus approach to moisture susceptibility testing is recommended if a performance based-design/specification and/or any form of life cycle cost-based design is desired. It should be noted, however, that these predictions are indicative of the potential reduction in performance seen in the field from moisture damage. Due to the nature in

which moisture damage occurs in hot mix asphalt and the limitations associated with pavement performance software such as PavementME, the predictions from pavements performance software should not be taken as absolute. These predictions are better suited to being used as a basis to compare the potential life cycle effects of different materials when significant moisture-induced damage is expected during the life of the pavement.

- The Hamburg wheel tracker was investigated in this project, as it has seen as rise in popularity in usage as a moisture susceptibility test both across the Unites States and within New England. For this study, Hamburg testing was conducted using following procedures used in the New England region and two separate analysis methods were used. The first is the traditional approach of using stripping inflection point to determine moisture susceptibility, while the second is an approach developed at TTI, which uses a two-parameter approach to assess moisture susceptibility. While the details are covered in the results discussion, both of these parameters were able to clearly and consistently distinguish good and poor performing materials. In addition to this, both methods were able to distinguish the effects of remedial additives in the materials, allowing their effects to be quantified. Considering the high quality results from both of the analysis methods as well as the practicality and simplicity of the test, it is recommended that the Hamburg test be pursued and adopted as a moisture susceptibility test for routine usage during mix design in New England. While more testing would need to be conducted to establish reliable thresholds and limits for the Hamburg analysis methods, both analysis methods can reliably screen and distinguish mixtures that would be expected to perform poorly in the field.

- It is recommended that ultrasonic pulse velocity testing be used as a screening test to identify poor performing materials during mix design. Because of the non-destructive and quick nature of the test, implementing the procedure would be relatively simple and straightforward, as no extra materials need to be produced for the test; it can be conducted on specimens prepared for standard moisture susceptibility tests during mix design. A study to develop appropriate drying times before conducting the test could be considered to further improve the accuracy of prediction with this test.

- The use of MiST (ASTM D7870) is recommended as a moisture conditioning procedure on a routine basis during mix design and evaluation. The equipment is relatively cheap (~$10k), has a small footprint, allows simultaneous conditioning of multiple samples, and the process takes a relatively small amount of time (can be completed in one day). The process also allows the users to experiment with pressure, temperature and number of cycles to conduct in-house studies to develop or fine tune the standard process.

6. References

Al-Swailmi, S., and R. L. Terrel. (1994) “Water Sensitivity of Asphalt–Aggregate Mixtures: Test Selection.” SHRP-A-403. Strategic Highway Research Program, National Research Council, Washington, D.C.

Aouad, M. F., Stokoe II, K. H., and Briggs, R. C. (1993) "Stiffness of Asphalt Concrete Surface Layer from Stress Wave Measurements,” Transportation Research Record 1384, Washington, DC, pp. 29-35.

Apeagyei, A., W. Buttlar, and B. Dempsey. (2006) “Moisture Damage Evaluation of Asphalt Mixtures using AASHTO T283 and DC(T) Fracture Test.” Proceedings of the 10th International Conference on Asphalt Pavements, International Society of Asphalt Pavements, ISBN: 978-1-61782-084, pp. 862-873, Red Hook NY.

Apeagyei, A. K., Grenfell, J. R., & Airey, G. D. (2014). “Moisture-induced strength degradation of aggregate–asphalt mastic bonds.” Road Materials and Pavement Design, 15(sup1), 239-262.

Aschenbrener, T. (1995). “Evalulation of Hamburg Wheel-Tracking Device to Predict Moisture Damage in Hot Mix-Asphalt.” Transportation Research Record 1492. Transportation Research Board, National Research Council, Washington, D.C. pp. 193-201.

Azari, H. and Mohseni, A.(2014) “Performance Testing of Asphalt Binder, Mastic and Mixture based on iRLPD Concept” PCCAS Meeting, Reno, NV

Bahia, H., Hanz, A., Kanitpong, K., & Wen, H. (2007).” Test Method to Determine Aggregate/Asphalt Adhesion Properties and Potential Moisture Damage,” Report No. WHRP 07-02, Wisconsin Department of Transportation..

Baker, J. J. (2012). “Cracking performance of asphalt mixtures containing taconite tailings using traditional and multiple freeze-thaw moisture conditioning methods,” Masters dissertation, University of Minnesota Duluth.

Baker, M. R., Crain, K., and Nazarian S., (1995) "Determination of Pavement Thickness with a New Ultrasonic Device," Research Report 1966-1, Center for Geotechnical and Highway

Materials Research, The University of Texas at El Paso, El Paso, TX, 53 p.

Birgisson, B., Roque, R., Tia, M., and Masad, E, (2007) "Development and evaluation of test methods to evaluate water damage and effectiveness of antistripping agents, Final report of UF Project 4910-4504-722-12, University of Florida, Gainesville, FL.

Birgisson, Bjorn, Reynaldo Roque and Gale C. Page. (2003) "Ultrasonic Pulse Wave Velocity Test for Monitoring Changes in Hot-Mix Asphalt Mixture Integrity from Exposure to Moisture." Transportation Research Record 1832, Transportation research Board, Washington DC.

Buchanan, S., Moore, V., Mallick, R. B., O'Brien, Sean and Regimand, Ali. (2004) "Accelerated Moisture Susceptibility Testing of Hot Mix Asphalt (HMA) Mixes." Proceedings of the 83rd Transportation Research Board Annual Meeting, Washington, DC.

Celaya, M., Young, G., and Nazarian, S. (2009) "Portable Seismic Property Analyzer Identification of Asphalt Pavement Layer", Publication No. FHWA-CFL/TD-09-002.

Chen, Xingwei and Huang Baoshan, (2008) "Evaluation of Moisture Damage in Hot Mix Asphalt Using Simple Performance and Superpave Indirect Tensile Tests", Construction and Building Materials, Volume 22, Issue 9, Pages 1950-1962.

Dave, E.V., and J.J. Baker, (2013) "Moisture Damage Evaluation of Asphalt Mixes Containing Mining By-Products: Results from Traditional and Fracture Energy Tests," *Transportation Research Record,* 2371, pp. 113-120.

Dave, E.V. and P. Koktan, (2011) "Synthesis of Performance Testing of Asphalt Concrete," Report No. MnDOT 2011-22. Minnesota Department of Transportation, Research Services Section, 395 John Ireland Boulevard, MS 330, St. Paul, Minnesota 55155.

Dave E.V., and J.J. Baker (2015). "Effects of Multiple Freeze-Thaw Cycling on Low Temperature Cracking Behavior of Asphalt Mixtures," submitted for journal publication.

Epps, J. A., P. E. Sebaaly, J. Penaranda, M. R. Maher, M. B. McCann, and A. J. Hand. (2000) "NCHRP Report 444: Compatibility of a Test for Moisture-Induced Damage with Superpave Volumetric Mix Design." Transportation Research Board, National Research Council, Washington, DC.

Fortin, G. (2010). “Variabilité et fréquence des cycles de gel-dégel dans la région de Québec”, 1977–2006. Le Géographe canadien, 54(2), 196–208. [In French].

Hand, A. J. T., (2015) “Testing for Moisture Damage in the Laboratory” Transportation Research Board Circular, Number E-C198.

Izzo, R., & Tahmoressi, M. (1999). “Use of the Hamburg wheel-tracking device for evaluating moisture susceptibility of hot-mix asphalt.” Transportation Research Record: Journal of the Transportation Research Board, (1681), 76-85.

Jackson, N., & Puccinelli, J. (2006). “Long-Term Pavement Performance (LTPP) Data Analysis Support: National Pooled Fund study TPF-5 (013)-Effects of Multiple Freeze Cycles and Deep Frost Penetration on Pavement Performance and Cost” (No. FHWA-HRT-06-121).

Jacques, C., (2013) “What happens to an asphalt pavement when it gets flooded?”, Final report to Hamel center for undergraduate research (Mentors: J.S. Daniel), University of New Hampshire.

Jailiardo, A., (2003) “Development of Specification Criteria to Mitigate Top-Down Cracking,” Master’s Thesis, University of Florida, Gainesville, FL.

Jimenez R. A. (1974) “Testing for Debonding of Asphalts from Aggregates.” In Transportation Research Record 515, TRB, National Research Council, Washington, DC.

Kandhal, P. S., Buchanan, M. S., Fee, F., & Epps, A. (2000). “Loaded wheel testers in the United States: State of the practice.” Transportation Research Board, National Research Council.

Kennedy, T. W., Roberts, F. L., & Anagnos, J. N. (1984). “Texas boiling test for evaluating moisture susceptibility of asphalt mixtures” (No. FHWA-TX-85-63+ 253-5). Center for Transportation Research, Bureau of Engineering Research, University of Texas at Austin.

Kiggundu B. M. and F. L. Roberts. (September 1988) “Stripping in HMA Mixtures: State-of-the-art and Critical Review of Test Methods.” In NCAT Report No. 88-2, National Center for Asphalt Technology, Auburn University.

Kringos, N., Khedoe, R., Scarpas, A., & de Bondt, A. (2011). A new asphalt concrete moisture susceptibility test methodology. In Transportation Research Board 90th Annual

Meeting (No. 11-0653).

Lamothe, S., Perraton, D., & Di Benedetto, H. (2015). “Contraction and expansion of partially saturated hot mix asphalt samples exposed to freeze–thaw cycles.” Road Materials and Pavement Design, 16(2), 277-299.

Li, Y., and S. Nazarian. (1994) “Evaluation of Aging of Hot Mix Asphalt Using Wave Propagation Techniques.” In STP 1265, ASTM, Philadelphia, PA.

Li, X., M. O. Marasteanu, N. Iverson, and J. F. Labuz. (2006) “Observation of Crack Propagation in Asphalt Mixtures with Acoustic Emission.” Transportation Research Record, No. 1970, Transportation Research Board of the National Academies, Washington, D.C., 2006, pp. 171-177.

Lottman, R.P. (1978) “Predicting Moisture-Induced Damage to Asphaltic Concrete - Field Evaluation.” TRB, NCHRP Report 192.

Mallick, R. B., Gould, J. S., Bhattacharjee, S., Regimand, Ali., James, L. H., and Brown, E. R. (2003) “Development of A Rational Procedure For Evaluation of Moisture Susceptibility of Asphalt Paving Mixes.” Proceedings of the Transportation Research Board 82nd Annual Meeting.

Mallick, R. B., Pelland, Robert and Hugo, Frederick. (2005) “Use of Accelerated Loading Equipment for Determination of Long Term Moisture Susceptibility of Hot Mix Asphalt”, International Journal of Pavement Engineering, Volume 6, Number 2.

Mallick, Rajib B., Das, A. and Nazarian, S. (2005) “Use of a Fast Non Destructive Field Test Method for Determination of Stiffness of Subsurface Layer in Thin Surface Hot Mix Asphalt (HMA)” Pavement. Journal of Transportation Research Board No. 1905, National Research Council, Washington, D.C.

Manning, T., Poudyal, B., and van der Heijden, R. (2014). “Strength of Asphalt over Freeze-Thaw Cycles,” Honors Project (Mentors: J.S. Daniel, C. Jacques), University of New Hampshire.

Martin, A. E. (2014). “Evaluation of the Moisture Susceptibility of WMA Technologies” (Vol. 763). Transportation Research Board.

Moraes, R., Velasquez, R., & Bahia, H. (2011). “Measuring the effect of moisture on asphalt-aggregate bond with the bitumen bond strength test.” Transportation Research Record: Journal of the Transportation Research Board, (2209), 70-81.

Nadkarni, A., Kaloush, K., Zeiada, W., & Biligiri, K. (2009). “Using dynamic modulus test to evaluate moisture susceptibility of asphalt mixtures.”Transportation Research Record: Journal of the Transportation Research Board, (2127), 29-35.

Nazarian, S., Baker, M.R and Crain, K. (1993), Fabrication and Testing of a Seismic Pavement Analyzer. SHRP Report H-375. SHRP National Research Council, Washington, D.C.

Nazarian, S., Deren Yuan, Vivek Tandon, and Miguel Arellano, (2005) “Quality Management of Flexible Pavement Layers with Seismic Methods” The Center for Transportation Infrastructure Systems The University of Texas at El Paso El Paso, TX 79968-0516.

Novak M, B. Birgisson and M. C. McVay. (2002) “Effects of Permeability and Vehicle Speed on Pore Pressure in Hot Mix Asphalt Pavements.” Proceedings of the Transportation Research Board 81st Annual Meeting.

Pinkham, Rudy, Cote, Sarah Ann, Mallick, R. B., Tao, Mingjiang, Bradbury, Richard L., Regimand, Ali. (2013) “Use of Moisture Induced Stress Testing to Evaluate Stripping Potential of Hot Mix Asphalt (HMA).” Proceedings of the 92nd Transportation Research Board (TRB) Annual Meeting.

Poulikakos, L. D., & Partl, M. N. (2009). “Evaluation of moisture susceptibility of porous asphalt concrete using water submersion fatigue tests.” Construction and Building materials, 23(12), 3475-3484.

Rahman, F., & Hossain, M. (2014). “Review and Analysis of Hamburg Wheel Tracking Device Test Data,” No. KS-14-1, Kansas Department of Transportation.

Saeed, A. and Hall, Jr., J. (2002) “Comparison of Non-Destructive Testing Devices to Determine In Situ Properties of Asphalt Concrete Pavement Layers.” Pavement Evaluation Conference, Roanoke, Virginia.

Schram, S., & Williams, R. C. (2012). “Ranking of HMA Moisture Sensitivity Tests in Iowa,” No. RB00-012, Iowa Department of Transporation.

Solaimanian, M., and T. W. Kennedy. (2000). Precision of the Moisture Susceptibility Test Method Tex 531-C. Research Report 4909-1F. Center for Transportation Research, University of Texas at Austin.

Solaimanian, M., Harvey, J., Tahmoressi, M., & Tandon, V. (2003). "Test methods to predict moisture sensitivity of hot-mix asphalt pavements." In Transportation Research Board National Seminar. San Diego, California (pp. 77-110).

Tandon, V. and S. Nazarian. (2001) "Modified Environmental Conditioning System: Validation and Optimization." Research Report TX - 01/1826 - 1F. Center for Highway Materials Research, University of Texas at El Paso.

Tunnicliff, D.G. and R.E. Root. (1984) "Use of Antistripping Additives in Asphaltic Concrete Mixtures." TRB, NCHRP 274.

Wagoner, M. P., W. G. Buttlar, and G. H. Paulino. (2005) "Disk-Shaped Compact Tension Test for Asphalt Concrete Fracture," Experimental Mechanics, Vol. 45, pp. 270-277.

Williams, R. C., & Breakah, T. M. (2010). "Evaluation of Hot Mix Asphalt Moisture Sensitivity Using the Nottingham Asphalt Test Equipment". Institute for Transportation, Iowa State University.

F. Yin, E. Arambula, R. Lytton, Epps Martin, A., Garcia Cucalon, L. Novel Method for Moisture Susceptibility and Rutting Evaluation Using Hamburg Wheel Tracking Test. In *Transportation Research Record 2446*, TRB, National Research Council, Washington, D. C., 2014, pp. 1-7.

Zhang, Z., Roque, R., Birgisson, B., and Sangpetngam, B., (2001) "Identification and Verification of a Suitable Crack Growth Law," Proceedings, AAPT, Vol. 70.

Appendix A: Mix Designs and Volumetrics

The following section contains the mix designs for the ten mixtures used in this study as well as some additional volumetric information.

VERMONT AGENCY OF TRANSPORTATION SP17- 980
HIGHWAY DIVISION - CONSTRUCTION & MATERIALS BUREAU - MATERIALS SECTION
SUPERPAVE BITUMINOUS CONCRETE MIXTURE DESIGN

January 6, 2017

Project Name: MASTER Project Number: N/A
Mix Type: Superpave Type IIIS w/ rap Gyrations, Nini / Ndes / Nmax: 8/80/160

PLANT TYPE: BATCH

Stockpile Gradations - % Passing (WET Sieve Analysis)

Size (mm)	% Used	50.0	37.5	25.0	19.0	12.5	9.5	4.75	2.36	1.18	0.600	0.300	0.150	0.075	RAP % AC	
WSS	19	100	100	100	100	100	100	99	68	30	15	7	3	2.0		
DSS	38	100	100	100	100	100	100	87	54	33	21	11	5	3.5		
9.5	13	100	100	100	100	100	90	5	4	3	2	2	2	1.5		
12.5	15	100	100	100	100	90	20	4	3	2	2	2	2	1.5		
RAP	15	100	100	100	100	100	72	50	41	31	27	22	16	11.0	4.74	
Resultant	**100.0**	**100**	**100**	**100**	**100**	**99**	**83**	**61**	**41**	**24**	**15**	**9**	**5**	**3.8**		3.8

Hot Bin Gradation - % Passing (WET Sieve Analysis)

Bin	% Used	50.0	37.5	25.0	19.0	12.5	9.5	4.75	2.36	1.18	0.600	0.300	0.150	0.075	RAP % AC	
Sand	59.0	100	100	100	100	100	100	90	61	35	21	11	6	4.0		
2	12.0	100	100	100	100	100	93	17	3	2	2	2	2	1.5		
3	14.0	100	100	100	100	100	90	15	5	4	3	2	2	2	1.5	
4																
5																
Mfg. Fines																
RAP	15.0	100	100	100	100	100	72	50	41	31	27	22	16	11.0	4.74	
Resultant	**100.0**	**100**	**100**	**100**	**100**	**99**	**83**	**63**	**43**	**26**	**17**	**10**	**6**	**4.4**		4.4

Design Blend HMA Plant's Fine Adjustment Factor = 0.6

Batch Weight (Kg)	Bin - Sand	Bin No. 2	Bin No. 3	Bin No. 4	Bin No. 5	Bin Mfg. Fines	RAP	Performance Graded Binder Virgin	Performance Graded Binder RAP	Performance Graded Binder Total	Total
	2519	520	629				680	188	32	220	4536

% PG Binder Content		Sieve (mm)	50.0	37.5	25.0	19.0	12.5	9.5	4.75	2.36	1.18	0.600	0.300	0.150	0.075
		Job Mix Formula	100	100	100	100	98	83	63	43	26	17	10	6	4.0
Virgin	Total	Job Aim	100	100	100	100	92	77	57	39	22	13	6	2	3
4.1	4.9	Spec. Limits	100 / 100	100 / 100	100 / 100	100 / 100	90 / 100	— / 90	— / 69	28 / 58	— / 30	— / 21	— / 14	— / 10	2 / 10

Aggregates		Performance Graded Binder		
	PG Grade:	PG 70-28	PG 70-28	PG 70-28
	Other:			
	Manufacturer:	PARCO - ATHENS, NY	GORMAN ASPHALT,	TRISTATE - ALBANY,
	Mixing Temp.:	171 °C ± 11 °C	170 °C ± 11 °C	171 °C ± 11 °C
	Comp. Temp.:	151 °C ± 5 °C	153 °C ± 5 °C	152 °C ± 5 °C

Mixing Times: Dry: 10 Wet: 40 Total: 50
Title: KP
Date: 4/17/17

Job Mix Formula		
VMA	15.5	+/- 1%

FOR STATE OF VERMONT USE ONLY

Comments: THIS DESIGN HAS BEEN APPROVED BASED ON THE SUBMITTED SUPERPAVE TESTS DATA. CONTINUED USE OF THIS DESIGN IS CONTINGENT ON PRODUCT TESTS RESULTS ABLE TO MEET ALL SPECIFICATIONS. IF DURING CONSTRUCTION, THE MIX DISPLAYS UNSATISFACTORY LAY-DOWN CHARACTERISTICS AND/OR UNCOMPACTABILITY, THE DESIGN MAY BE DISCONTINUED.

Signature: 4/28/2017
Title: Bituminous Concrete Engineer or Designee Date:

Date & Time Received Stamped Below

Received
Received
APR 17 2017
VTrans Highway Division
VTrans Highway Division
Materials Lab

This document is intended for receivers use only. If you received this by mistake please delete.

Figure 51: VTG1 Mix Design

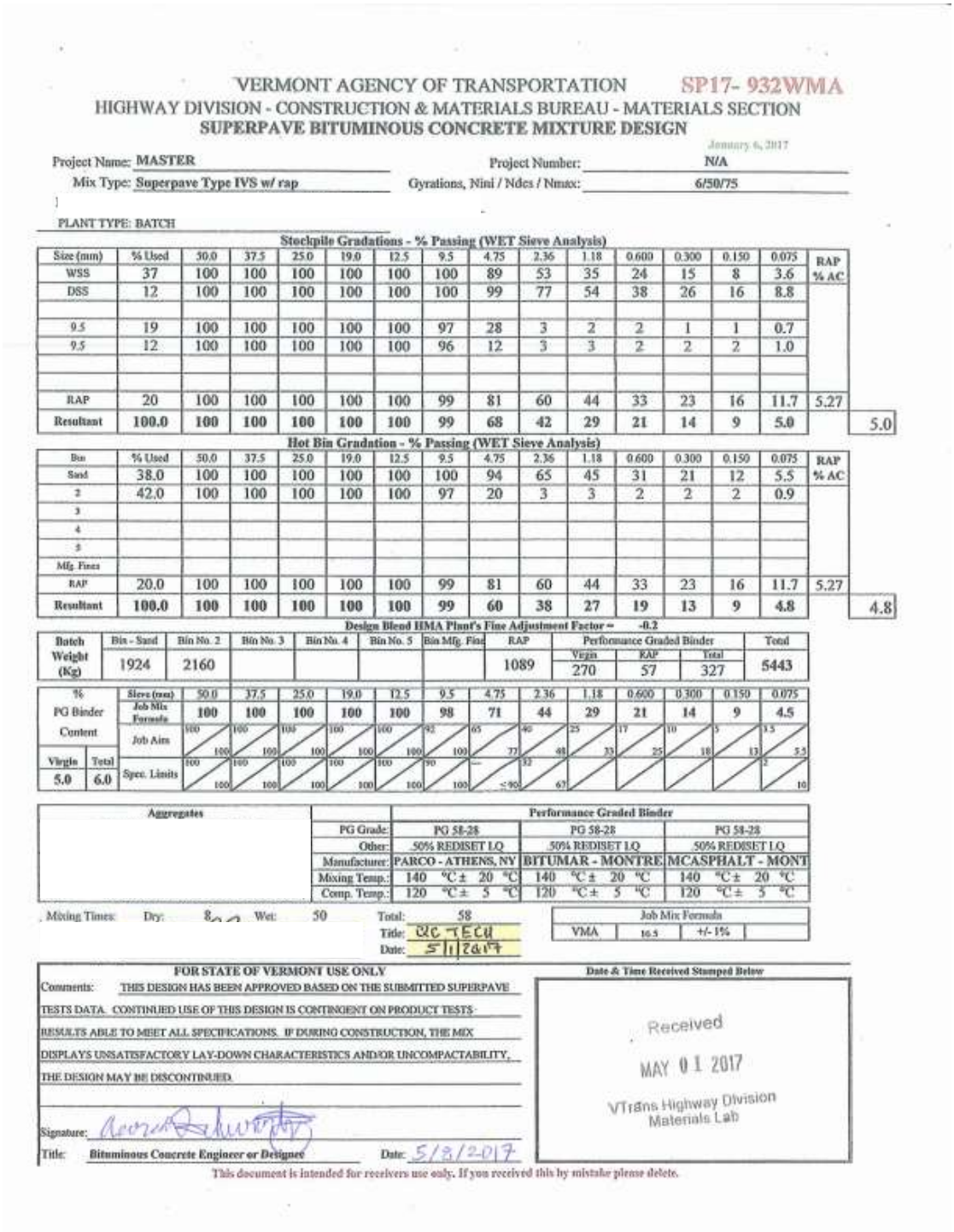

VERMONT AGENCY OF TRANSPORTATION SP17- 932WMA

HIGHWAY DIVISION - CONSTRUCTION & MATERIALS BUREAU - MATERIALS SECTION

SUPERPAVE BITUMINOUS CONCRETE MIXTURE DESIGN

January 6, 2017

Project Name: MASTER Project Number: N/A

Mix Type: Superpave Type IVS w/ rap Gyrations, Nini / Ndes / Nmax: 6/50/75

PLANT TYPE: BATCH

Stockpile Gradations - % Passing (WET Sieve Analysis)

Size (mm)	% Used	50.0	37.5	25.0	19.0	12.5	9.5	4.75	2.36	1.18	0.600	0.300	0.150	0.075	RAP % AC	
WSS	37	100	100	100	100	100	100	89	53	35	24	15	8	3.6		
DSS	12	100	100	100	100	100	100	99	77	54	38	26	16	8.8		
9.5	19	100	100	100	100	100	97	28	3	2	2	1	1	0.7		
9.5	12	100	100	100	100	100	96	12	3	3	2	2	2	1.0		
RAP	20	100	100	100	100	100	99	81	60	44	33	23	16	11.7	5.27	
Resultant	**100.0**	**100**	**100**	**100**	**100**	**100**	**99**	**68**	**42**	**29**	**21**	**14**	**9**	**5.0**		5.0

Hot Bin Gradation - % Passing (WET Sieve Analysis)

Bin	% Used	50.0	37.5	25.0	19.0	12.5	9.5	4.75	2.36	1.18	0.600	0.300	0.150	0.075	RAP % AC	
Sand	38.0	100	100	100	100	100	100	94	65	45	31	21	12	5.5		
2	42.0	100	100	100	100	100	97	20	3	3	2	2	2	0.9		
3																
4																
5																
Mfg. Fines																
RAP	20.0	100	100	100	100	100	99	81	60	44	33	23	16	11.7	5.27	
Resultant	**100.0**	**100**	**100**	**100**	**100**	**100**	**99**	**60**	**38**	**27**	**19**	**13**	**9**	**4.8**		4.8

Design Blend HMA Plant's Fine Adjustment Factor = -0.2

Batch Weight (Kg)	Bin - Sand	Bin No. 2	Bin No. 3	Bin No. 4	Bin No. 5	Bin Mfg. Fine	RAP	Performance Graded Binder			Total
								Virgin	RAP	Total	
	1924	2160					1089	270	57	327	5443

% PG Binder Content		Sieve (mm)	50.0	37.5	25.0	19.0	12.5	9.5	4.75	2.36	1.18	0.600	0.300	0.150	0.075
		Job Mix Formula	100	100	100	100	100	98	71	44	29	21	14	9	4.5
		Job Min	100	100	100	100	100	92	65	40	25	17	10	5	3.5
		Job Max	100	100	100	100	100	104	77	48	33	25	18	13	5.5
Virgin	Total	Spec. Limits	100	100	100	100	100	90	—	32					2
5.0	6.0		100	100	100	100	100	100	≤ 90	67					10

Aggregates		Performance Graded Binder		
	PG Grade:	PG 58-28	PG 58-28	PG 58-28
	Other:	50% REDISET LQ	50% REDISET LQ	50% REDISET LQ
	Manufacturer:	PARCO - ATHENS, NY	BITUMAR - MONTRE	MCASPHALT - MONT
	Mixing Temp.:	140 °C ± 20 °C	140 °C ± 20 °C	140 °C ± 20 °C
	Comp. Temp.:	120 °C ± 5 °C	120 °C ± 5 °C	120 °C ± 5 °C

Mixing Times: Dry: 80 Wet: 50 Total: 58

Title: QC TECH

Date: 5/1/2017

Job Mix Formula			
VMA	16.5	+/- 1%	

FOR STATE OF VERMONT USE ONLY

Comments: THIS DESIGN HAS BEEN APPROVED BASED ON THE SUBMITTED SUPERPAVE TESTS DATA. CONTINUED USE OF THIS DESIGN IS CONTINGENT ON PRODUCT TESTS RESULTS ABLE TO MEET ALL SPECIFICATIONS. IF DURING CONSTRUCTION, THE MIX DISPLAYS UNSATISFACTORY LAY-DOWN CHARACTERISTICS AND/OR UNCOMPACTABILITY, THE DESIGN MAY BE DISCONTINUED.

Signature:

Title: Bituminous Concrete Engineer or Designee Date: 5/8/2017

Date & Time Received Stamped Below

Received

MAY 01 2017

VTrans Highway Division
Materials Lab

This document is intended for receivers use only. If you received this by mistake please delete.

Figure 52: VTP1 Mix Design

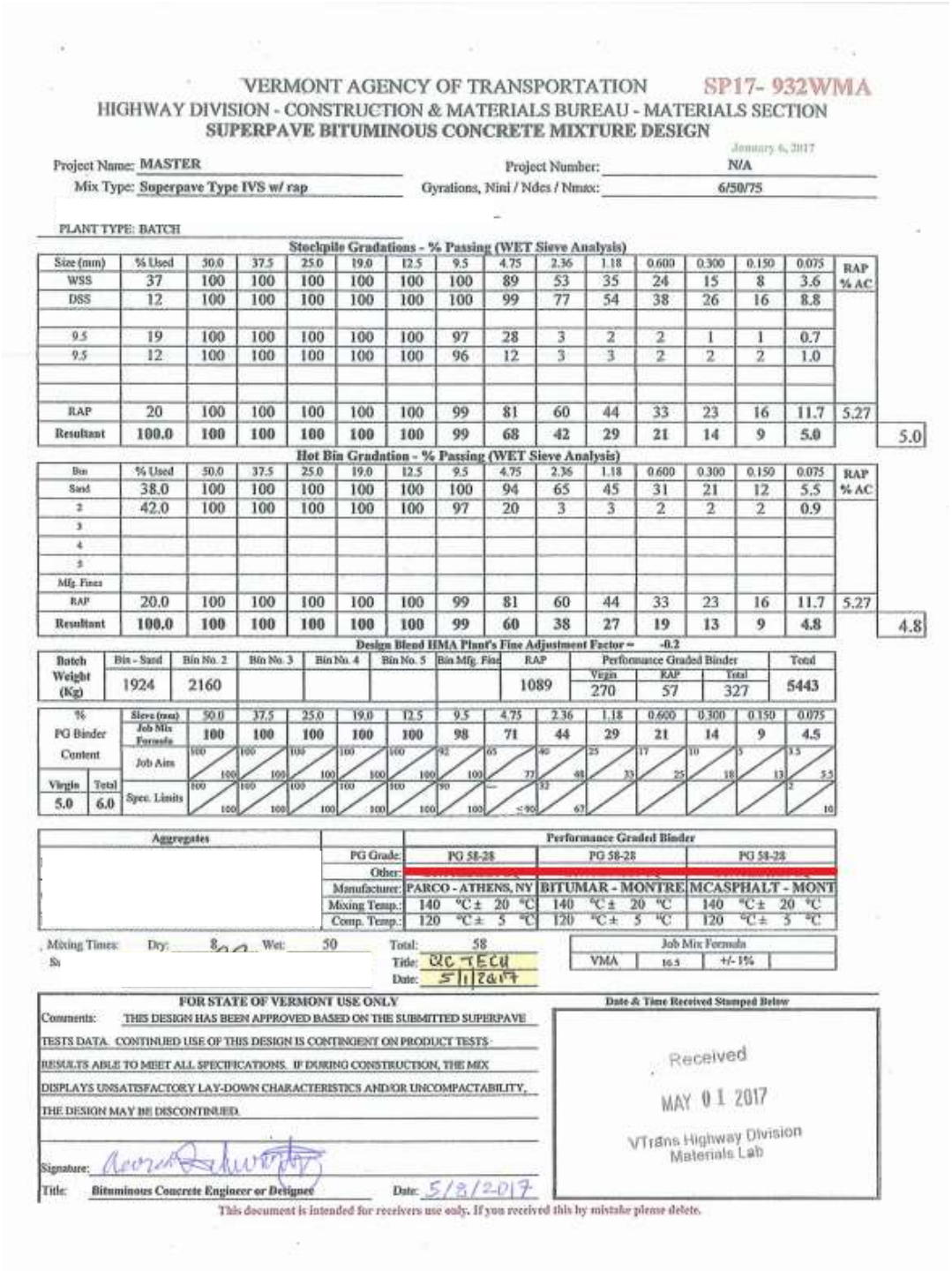

VERMONT AGENCY OF TRANSPORTATION SP17- 932WMA

HIGHWAY DIVISION - CONSTRUCTION & MATERIALS BUREAU - MATERIALS SECTION

SUPERPAVE BITUMINOUS CONCRETE MIXTURE DESIGN

January 6, 2017

Project Name: MASTER Project Number: N/A

Mix Type: Superpave Type IVS w/ rap Gyrations, Nini / Ndes / Nmax: 6/50/75

PLANT TYPE: BATCH

Stockpile Gradations - % Passing (WET Sieve Analysis)

Size (mm)	% Used	50.0	37.5	25.0	19.0	12.5	9.5	4.75	2.36	1.18	0.600	0.300	0.150	0.075	RAP % AC	
WSS	37	100	100	100	100	100	100	89	53	35	24	15	8	3.6		
DSS	12	100	100	100	100	100	100	99	77	54	38	26	16	8.8		
9.5	19	100	100	100	100	100	97	28	3	2	2	1	1	0.7		
9.5	12	100	100	100	100	100	96	12	3	3	2	2	2	1.0		
RAP	20	100	100	100	100	100	99	81	60	44	33	23	16	11.7	5.27	
Resultant	**100.0**	**100**	**100**	**100**	**100**	**100**	**99**	**68**	**42**	**29**	**21**	**14**	**9**	**5.0**		5.0

Hot Bin Gradation - % Passing (WET Sieve Analysis)

Bin	% Used	50.0	37.5	25.0	19.0	12.5	9.5	4.75	2.36	1.18	0.600	0.300	0.150	0.075	RAP % AC	
Sand	38.0	100	100	100	100	100	100	94	65	45	31	21	12	5.5		
2	42.0	100	100	100	100	100	97	20	3	3	2	2	2	0.9		
3																
4																
5																
Mfg. Fines																
RAP	20.0	100	100	100	100	100	99	81	60	44	33	23	16	11.7	5.27	
Resultant	**100.0**	**100**	**100**	**100**	**100**	**100**	**99**	**60**	**38**	**27**	**19**	**13**	**9**	**4.8**		4.8

Design Blend HMA Plant's Fine Adjustment Factor = -0.2

Batch Weight (Kg)	Bin - Sand	Bin No. 2	Bin No. 3	Bin No. 4	Bin No. 5	Bin Mfg. Fine	RAP	Performance Graded Binder Virgin	Performance Graded Binder RAP	Performance Graded Binder Total	Total
	1924	2160					1089	270	57	327	5443

% PG Binder Content		Sieve (mm)	50.0	37.5	25.0	19.0	12.5	9.5	4.75	2.36	1.18	0.600	0.300	0.150	0.075
		Job Mix Formula	100	100	100	100	100	98	71	44	29	21	14	9	4.5
		Job Mix Aim	100 / 100	100 / 100	100 / 100	100 / 100	100 / 100	92 / 100	65 / 77	40 / 48	25 / 33	17 / 25	10 / 18	5 / 13	3.5 / 5.5
Virgin	Total	Spec. Limits	100 / 100	100 / 100	100 / 100	100 / 100	100 / 100	90 / 100	— / ≤90	32 / 67					2 / 10
5.0	6.0														

Aggregates		Performance Graded Binder		
	PG Grade:	PG 58-28	PG 58-28	PG 58-28
	Other:			
	Manufacturer:	PARCO - ATHENS, NY	BITUMAR - MONTRE.	MCASPHALT - MONT
	Mixing Temp.:	140 °C ± 20 °C	140 °C ± 20 °C	140 °C ± 20 °C
	Comp. Temp.:	120 °C ± 5 °C	120 °C ± 5 °C	120 °C ± 5 °C

Mixing Times: Dry: 8:00 Wet: 50 Total: 58

Si

Title: QC TECH

Date: 5/1/2017

Job Mix Formula			
VMA	16.5	+/- 1%	

FOR STATE OF VERMONT USE ONLY

Comments: THIS DESIGN HAS BEEN APPROVED BASED ON THE SUBMITTED SUPERPAVE TESTS DATA. CONTINUED USE OF THIS DESIGN IS CONTINGENT ON PRODUCT TESTS RESULTS ABLE TO MEET ALL SPECIFICATIONS. IF DURING CONSTRUCTION, THE MIX DISPLAYS UNSATISFACTORY LAY-DOWN CHARACTERISTICS AND/OR UNCOMPACTABILITY, THE DESIGN MAY BE DISCONTINUED.

Signature:

Title: Bituminous Concrete Engineer or Designee Date: 5/8/2017

Date & Time Received Stamped Below

Received

MAY 01 2017

VTrans Highway Division
Materials Lab

This document is intended for receivers use only. If you received this by mistake please delete.

Figure 53: VTP2 Mix Design

12 Desert Rd, Freeport MaineDOT TESTING LABORATORIES 219 Hogan Rd, Bangor

MaineDOT

ASPHALT MIX DESIGN
BASE JMN: PII-WE17-50B-12R

Mix Grading	Submittal	Submitted By
HMA MIX-12.5MM (FINE-GRADED WITH 20% RAP)	2/27/2017	

Plant	Plant No.	Make	Size	Type
			5 TON	BATCH

Approved MaineDOT Job Mix No.'s	Binder	1st Item No.	2nd Item No.	3rd Item No.	4th Item No.	5th Item No.
PII-WE17-50B-12R-64	PG64-28	403.208	403.213			

ARGG = Asphalt Rubber Gap-Graded; C = Colored; SB = Hot Stabilized Asphalt Base; L = Liquid Latex Modified or Hydrated Lime; MTA = Maine Turnpike Authority; P = Polymer Modified; RB = Rich Base; WMA = Warm Mix Asphalt

Binder	Binder Supplier	WMA Additive	%	Temperature, °F	Start Date
PG64-28					2/7/2017

Current Superpave Design Data									
Gyrations	ESAL's	Nominal Size	Gmm	Gsb	% Binder	New % Binder	Fbe Ratio	Gmb, weight, g	Verif. Ref No
50 GYRATIONS	3 to <10	12.5mm	2.460	2.67	5.8	4.9	0.8	4750	247559

Current Gradation Aims (Percentages Passing Sieve Sizes)												
	1 in. 25.0 mm	¾ in. 19.0 mm	½ in. 12.5 mm	⅜ in. 9.5 mm	1/4 in. 6.3 mm	No. 4 4.75 mm	No. 8 2.36 mm	No. 16 1.18 mm	No. 30 0.600 mm	No. 50 0.300 mm	No. 100 0.150 mm	No. 200 0.075 mm
Aim		100	99	86		58	43	32	21	12	7	4.5
Lower		100	92	79		51	39	28	18	10	5	2.5
Upper		100	100	90		65	47	36	24	14	9	6.0
Spec.		100	90 - 100	- 90			28 - 58					2 - 6

Aggregate Data			RAP Pile Replaced
%	Size	Original Source/Owner	
22	12.5MM LEDGE		
21	9.5MM LEDGE		
11	WASHED STONE SCREENINGS		
9	DRY STONE SCREENINGS		
17	SAND		
20	RAP		

Comments

Authorized by: DEREK NENER-PLANTE Initial Approved Date: 5/5/2017

Paper Copy: Lab File Electronic: Area Supervisor; Resident; Contractor

12 Desert Rd, Freeport MaineDOT TESTING LABORATORIES 219 Hogan Rd, Bangor

Page 1 of 2

Figure 54: MEG1 Mix Design (Page 1 of 2)

MaineDOT

Base JMN	Consensus Ref No	Oven Ref No	Specification Date
PII-WE17-50B-12R	17AGG3	17002	01/01/17

Design Criteria

Start Date	End Date	Specification Date	Resubmittal Date	Change Type	Verification Ref No	Total AC Aim, %	Virgin AC Aim, %	Fbe Ratio	Gmm	State Gsb	Contr Gsb
2/7/2017		01/01/17		Initial Design	247559	5.8	4.9	0.8	2.460	2.67	2.67

Gradation Aims (Percentages Passing Sieve Sizes)

Start Date	1 in. 25.0 mm	¾ in. 19.0 mm	½ in. 12.5 mm	⅜ in. 9.5 mm	1/4 in. 6.3 mm	No. 4 4.75 mm	No. 8 2.36 mm	No. 16 1.18 mm	No. 30 0.600 mm	No. 50 0.300 mm	No. 100 0.150 mm	No. 200 0.075 mm
2/7/2017		100	99	86		58	43	32	21	12	7	4.5

Additional Additives

Start Date	Antistrip Additive	Antistrip, %	Antistrip Supplier	Other Additive	Other, %	Other Supplier
2/7/2017						

Aggregate Quality Tests	Original	Retest 1	Retest 2	Results to Use	Specification	Meets?
Fractured, 1 Face (ASTM D 5821), %	99			99	85%, min.	YES
Fractured, 2 Face (ASTM D 5821), %	99			99	80%, min.	
F.A. Angularity (T 304, Method A)	46			46	45, min.	YES
Flat & Elongated Part. (ASTM D 4791), %	0			0	10%, max.	YES
Sand Equivalent (T 176)	84			84	45, min.	YES
Coarse Micro-Deval (T 327), %	7.2			7.2		YES
Method B Machine Used	MD3				Passing No. 16, %	7.3
Control Agg., Current Result, %	20.6				Weighted Avg Loss, %	11.80
Control Agg., Avg. of Last 20 Results, %	20.4				Area Btwn Curves, %-mm	105.68
Fine Micro-Deval (ASTM D7428), %	8.0			8.0		N/A
Machine Used	MD2				Passing No. 200, %	9.8
Control Agg., Current Result, %	18.6				Weighted Avg Loss, %	12.16
Control Agg., Avg. of Last 20 Results, %	18.9				Area Btwn Curves, %-mm	20.19
Los Angeles Wear (T 96), %						
					Passing No. 12, %	
					Weighted Avg Loss, %	
					Area Btwn Curves, %-mm	
Washington Degradation (MeDOT)					30, min.	
Combined Aggregate, Gsb (PP 28)					±0.02	
Fine Aggregate Specific Gravity (T 84)	2.65			2.65		
Fine Aggregate Absorption (T 84), %	0.5			0.5		N/A
Coarse Aggregate Specific Gravity (T 85)						
Coarse Aggregate Absorption (T 85), %						
Avg. Draindown at °F, % (Anticipated Plant Production)						
Avg. Draindown at °F, %						

Page 2 of 2

Figure 55: MEG1 Mix Design (Page 2 of 2)

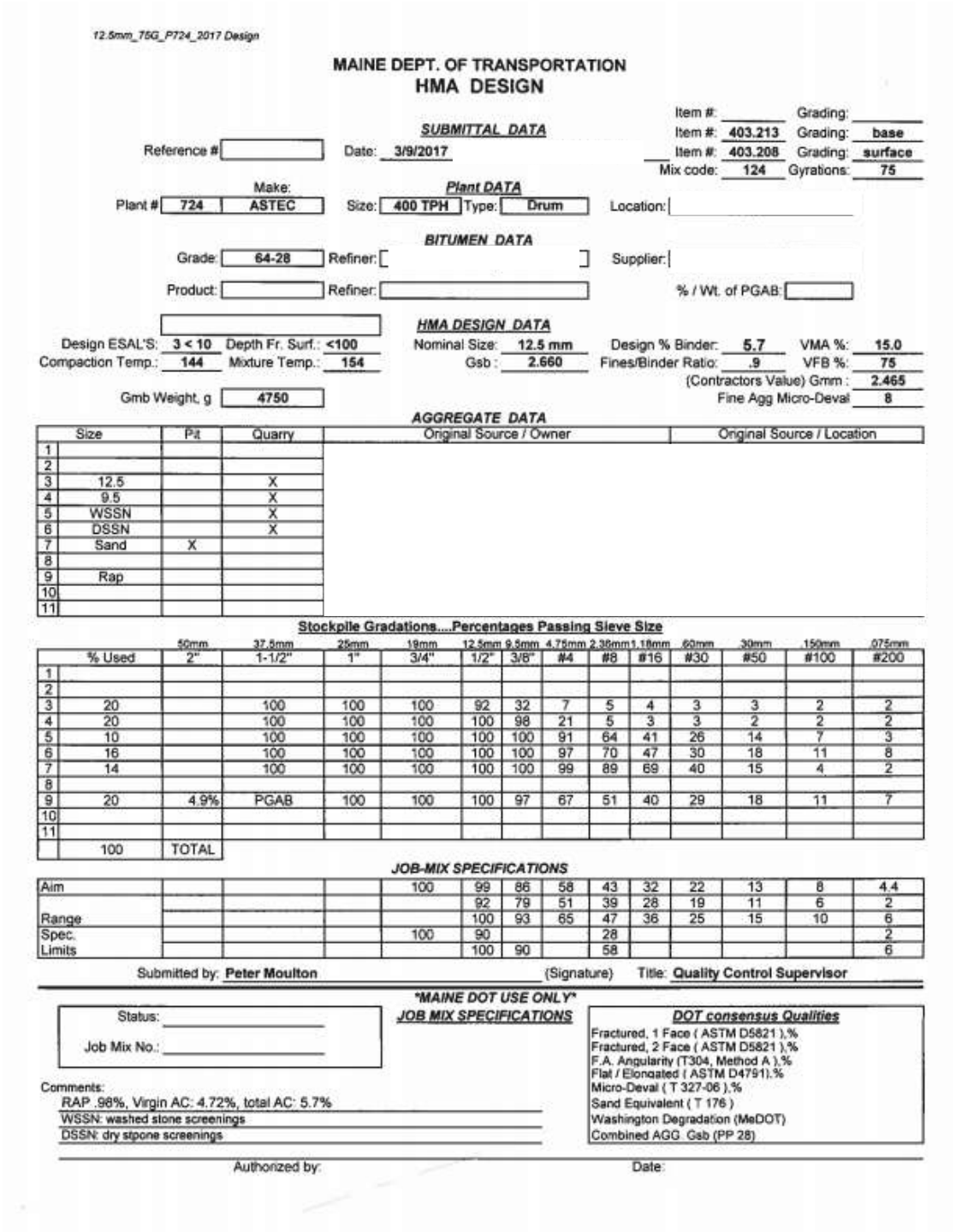

12.5mm_75G_P724_2017 Design

MAINE DEPT. OF TRANSPORTATION
HMA DESIGN

SUBMITTAL DATA

Reference #: Date: 3/9/2017

Item #: Grading:
Item #: 403.213 Grading: base
Item #: 403.208 Grading: surface
Mix code: 124 Gyrations: 75

Plant DATA

Plant #: 724 Make: ASTEC Size: 400 TPH Type: Drum Location:

BITUMEN DATA

Grade: 64-28 Refiner: Supplier:

Product: Refiner: % / Wt. of PGAB:

HMA DESIGN DATA

Design ESAL'S: 3 < 10 Depth Fr. Surf.: <100
Compaction Temp.: 144 Mixture Temp.: 154
Gmb Weight, g: 4750

Nominal Size: 12.5 mm Design % Binder: 5.7 VMA %: 15.0
Gsb: 2.660 Fines/Binder Ratio: .9 VFB %: 75
(Contractors Value) Gmm: 2.465
Fine Agg Micro-Deval: 8

AGGREGATE DATA

	Size	Pit	Quarry	Original Source / Owner	Original Source / Location
1					
2					
3	12.5		X		
4	9.5		X		
5	WSSN		X		
6	DSSN		X		
7	Sand	X			
8					
9	Rap				
10					
11					

Stockpile Gradations....Percentages Passing Sieve Size

	% Used	50mm 2"	37.5mm 1-1/2"	25mm 1"	19mm 3/4"	12.5mm 1/2"	9.5mm 3/8"	4.75mm #4	2.36mm #8	1.18mm #16	.60mm #30	.30mm #50	.150mm #100	.075mm #200
1														
2														
3	20		100	100	100	92	32	7	5	4	3	3	2	2
4	20		100	100	100	100	98	21	5	3	3	2	2	2
5	10		100	100	100	100	100	91	64	41	26	14	7	3
6	16		100	100	100	100	100	97	70	47	30	18	11	8
7	14		100	100	100	100	100	99	89	69	40	15	4	2
8														
9	20	4.9%	PGAB	100	100	100	97	67	51	40	29	18	11	7
10														
11														
	100	TOTAL												

JOB-MIX SPECIFICATIONS

Aim					100	99	86	58	43	32	22	13	8	4.4
						92	79	51	39	28	19	11	6	2
Range						100	93	65	47	36	25	15	10	6
Spec.					100	90			28					2
Limits						100	90		58					6

Submitted by: Peter Moulton (Signature) Title: Quality Control Supervisor

MAINE DOT USE ONLY

Status:
Job Mix No.:

JOB MIX SPECIFICATIONS

DOT consensus Qualities

Fractured, 1 Face (ASTM D5821),%
Fractured, 2 Face (ASTM D5821),%
F.A. Angularity (T304, Method A),%
Flat / Elongated (ASTM D4791),%
Micro-Deval (T 327-06),%
Sand Equivalent (T 176)
Washington Degradation (MeDOT)
Combined AGG. Gsb (PP 28)

Comments:
RAP .98%, Virgin AC: 4.72%, total AC: 5.7%
WSSN: washed stone screenings
DSSN: dry stpone screenings

Authorized by: Date:

Figure 56: MEP3 Mix Design

12 Desert Rd, Freeport MaineDOT TESTING LABORATORIES 219 Hogan Rd, Bangor

MaineDOT

ASPHALT MIX DESIGN
BASE JMN: LAN-HE15-50B-12R-V1

Mix Grading	Submittal	Submitted By
HMA MIX-12.5MM (FINE-GRADED WITH 20% RAP)	4/15/2015	

Plant	Plant No.	Make	Size	Type
			7 TON	BATCH

Approved MaineDOT Job Mix No.'s	Binder	1st Item No.	2nd Item No.	3rd Item No.	4th Item No.	5th Item No.
LAN-HE15-50B-12R-V1-58	PG58-28	403.208	403.213			
LAN-HE15-50B-12R-V1-64	PG64-28	403.208	403.213			
LAN-HE15-50B-12R-V1-64E	PG64E-28	403.2081	403.2131			

ARGG = Asphalt Rubber Gap-Graded; C = Colored; SB = Hot Stabilized Asphalt Base; L = Liquid Latex Modified or Hydrated Lime; MTA = Maine Turnpike Authority; P = Polymer Modified; RB = Rich Base; WMA = Warm Mix Asphalt

Binder	Binder Supplier	WMA Additive	%	Temperature, °F	Start Date
PG58-28					7/9/2015
PG64E-28					4/15/2015
PG64-28					10/22/2015

Current Superpave Design Data									
Gyrations	ESAL's	Nominal Size	Gmm	Gsb	% Binder	New % Binder	Fbe Ratio	Gmb, weight, g	Verif. Ref No
50 GYRATIONS	3 to <10	12.5mm	2.475	2.67	5.6	4.6	1.0	4750	

Current Gradation Aims (Percentages Passing Sieve Sizes)												
	1 in. 25.0 mm	¾ in. 19.0 mm	½ in. 12.5 mm	⅜ in. 9.5 mm	1/4 in. 6.3 mm	No. 4 4.75 mm	No. 8 2.36 mm	No. 16 1.18 mm	No. 30 0.600 mm	No. 50 0.300 mm	No. 100 0.150 mm	No. 200 0.075 mm
		100	99	85		57	39	26	17	11	7	5
Lower		100	92	78		50	35	22	14	9	5	3.0
Upper		100	100	90		64	43	30	20	13	9	6.0
Spec.		100	90 - 100	- 90			28 - 58					2 - 6

Aggregate Data			RAP Pile Replaced
%	Size	Original Source/Owner	
20	12.5MM LEDGE		
15	9.5MM LEDGE		
10	CRUSHER DUST		
20	NATURAL SAND		
15	WASHED LEDGE SAND LEDGE		
20	RAP		

Comments
1/4" MINUS renamed to CRUSHER DUST; SAND changed to NATURAL SAND

Authorized by: DEREK NENER-PLANTE Initial Approved Date: 5/20/2015 Reissued Date: 2/17/2017

Paper Copy: Lab File Electronic: Area Supervisor; Resident; Contractor

Page 1 of 2

Figure 57: MEP4 Mix Design (Page 1 of 2)

12 Desert Rd, Freeport MaineDOT TESTING LABORATORIES 219 Hogan Rd, Bangor

MaineDOT

Base JMN	Consensus Ref No	Oven Ref No	Specification Date
LAN-HE15-50B-12R-V1	15015	15015	01/15/16

Design Criteria

Start Date	End Date	Specification Date	Resubmittal Date	Change Type	Verification Ref No	Total AC Aim, %	Virgin AC Aim, %	Fbe Ratio	Gmm	State Gsb	Contr. Gsb
4/15/2015	2/17/2017	01/15/16		Initial Design		5.6	4.6	1.0	2.475	2.66	2.68
2/18/2017		01/15/16		RAP Change		5.6	4.6	1.0	2.475	2.67	2.68

2017 Carryover

Gradation Aims (Percentages Passing Sieve Sizes)

Start Date	1 in. 25.0 mm	¾ in. 19.0 mm	½ in. 12.5 mm	⅜ in. 9.5 mm	1/4 in. 6.3 mm	No. 4 4.75 mm	No. 8 2.36 mm	No. 16 1.18 mm	No. 30 0.600 mm	No. 50 0.300 mm	No. 100 0.150 mm	No. 200 0.075 mm
4/15/2015		100	99	85		57	39	26	17	11	7	5
2/18/2017		100	99	85		57	39	26	17	11	7	5

Additional Additives

Start Date	Antistrip Additive	Antistrip, %	Antistrip Supplier	Other Additive	Other, %	Other Supplier
4/15/2015						
2/18/2017						

Aggregate Quality Tests	Original	Retest 1	Retest 2	Results to Use	Specification	Meets?
Fractured, 1 Face (ASTM D 5821), %	97			97	85%, min.	YES
Fractured, 2 Face (ASTM D 5821), %	96			96	80%, min.	
F.A. Angularity (T 304, Method A)	48			48	45, min.	YES
Flat & Elongated Part. (ASTM D 4791), %	1			1	10%, max.	YES
Sand Equivalent (T 176)	77			77	45, min.	YES
Coarse Micro-Deval (T 327), %	16.0			16.0	18.0%, max.	YES
Method B / Machine Used	MD3			Passing No. 16, %		
Control Agg., Current Result, %	19.8			Weighted Avg Loss, %		
Control Agg., Avg. of Last 20 Results, %	20.4			Area Btwn Curves, %-mm		
Fine Micro-Deval (ASTM D7428), %	15.0			15.0		N/A
Machine Used	MD2			Passing No. 200, %		16.1
Control Agg., Current Result, %	18.1			Weighted Avg Loss, %		14.02
Control Agg., Avg. of Last 20 Results, %	18.0			Area Btwn Curves, %-mm		21.44
Los Angeles Wear (T 96), %						
				Passing No. 12, %		
				Weighted Avg Loss, %		
				Area Btwn Curves, %-mm		
Washington Degradation (MeDOT)					30, min	
Combined Aggregate, Gsb (PP 28)	2.66				2.67 ±0.02	YES
Fine Aggregate Specific Gravity (T 84)	2.68			2.68		
Fine Aggregate Absorption (T 84), %	0.4			0.4		N/A
Coarse Aggregate Specific Gravity (T 85)						
Coarse Aggregate Absorption (T 85), %						
Avg. Draindown at °F, % (Anticipated Plant Production)						
Avg. Draindown at °F, %						

Page 2 of 2

Figure 58: MEP4 Mix Design (Page 2 of 2)

12 Desert Rd, Freeport MaineDOT TESTING LABORATORIES 219 Hogan Rd, Bangor

MaineDOT

ASPHALT MIX DESIGN
BASE JMN: LAN-PI17-50B-12CR

Mix Grading	Submittal	Submitted By
HMA MIX-12.5MM (FINE-GRADED WITH 10% RAP)	4/26/2017	

Plant	Plant No.	Make	Size	Type
			3 TON	BATCH

Approved MaineDOT Job Mix No.'s	Binder	1st Item No.	2nd Item No.	3rd Item No.	4th Item No.	5th Item No.
LAN-PI17-50B-12CR-58	PG58-28	403.208	403.213			
LAN-PI17-50B-12CR-64	PG64-28	403.208	403.213			
LAN-PI17-50B-12CR-64E	PG64E-28	403.2081	403.2131			
LAN-PI17-50B-12CR-AS64	PG64-28	403.208	403.213			

ARGG = Asphalt Rubber Gap-Graded; C = Colored; SB = Hot Stabilized Asphalt Base; L = Liquid Latex Modified or Hydrated Lime; MTA = Maine Turnpike Authority; P = Polymer Modified; RB = Rich Base; WMA = Warm Mix Asphalt; AS = Anti-strip

Binder	Binder Supplier	WMA Additive	%	Temperature, °F	Start Date
PG58-28					4/26/2017
PG64E-28					4/26/2017
PG64-28					6/14/2017

Current Superpave Design Data									
Gyrations	ESAL's	Nominal Size	Gmm	Gsb	% Binder	New % Binder	Fbe Ratio	Gmb, weight, g	Verif. Ref No
50 GYRATIONS	3 to <10	12.5mm	2.485	2.71	5.9	5.4	0.9	4750	

Current Gradation Aims (Percentages Passing Sieve Sizes)												
	1 in. 25.0 mm	¾ in. 19.0 mm	½ in. 12.5 mm	⅜ in. 9.5 mm	1/4 in. 6.3 mm	No. 4 4.75 mm	No. 8 2.36 mm	No. 16 1.18 mm	No. 30 0.600 mm	No. 50 0.300 mm	No. 100 0.150 mm	No. 200 0.075 mm
Aim		100	93	82		58	39	25	16	10	7	5.1
Lower		100	90	75		51	35	21	13	8	5	3.1
Upper		100	100	89		65	43	29	19	12	9	6.0
Spec		100	90 - 100	- 90			28 - 58					2 - 6

Aggregate Data			RAP Pile Replaced
%	Size	Original Source/Owner	
15	NATURAL SAND		
20	WASHED LEDGE SAND LEDGE		
15	CRUSHER DUST		
25	12.5MM LEDGE		
15	19.0MM LEDGE		
10	RAP		

Mix temp 155

Comp temp 145

Comments
Mix design meeets maximum Fine Micro-Deval loss of 14.0% for projects that require it by special provision.

Authorized by: DEREK NENER-PLANTE Initial Approved Date: 6/8/2017 Reissued Date: 6/28/2017

Paper Copy: Lab File Electronic: Area Supervisor; Resident; Contractor

Page 1 of 2

Figure 59: MEP1 Mix Design (Page 1 of 2)

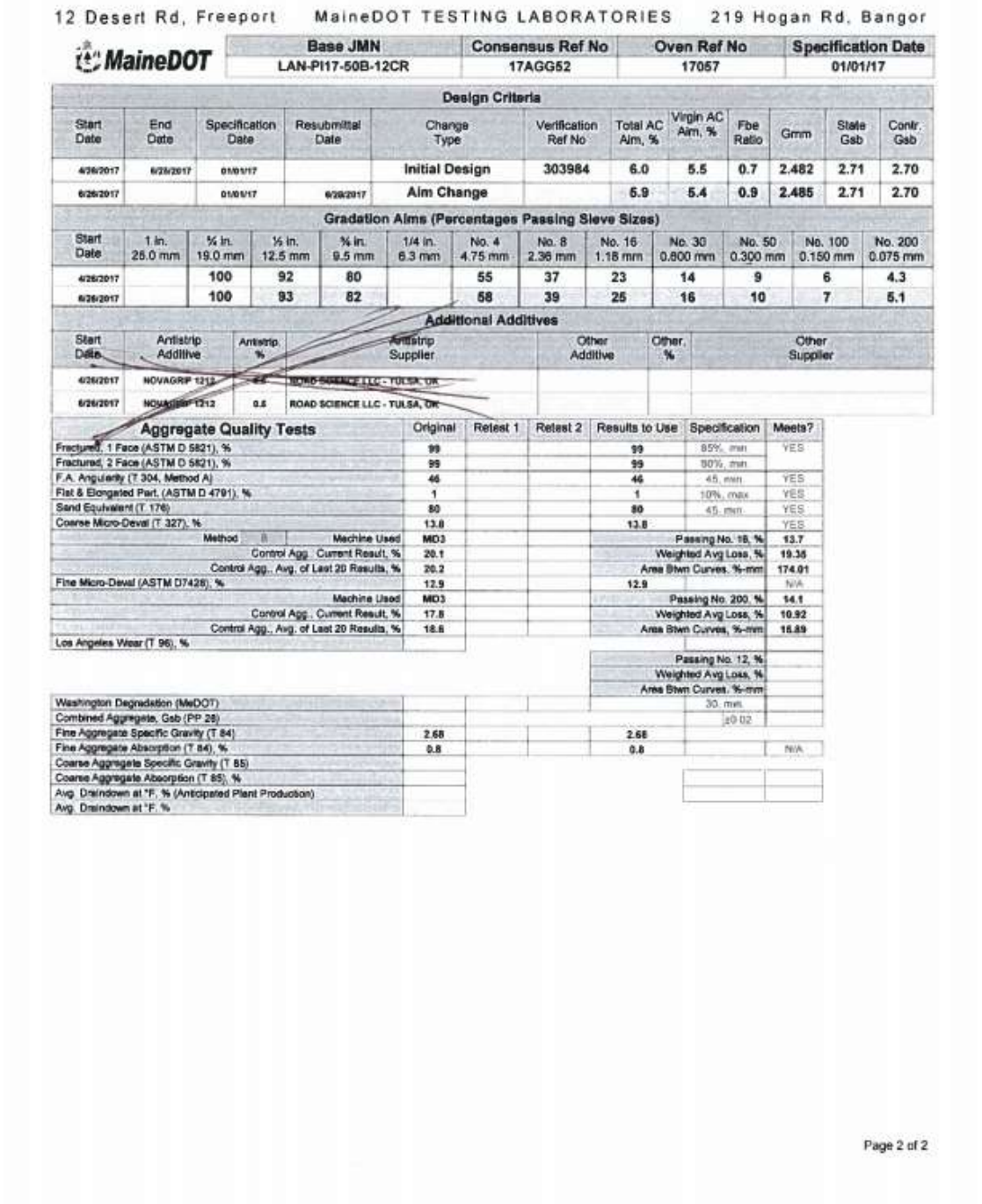

12 Desert Rd, Freeport MaineDOT TESTING LABORATORIES 219 Hogan Rd, Bangor

MaineDOT

Base JMN	Consensus Ref No	Oven Ref No	Specification Date
LAN-PI17-50B-12CR	17AGG52	17057	01/01/17

Design Criteria

Start Date	End Date	Specification Date	Resubmittal Date	Change Type	Verification Ref No	Total AC Aim, %	Virgin AC Aim, %	Fbe Ratio	Gmm	State Gsb	Contr. Gsb
4/26/2017	6/25/2017	01/01/17		Initial Design	303984	6.0	5.5	0.7	2.482	2.71	2.70
6/26/2017		01/01/17	6/26/2017	Aim Change		5.9	5.4	0.9	2.485	2.71	2.70

Gradation Aims (Percentages Passing Sieve Sizes)

Start Date	1 in. 25.0 mm	¾ in. 19.0 mm	½ in. 12.5 mm	⅜ in. 9.5 mm	1/4 in. 6.3 mm	No. 4 4.75 mm	No. 8 2.36 mm	No. 16 1.18 mm	No. 30 0.600 mm	No. 50 0.300 mm	No. 100 0.150 mm	No. 200 0.075 mm
4/25/2017		100	92	80		55	37	23	14	9	6	4.3
6/26/2017		100	93	82		58	39	25	16	10	7	5.1

Additional Additives

Start Date	Antistrip Additive	Antistrip %	Antistrip Supplier	Other Additive	Other %	Other Supplier
4/26/2017	NOVAGRIP 1212	0.5	ROAD SCIENCE LLC - TULSA, OK			
6/26/2017	NOVAGRIP 1212	0.5	ROAD SCIENCE LLC - TULSA, OK			

Aggregate Quality Tests	Original	Retest 1	Retest 2	Results to Use	Specification	Meets?
Fractured, 1 Face (ASTM D 5821), %	99			99	85%, min	YES
Fractured, 2 Face (ASTM D 5821), %	99			99	80%, min	
F.A. Angularity (T 304, Method A)	46			46	45, min	YES
Flat & Elongated Part. (ASTM D 4791), %	1			1	10%, max	YES
Sand Equivalent (T 176)	80			80	45, min	YES
Coarse Micro-Deval (T 327), %	13.8			13.8		YES
Method B / Machine Used	MD3			Passing No. 18, %		13.7
Control Agg., Current Result, %	20.1			Weighted Avg Loss, %		19.35
Control Agg., Avg. of Last 20 Results, %	20.2			Area Btwn Curves, %-mm		174.01
Fine Micro-Deval (ASTM D7428), %	12.9			12.9		N/A
Machine Used	MD3			Passing No. 200, %		14.1
Control Agg., Current Result, %	17.8			Weighted Avg Loss, %		10.92
Control Agg., Avg. of Last 20 Results, %	18.6			Area Btwn Curves, %-mm		16.89
Los Angeles Wear (T 96), %						
				Passing No. 12, %		
				Weighted Avg Loss, %		
				Area Btwn Curves, %-mm		
Washington Degradation (MeDOT)					30, min	
Combined Aggregate, Gsb (PP 28)					±0.02	
Fine Aggregate Specific Gravity (T 84)	2.68			2.68		
Fine Aggregate Absorption (T 84), %	0.8			0.8		N/A
Coarse Aggregate Specific Gravity (T 85)						
Coarse Aggregate Absorption (T 85), %						
Avg. Draindown at °F, % (Anticipated Plant Production)						
Avg. Draindown at °F, %						

Page 2 of 2

Figure 60: MEP1 Mix Design (Page 2 of 2)

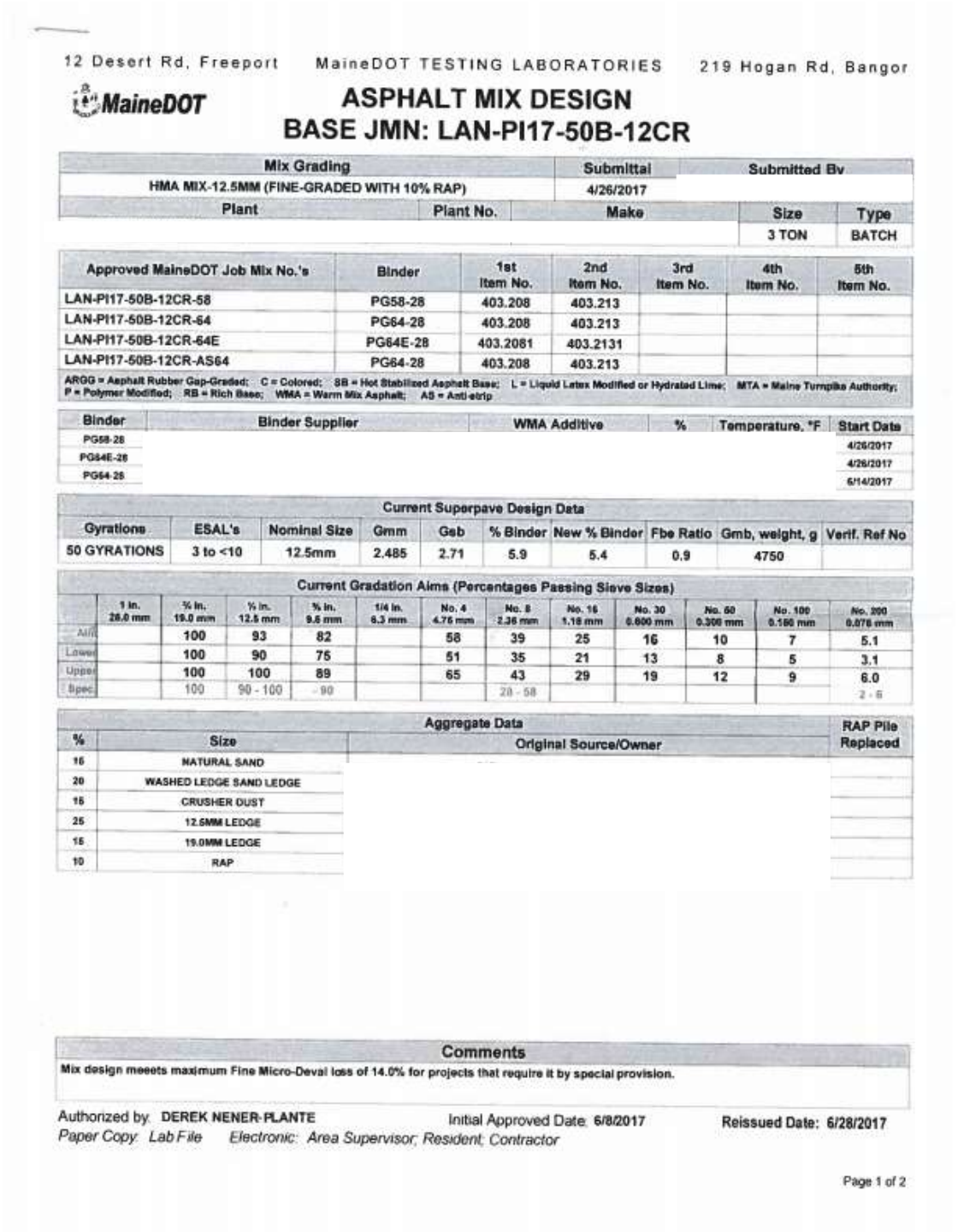

12 Desert Rd, Freeport MaineDOT TESTING LABORATORIES 219 Hogan Rd, Bangor

MaineDOT

ASPHALT MIX DESIGN
BASE JMN: LAN-PI17-50B-12CR

Mix Grading	Submittal	Submitted By
HMA MIX-12.5MM (FINE-GRADED WITH 10% RAP)	4/26/2017	

Plant	Plant No.	Make	Size	Type
			3 TON	BATCH

Approved MaineDOT Job Mix No.'s	Binder	1st Item No.	2nd Item No.	3rd Item No.	4th Item No.	5th Item No.
LAN-PI17-50B-12CR-58	PG58-28	403.208	403.213			
LAN-PI17-50B-12CR-64	PG64-28	403.208	403.213			
LAN-PI17-50B-12CR-64E	PG64E-28	403.2081	403.2131			
LAN-PI17-50B-12CR-AS64	PG64-28	403.208	403.213			

ARGG = Asphalt Rubber Gap-Graded; C = Colored; SB = Hot Stabilized Asphalt Base; L = Liquid Latex Modified or Hydrated Lime; MTA = Maine Turnpike Authority; P = Polymer Modified; RB = Rich Base; WMA = Warm Mix Asphalt; AS = Anti-strip

Binder	Binder Supplier	WMA Additive	%	Temperature, °F	Start Date
PG58-28					4/26/2017
PG64E-28					4/26/2017
PG64-28					5/14/2017

Current Superpave Design Data									
Gyrations	ESAL's	Nominal Size	Gmm	Gsb	% Binder	New % Binder	Fbe Ratio	Gmb, weight, g	Verif. Ref No
50 GYRATIONS	3 to <10	12.5mm	2.485	2.71	5.9	5.4	0.9	4750	

Current Gradation Aims (Percentages Passing Sieve Sizes)												
	1 in. 25.0 mm	¾ in. 19.0 mm	½ in. 12.5 mm	⅜ in. 9.5 mm	1/4 in. 6.3 mm	No. 4 4.75 mm	No. 8 2.36 mm	No. 16 1.18 mm	No. 30 0.600 mm	No. 50 0.300 mm	No. 100 0.150 mm	No. 200 0.075 mm
Aim		100	93	82		58	39	25	16	10	7	5.1
Lower		100	90	75		51	35	21	13	8	5	3.1
Upper		100	100	89		65	43	29	19	12	9	6.0
Spec		100	90 - 100	- 90			28 - 58					2 - 6

Aggregate Data			RAP Pile Replaced
%	Size	Original Source/Owner	
15	NATURAL SAND		
20	WASHED LEDGE SAND LEDGE		
15	CRUSHER DUST		
25	12.5MM LEDGE		
15	19.0MM LEDGE		
10	RAP		

Comments
Mix design meeets maximum Fine Micro-Deval loss of 14.0% for projects that require it by special provision.

Authorized by: DEREK NENER-PLANTE Initial Approved Date: 6/8/2017 Reissued Date: 6/28/2017

Paper Copy: Lab File Electronic: Area Supervisor; Resident; Contractor

Page 1 of 2

Figure 61: MEP2 Mix Design (Page 1 of 2)

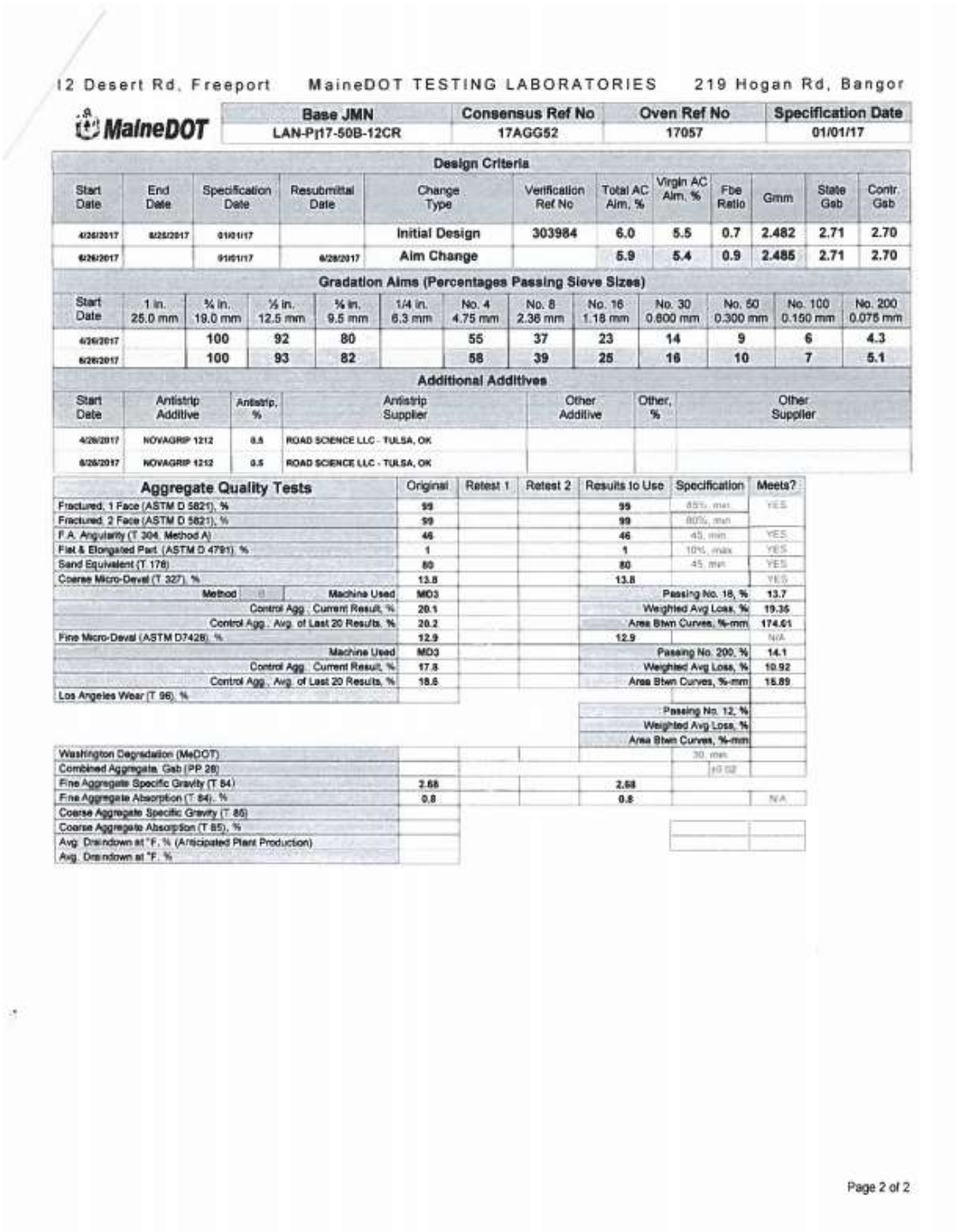

12 Desert Rd, Freeport MaineDOT TESTING LABORATORIES 219 Hogan Rd, Bangor

MaineDOT

Base JMN	Consensus Ref No	Oven Ref No	Specification Date
LAN-P(17-50B-12CR	17AGG52	17057	01/01/17

Design Criteria

Start Date	End Date	Specification Date	Resubmittal Date	Change Type	Verification Ref No	Total AC Aim, %	Virgin AC Aim, %	Fbe Ratio	Gmm	State Gsb	Contr Gsb
4/26/2017	6/25/2017	01/01/17		Initial Design	303984	6.0	5.5	0.7	2.482	2.71	2.70
6/26/2017		01/01/17	6/28/2017	Aim Change		5.9	5.4	0.9	2.485	2.71	2.70

Gradation Aims (Percentages Passing Sieve Sizes)

Start Date	1 in. 25.0 mm	¾ in. 19.0 mm	½ in. 12.5 mm	⅜ in. 9.5 mm	1/4 in. 6.3 mm	No. 4 4.75 mm	No. 8 2.36 mm	No. 16 1.18 mm	No. 30 0.600 mm	No. 50 0.300 mm	No. 100 0.150 mm	No. 200 0.075 mm
4/26/2017		100	92	80		55	37	23	14	9	6	4.3
6/26/2017		100	93	82		58	39	25	16	10	7	5.1

Additional Additives

Start Date	Antistrip Additive	Antistrip, %	Antistrip Supplier	Other Additive	Other, %	Other Supplier
4/26/2017	NOVAGRIP 1212	0.5	ROAD SCIENCE LLC - TULSA, OK			
6/26/2017	NOVAGRIP 1212	0.5	ROAD SCIENCE LLC - TULSA, OK			

Aggregate Quality Tests	Original	Retest 1	Retest 2	Results to Use	Specification	Meets?
Fractured, 1 Face (ASTM D 5821), %	99			99	85%, min	YES
Fractured, 2 Face (ASTM D 5821), %	99			99	80%, min	
F.A. Angularity (T 304, Method A)	46			46	45, min	YES
Flat & Elongated Part. (ASTM D 4791), %	1			1	10%, max	YES
Sand Equivalent (T 176)	80			80	45, min	YES
Coarse Micro-Deval (T 327), %	13.8			13.8		YES
Method B / Machine Used	MD3			Passing No. 16, %		13.7
Control Agg., Current Result, %	20.1			Weighted Avg Loss, %		19.35
Control Agg., Avg. of Last 20 Results, %	20.2			Area Btwn Curves, %-mm		174.61
Fine Micro-Deval (ASTM D7428), %	12.9			12.9		N/A
Machine Used	MD3			Passing No. 200, %		14.1
Control Agg., Current Result, %	17.8			Weighted Avg Loss, %		10.92
Control Agg., Avg. of Last 20 Results, %	18.6			Area Btwn Curves, %-mm		16.89
Los Angeles Wear (T 96), %						
				Passing No. 12, %		
				Weighted Avg Loss, %		
				Area Btwn Curves, %-mm		
Washington Degradation (MeDOT)					30, min	
Combined Aggregate, Gsb (PP 28)					±0.02	
Fine Aggregate Specific Gravity (T 84)	2.68			2.68		
Fine Aggregate Absorption (T 84), %	0.8			0.8		N/A
Coarse Aggregate Specific Gravity (T 85)						
Coarse Aggregate Absorption (T 85), %						
Avg. Draindown at °F, % (Anticipated Plant Production)						
Avg. Draindown at °F, %						

Page 2 of 2

Figure 62: MEP2 Mix Design (Page 2 of 2)

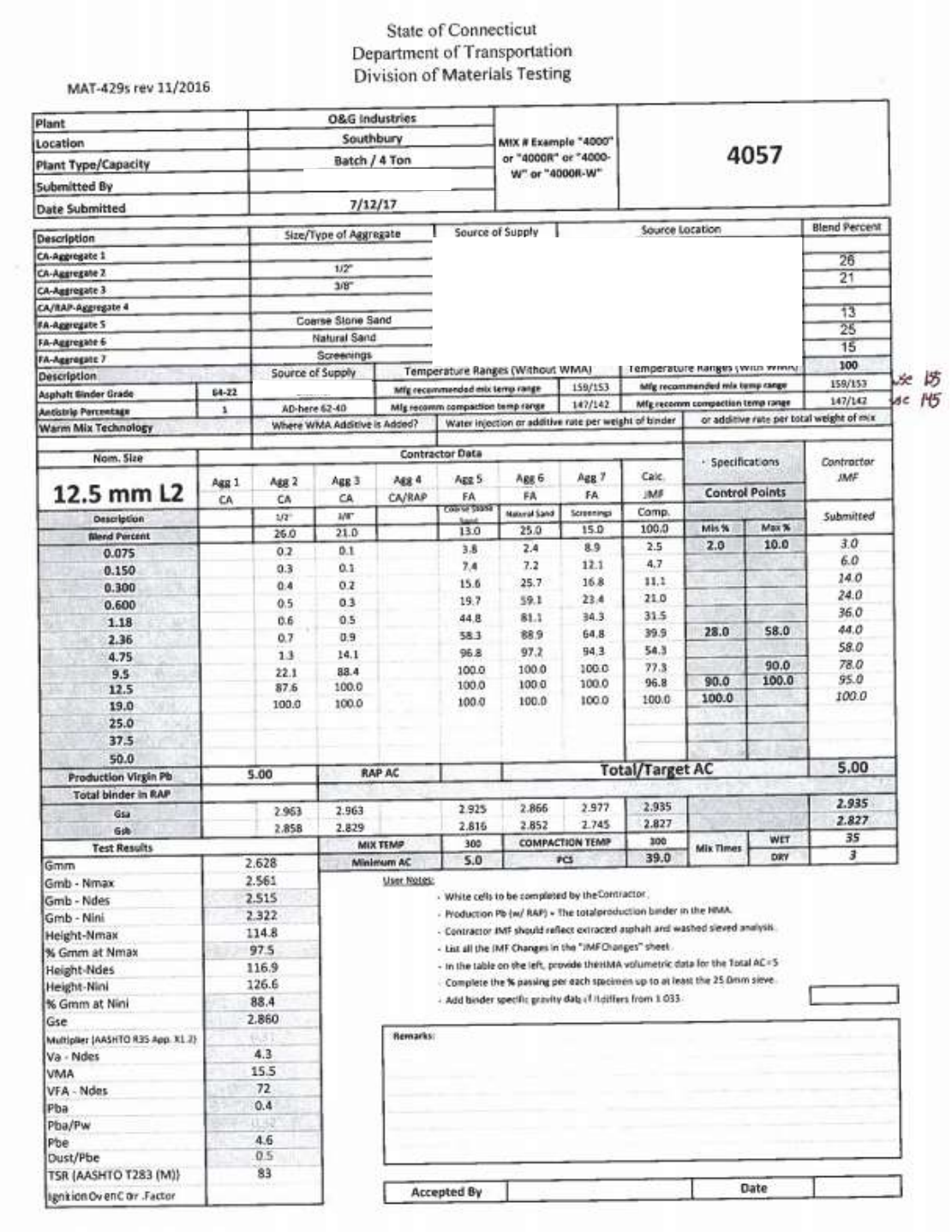

State of Connecticut
Department of Transportation
Division of Materials Testing

MAT-429s rev 11/2016

Plant	O&G Industries
Location	Southbury
Plant Type/Capacity	Batch / 4 Ton
Submitted By	
Date Submitted	7/12/17

MIX # Example "4000" or "4000R" or "4000-W" or "4000R-W": **4057**

Description	Size/Type of Aggregate	Source of Supply	Source Location	Blend Percent
CA-Aggregate 1				
CA-Aggregate 2	1/2"			26
CA-Aggregate 3	3/8"			21
CA/RAP-Aggregate 4				
FA-Aggregate 5	Coarse Stone Sand			13
FA-Aggregate 6	Natural Sand			25
FA-Aggregate 7	Screenings			15
				100

Description		Source of Supply	Temperature Ranges (Without WMA)		Temperature Ranges (With WMA)	
Asphalt Binder Grade	64-22		Mfg recommended mix temp range	159/153	Mfg recommended mix temp range	159/153
Antistrip Percentage	1	AD-here 62-40	Mfg recomm compaction temp range	147/142	Mfg recomm compaction temp range	147/142
Warm Mix Technology		Where WMA Additive is Added?	Water injection or additive rate per weight of binder		or additive rate per total weight of mix	

use 155
use 145

12.5 mm L2

Nom. Size	Contractor Data								Specifications		Contractor JMF
	Agg 1	Agg 2	Agg 3	Agg 4	Agg 5	Agg 6	Agg 7	Calc.	Control Points		
	CA	CA	CA	CA/RAP	FA	FA	FA	JMF			
Description		1/2"	3/8"		Coarse Stone Sand	Natural Sand	Screenings	Comp.			Submitted
Blend Percent		26.0	21.0		13.0	25.0	15.0	100.0	Min %	Max %	
0.075		0.2	0.1		3.8	2.4	8.9	2.5	2.0	10.0	3.0
0.150		0.3	0.1		7.4	7.2	12.1	4.7			6.0
0.300		0.4	0.2		15.6	25.7	16.8	11.1			14.0
0.600		0.5	0.3		19.7	59.1	23.4	21.0			24.0
1.18		0.6	0.5		44.8	81.1	34.3	31.5			36.0
2.36		0.7	0.9		58.3	88.9	64.8	39.9	28.0	58.0	44.0
4.75		1.3	14.1		96.8	97.2	94.3	54.3			58.0
9.5		22.1	88.4		100.0	100.0	100.0	77.3		90.0	78.0
12.5		87.6	100.0		100.0	100.0	100.0	96.8	90.0	100.0	95.0
19.0		100.0	100.0		100.0	100.0	100.0	100.0	100.0		100.0
25.0											
37.5											
50.0											

Production Virgin Pb	5.00	RAP AC		Total/Target AC						5.00
Total binder in RAP										
Gsa	2.963	2.963		2.925	2.866	2.977	2.935			2.935
Gsb	2.858	2.829		2.816	2.852	2.745	2.827			2.827
Test Results		MIX TEMP	300	COMPACTION TEMP			300	Mix Times	WET	35
		Minimum AC	5.0	PCS			39.0		DRY	3

Test Results	
Gmm	2.628
Gmb - Nmax	2.561
Gmb - Ndes	2.515
Gmb - Nini	2.322
Height-Nmax	114.8
% Gmm at Nmax	97.5
Height-Ndes	116.9
Height-Nini	126.6
% Gmm at Nini	88.4
Gse	2.860
Multiplier (AASHTO R35 App. X1.2)	
Va - Ndes	4.3
VMA	15.5
VFA - Ndes	72
Pba	0.4
Pba/Pw	
Pbe	4.6
Dust/Pbe	0.5
TSR (AASHTO T283 (M))	83
Ignition Oven Correction Factor	

User Notes:

- White cells to be completed by the Contractor.
- Production Pb (w/ RAP) = The total production binder in the HMA.
- Contractor JMF should reflect extracted asphalt and washed sieved analysis.
- List all the JMF Changes in the "JMF Changes" sheet.
- In the table on the left, provide the HMA volumetric data for the Total AC +5
- Complete the % passing per each specimen up to at least the 25.0mm sieve.
- Add binder specific gravity data if it differs from 1.033.

Remarks:

Accepted By		Date	

Figure 63: CTP1 Mix Design

Report on Hot Mix Asphalt (HMA) Job Mix Formula						
					Approved 9/29/17	
Project: Concord - Pembroke 40405					MBC	
Contractor:					4.60% asphalt content	
Asphalt Plant Supplier:					used for adjustment	
Asphalt Plant:						
Mix Type:	12.5mm w rap 75 gyr (CPI-CO-3-75-12)				LOT GTA	
Aggregate Fractions			Percent Passing Material			
Eng.	Metric		DRY AIM JMF		New Aim GTA	
1-1/2"	37.5 mm					
1-1/4"	31.5 mm					
1"	25 mm					
3/4"	19 mm					
1/2"	12.5 mm		99		99	
3/8"	9.5 mm		88		88	
#4	4.75 mm		58		60	
#8	2.36 mm		44		44	
#16	1.18 mm		34		34	
#30	0.600 mm		23		24	
#50	0.300 mm		14		14	
#100	0.150 mm		7		7.5	
#200	0.075 mm		3.8		4.1	
%AC			5.6		5.7	
Gmm			-		2.470	

Figure 64: NHG1 Mix Design

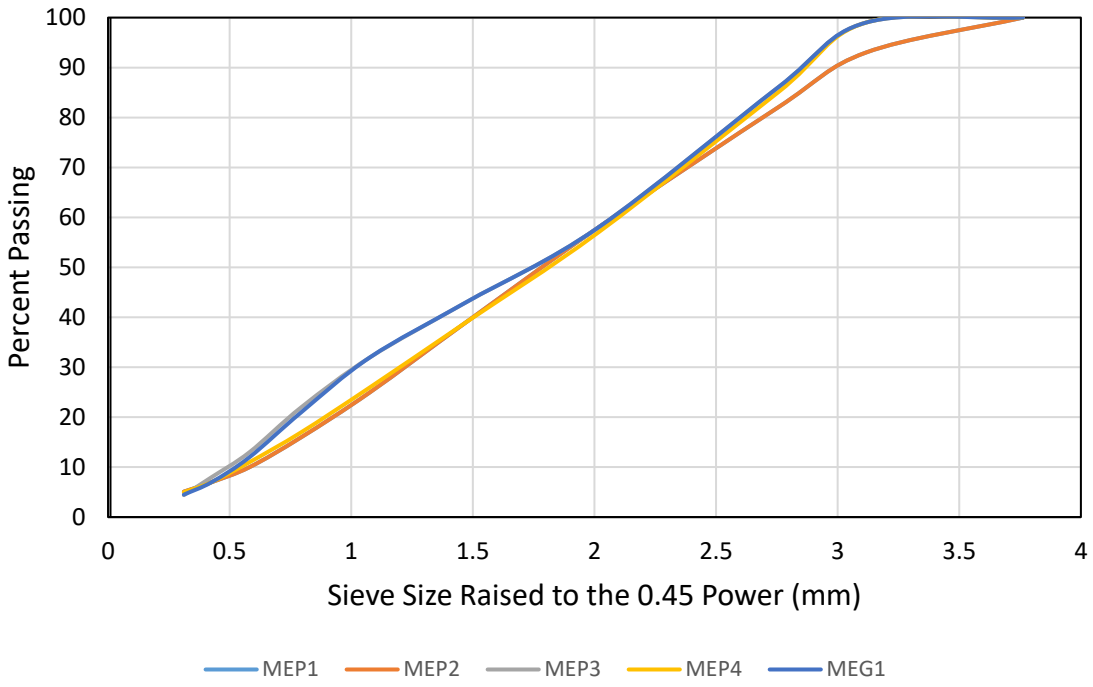

Figure 65: Maine Mixture Gradation Chart

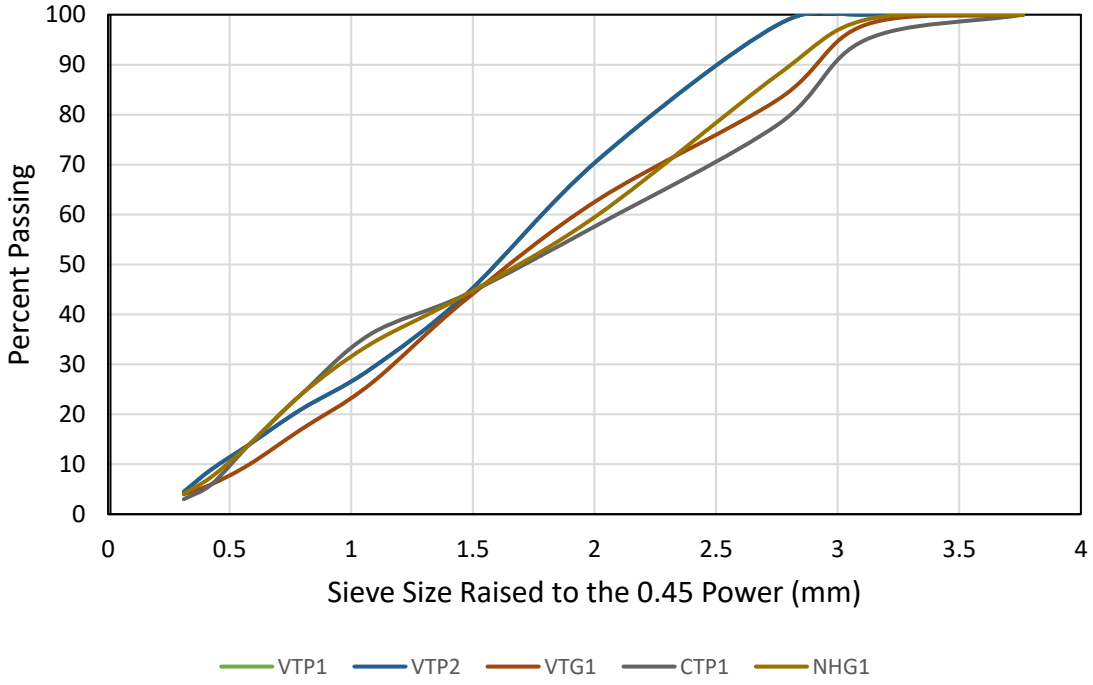

Figure 66: Vermont, New Hampshire, and Connecticut Mixture Gradation Chart

Appendix B: Indirect Tensile Strength (ITS) Specimen Data

The following section contains individual specimen data from the ITS testing. This includes the specimen I.D., conditioning method, peak load during the test, dimensions, and air voids.

Table 16: VTG-1 ITS Individual Specimen Data

Mix	Specimen ID	Conditioning Method	Peak Load (kN)	Height (mm)	Diameter (mm)	Air Voids (%)	Strength (kPa)
VTG-1	ITSU-6	Unconditioned	19	95	150	7.5	848.8
	ITSU-7	Unconditioned	18.4	95	150	7.5	822.0
	ITSU-12	Unconditioned	18.3	95	150	7.5	817.6
	ITS-14	T283	17.1	95	150	7.44	763.9
	ITS-15	T283	17.1	95	150	7.14	763.9
	ITS-16	T283	17.3	95	150	7.17	772.9
	WPI-10	MIST	16.2	95	150	6.9	723.7
	WPI-11	MIST	15.5	95	150	6.5	692.5
	WPI-12	MIST	18.6	95	150	6.3	831.0

Table 17: VTP-1 ITS Individual Specimen Data

Mix	Specimen ID	Conditioning Method	Peak Load (kN)	Height (mm)	Diameter (mm)	Air Voids (%)	Strength (kPa)
VTP-1	ITSU-7	Unconditioned	12.2	95	150	7.09	545.0
	ITSU-8	Unconditioned	12.6	95	150	7.02	562.9
	ITSU-9	Unconditioned	12.3	95	150	7.01	549.5
	ITS-10	T283	10.7	95	150	7.12	478.0
	ITS-11	T283	10.6	95	150	7.3	473.6
	ITS-12	T283	11.1	95	150	7.04	495.9
	WPI-10	MIST	11.4	95	150	6.6	509.3
	WPI-11	MIST	11.6	95	150	6.5	518.2
	WPI-12	MIST	7.9	95	150	6.9	352.9

Table 18: VTP-2 ITS Individual Specimen Data

Mix	Specimen ID	Conditioning Method	Peak Load (kN)	Height (mm)	Diameter (mm)	Air Voids (%)	Strength (kPa)
VTP-2	ITSU-3	Unconditioned	11.5	95	150	6.96	513.8
	ITSU-4	Unconditioned	12.5	95	150	6.91	558.4
	ITSU-5	Unconditioned	11	95	150	6.93	491.4
	ITS-1	T283	11.1	95	150	7.13	495.9
	ITS-2	T283	10.5	95	150	7.15	469.1
	ITS-6	T283	9.3	95	150	6.9	415.5
	WPI-10	MIST	11.6	95	150	6.8	518.2
	WPI-11	MIST	10.5	95	150	6.7	469.1
	WPI-12	MIST	10.3	95	150	7.3	460.2

Table 19: MEG-1 ITS Individual Specimen Data

Mix	Specimen ID	Conditioning Method	Peak Load (kN)	Height (mm)	Diameter (mm)	Air Voids (%)	Strength (kPa)
MEG-1	ITSU-8	Unconditioned	11.6	95	150	7.34	518.2
	ITSU-9	Unconditioned	11.5	95	150	7.31	513.8
	ITSU-10	Unconditioned	11.6	95	150	7.33	518.2
	ITS-2	T283	11.9	95	150	7.3	531.6
	ITS-11	T283	12	95	150	7.2	536.1
	ITS-12	T283	12.4	95	150	7.2	554.0
	ITS-1	MIST	10.8	95	150	6.8	482.5
	ITS-14	MIST	11.6	95	150	7.3	518.2
	ITS-15	MIST	11	95	150	7.3	491.4

Table 20: MEP-3 ITS Individual Specimen Data

Mix	Specimen ID	Conditioning Method	Peak Load (kN)	Height (mm)	Diameter (mm)	Air Voids (%)	Strength (kPa)
MEP-3	ITSU-8	Unconditioned	11.4	95	150	6.94	509.3
	ITSU-9	Unconditioned	12.3	95	150	7.04	549.5
	ITSU-11	Unconditioned	12.6	95	150	6.97	562.9
	ITS-6	T283	11.1	95	150	6.73	495.9
	ITS-7	T283	10.2	95	150	7.48	455.7
	ITS-10	T283	11.2	95	150	6.83	500.4
	ITS-12	MIST	11.2	95	150	7.2	500.4
	ITS-13	MIST	11.3	95	150	6.7	504.8
	ITS-14	MIST	11.5	95	150	6.9	513.8

Table 21: MEP-4 ITS Individual Specimen Data

Mix	Specimen ID	Conditioning Method	Peak Load (kN)	Height (mm)	Diameter (mm)	Air Voids (%)	Strength (kPa)
MEP-4	ITSU-8	Unconditioned	11.9	95	150	7.06	531.6
	ITSU-9	Unconditioned	13.7	95	150	7.08	612.0
	ITSU-10	Unconditioned	13.9	95	150	7.06	621.0
	ITS-5	T283	11.5	95	150	7.2	513.8
	ITS-6	T283	12.4	95	150	7.13	554.0
	ITS-12	T283	12.4	95	150	7.12	554.0
	ITS-3	MIST	12.4	95	150	6.6	554.0
	ITS-10	MIST	12.9	95	150	7.3	576.3
	ITS-14	MIST	13.9	95	150	6.9	621.0

Table 22: MEP-1 ITS Individual Specimen Data

Mix	Specimen ID	Conditioning Method	Peak Load (kN)	Height (mm)	Diameter (mm)	Air Voids (%)	Strength (kPa)
MEP-1	ITS-1	Unconditioned	8.2	95	150	7.19	366.3
	ITS-8	Unconditioned	9.2	95	150	7.01	411.0
	ITS-11	Unconditioned	9.7	95	150	6.89	433.3
	ITS-2	T283	7.9	95	150	7.25	352.9
	ITS-9	T283	7.3	95	150	7.04	326.1
	ITS-12	T283	9.5	95	150	6.71	424.4
	ITS-7	MIST	7.1	95	150	7	317.2
	ITS-10	MIST	7.3	95	150	6.9	326.1
	ITS-13	MIST	7.9	95	150	6.9	352.9

Table 23: MEP-2 ITS Individual Specimen Data

Mix	Specimen ID	Conditioning Method	Peak Load (kN)	Height (mm)	Diameter (mm)	Air Voids (%)	Strength (kPa)
MEP-2	ITS-4	Unconditioned	9.3	95	150	6.9	415.5
	ITS-5	Unconditioned	9.9	95	150	6.9	442.3
	ITS-6	Unconditioned	10.1	95	150	6.8	451.2
	ITS-1	T283	6.7	95	150	7.5	299.3
	ITS-2	T283	7.5	95	150	7.4	335.1
	ITS-3	T283	7.8	95	150	7.1	348.5
	ITS-6	MIST	7	95	150	6.9	312.7
	ITS-7	MIST	6.4	95	150	7.2	285.9
	Its-8	MIST	6.6	95	150	7.3	294.9

Table 24: CTP-1 ITS Individual Specimen Data

Mix	Specimen ID	Conditioning Method	Peak Load (kN)	Height (mm)	Diameter (mm)	Air Voids (%)	Strength (kPa)
CTP-1	ITS-10	Unconditioned	17.5	95	150	6.83	781.8
	ITS-11	Unconditioned	18.6	95	150	7.04	831.0
	ITS-12	Unconditioned	18.7	95	150	6.84	835.4
	ITS-2	T283	13.4	95	150	7.05	598.6
	ITS-8	T283	12.7	95	150	7.07	567.4
	ITS-9	T283	12.8	95	150	6.97	571.8
	ITS-13	MIST	14.4	95	150	6.9	643.3
	ITS-14	MIST	13.4	95	150	6.7	598.6
	ITS-15	MIST	14.6	95	150	6.6	652.3

Table 25: NHG-1 ITS Individual Specimen Data

Mix	Specimen ID	Conditioning Method	Peak Load (kN)	Height (mm)	Diameter (mm)	Air Voids (%)	Strength (kPa)
NHG-1	ITS-2	Unconditioned	19.7	95	150	5.6	880.1
	ITS-5	Unconditioned	19.3	95	150	6.2	862.2
	ITS-8	Unconditioned	18.8	95	150	6.1	839.9
	ITS-3	T283	16.8	95	150	5.9	750.5
	ITS-4	T283	16.6	95	150	6	741.6
	ITS-9	T283	16.1	95	150	6	719.3
	ITS-1	MIST	15.9	95	150	6.2	710.3
	ITS-6	MIST	16.2	95	150	5.8	723.7
	ITS-7	MIST	16.5	95	150	6.1	737.1

Appendix C: Dynamic Modulus Specimen Data

The following section contains the calculated dynamic modulus and phase angle values at the various temperatures and frequencies the test is run at. These data points were shifted to produce the master curves shown in the results chapter.

Table 26: VTG1 Unconditioned Dynamic Modulus and Phase Angle Data at 4.4° C

	VTG1 Unconditioned 4.4° C					
	25 Hz	**10 Hz**	**5 Hz**	**1 Hz**	**0.5 Hz**	**0.1 Hz**
Specimen	**Dynamic Modulus (MPa)**					
1	13710	12270	11215	8744	7817	5729
2	13386	12437	11372	8831	7814	5617
3	12838	11536	10577	8325	7447	5377
Average	**13311.33**	**12081.00**	**11054.67**	**8633.33**	**7692.67**	**5574.33**
	Phase Angle (Degrees)					
1	12	11.2	12.8	16	17.2	21.2
2	9	12.4	14	16.2	18	22.6
3	13	12	13.2	15.8	17.4	22.8
Average	**11.33**	**11.87**	**13.33**	**16.00**	**17.53**	**22.20**

Table 27: VTG1 Unconditioned Dynamic Modulus and Phase Angle Data at 21.1° C

	VTG1 Unconditioned 21.1° C					
	25 Hz	**10 Hz**	**5 Hz**	**1 Hz**	**0.5 Hz**	**0.1 Hz**
Specimen	**Dynamic Modulus (MPa)**					
1	5863	4619	3819	2309	1835	1059
2	5541	4375	3621	2196	1768	1017
3	5868	4704	3895	2375	1882	1093
Average	**5757.33**	**4566.00**	**3778.33**	**2293.33**	**1828.33**	**1056.33**
	Phase Angle (Degrees)					
1	27	26.6	28.4	31.2	31.8	33.6
2	27	26	27.6	30.6	32.2	33.6
3	18	25.4	27	29.8	30.8	32.2
Average	**24.00**	**26.00**	**27.67**	**30.53**	**31.60**	**33.13**

Table 28: VTG1 Unconditioned Dynamic Modulus and Phase Angle Data at 37.8° C

	VTG1 Unconditioned 37.8° C					
	25 Hz	**10 Hz**	**5 Hz**	**1 Hz**	**0.5 Hz**	**0.1 Hz**
Specimen	**Dynamic Modulus (MPa)**					
1	2208.00	1733.00	1432.00	880.00	736.00	508.00
2	1636.00	1197.00	947.00	578.00	493.00	351.00
3	1664.00	1211	960.00	589.00	501.00	361.00
Average	**1836.00**	**1380.33**	**1113.00**	**682.33**	**576.67**	**406.67**
	Phase Angle (Degrees)					
1	36.00	31.00	27.00	26.00	23.00	17.00
2	36.00	36.00	34.20	30.40	27.80	24.80
3	36.00	35.20	33.80	30.00	26.40	25.00
Average	**36.00**	**34.07**	**31.67**	**28.80**	**25.73**	**22.27**

Table 29: VTG1 MiST Conditioned Dynamic Modulus and Phase Angle Data at 4.4° C

	VTG1 MiST 4.4° C					
	25 Hz	**10 Hz**	**5 Hz**	**1 Hz**	**0.5 Hz**	**0.1 Hz**
Specimen	**Dynamic Modulus (MPa)**					
1	14864	13285	12109	9495	8347	5906
2	11789	10450	9438	7145	6264	4366
3	11039	9783	8893	6738	5887	4072
Average	**12564.00**	**11172.67**	**10146.67**	**7792.67**	**6832.67**	**4781.33**
	Phase Angle (Degrees)					
1	9	12.4	13.6	16.2	17	22.6
2	18	13.6	14.8	17.2	19.4	24
3	10	14	15	19.2	20.4	25.2
Average	**12.33**	**13.33**	**14.47**	**17.53**	**18.93**	**23.93**

Table 30: VTG1 MiST Conditioned Dynamic Modulus and Phase Angle Data at 21.1° C

	VTG1 MiST 21.1° C					
	25 Hz	**10 Hz**	**5 Hz**	**1 Hz**	**0.5 Hz**	**0.1 Hz**
Specimen	**Dynamic Modulus (MPa)**					
1	4734	3716	3045	1818	1443	826
2	5159	4024	3289	1927	1532	875
3	4478	3478	2811	1633	1295	731
Average	**4790.33**	**3739.33**	**3048.33**	**1792.67**	**1423.33**	**810.67**
	Phase Angle (Degrees)					
1	24.5	27.4	28.2	31.8	31.8	32.6
2	27	27.8	28.8	32.4	31.8	33
3						
Average	**25.75**	**27.60**	**28.50**	**32.10**	**31.80**	**32.80**

Table 31: VTG1 MiST Conditioned Dynamic Modulus and Phase Angle Data at 37.8° C

	VTG1 MiST 37.8° C					
	25 Hz	**10 Hz**	**5 Hz**	**1 Hz**	**0.5 Hz**	**0.1 Hz**
Specimen	**Dynamic Modulus (MPa)**					
1	1657.00	1180.00	917.00	548.00	462.00	331.00
2	1368.00	978.00	754.00	451.00	377.00	270.00
3	1398.00	999	769.00	461.00	385.00	274.00
Average	**1474.33**	**1052.33**	**813.33**	**486.67**	**408.00**	**291.67**
	Phase Angle (Degrees)					
1	36.00	34.60	32.80	28.60	25.80	22.20
2	36.00	34.40	32.80	28.20	25.20	22.20
3	36.00	35.00	33.00	28.40	25.20	21.80
Average	**36.00**	**34.67**	**32.87**	**28.40**	**25.40**	**22.07**

Table 32: VTP1 Unconditioned Dynamic Modulus and Phase Angle Data at 4.4° C

	VTP1 Unconditioned 4.4° C					
	25 Hz	**10 Hz**	**5 Hz**	**1 Hz**	**0.5 Hz**	**0.1 Hz**
Specimen	**Dynamic Modulus (MPa)**					
1	13627	12117	10943	8248	7168	4832
2	11863	10505	9488	7076	6218	4167
3	11989	10593	9533	7167	6150	4157
Average	**12493.00**	**11071.67**	**9988.00**	**7497.00**	**6512.00**	**4385.33**
	Phase Angle (Degrees)					
1	9	12.6	14.4	17.4	20.4	25.2
2	9	13.2	14.6	17.8	20	25.8
3	9	14	15.8	19.4	21	27.6
Average	**9.00**	**13.27**	**14.93**	**18.20**	**20.47**	**26.20**

Table 33: VTP1 Unconditioned Dynamic Modulus and Phase Angle Data at 21.1° C

	VTP1 Unconditioned 21.1° C					
	25 Hz	**10 Hz**	**5 Hz**	**1 Hz**	**0.5 Hz**	**0.1 Hz**
Specimen	**Dynamic Modulus (MPa)**					
1	4646	3552	2836	1542	1163	618
2	4229	3215	2558	1409	1083	578
3	4223	3226	2585	1406	1070	596
Average	**4366.00**	**3331.00**	**2659.67**	**1452.33**	**1105.33**	**597.33**
	Phase Angle (Degrees)					
1	27	29.6	31.2	35.6	34.8	34.4
2	28.5	31	32.8	36	35.8	35.8
3	27	31.2	32.8	36.4	36.4	35.6
Average	**27.50**	**30.60**	**32.27**	**36.00**	**35.67**	**35.27**

Table 34: VTP1 Unconditioned Dynamic Modulus and Phase Angle Data at 37.8° C

	VTP1 Unconditioned 37.8° C					
	25 Hz	**10 Hz**	**5 Hz**	**1 Hz**	**0.5 Hz**	**0.1 Hz**
Specimen	**Dynamic Modulus (MPa)**					
1	1124.00	752.00	553.00	307.00	248.00	173.00
2	1126.00	760.00	565.00	317.00	260.00	181.00
3	1172.00	782	580.00	314.00	256.00	175.00
Average	**1140.67**	**764.67**	**566.00**	**312.67**	**254.67**	**176.33**
	Phase Angle (Degrees)					
1	41.50	38.80	36.60	31.40	27.60	24.00
2	39.00	37.80	35.60	29.60	27.40	22.80
3	37.50	38.60	36.60	31.60	28.00	24.00
Average	**39.33**	**38.40**	**36.27**	**30.87**	**27.67**	**23.60**

Table 35: VTP1 MiST Conditioned Dynamic Modulus and Phase Angle Data at 4.4° C

	VTP1 MiST 4.4° C					
	25 Hz	**10 Hz**	**5 Hz**	**1 Hz**	**0.5 Hz**	**0.1 Hz**
Specimen	**Dynamic Modulus (MPa)**					
1	9933	8710	7766	5641	4812	3056
2	9140	7966	7061	5080	4307	2733
3	10288	8982	8002	5748	4846	3063
Average	**9787.00**	**8552.67**	**7609.67**	**5489.67**	**4655.00**	**2950.67**
	Phase Angle (Degrees)					
1	9	16.8	18.4	22	25	31
2	9	15.6	17.4	21.6	24	30
3	9	15.6	18.2	21.6	24.4	30.6
Average	**9.00**	**16.00**	**18.00**	**21.73**	**24.47**	**30.53**

Table 36: VTP1 MiST Conditioned Dynamic Modulus and Phase Angle Data at 21.1° C

	VTP1 MiST 21.1° C					
	25 Hz	**10 Hz**	**5 Hz**	**1 Hz**	**0.5 Hz**	**0.1 Hz**
Specimen	**Dynamic Modulus (MPa)**					
1	3281	2426	1872	968	719	359
2	3006	2228	1734	902	669	340
3	3514	2567	1981	1012	751	380
Average	**3267.00**	**2407.00**	**1862.33**	**960.67**	**713.00**	**359.67**
	Phase Angle (Degrees)					
1	33.5	33.4	35.6	37.2	37.2	36.6
2	36	34	35.8	38.6	38.4	37.2
3	36	34.2	36.6	38	37.6	35.6
Average	**35.17**	**33.87**	**36.00**	**37.93**	**37.73**	**36.47**

Table 37: VTP1 MiST Conditioned Dynamic Modulus and Phase Angle Data at 37.8° C

	VTP1 MiST 37.8° C					
	25 Hz	**10 Hz**	**5 Hz**	**1 Hz**	**0.5 Hz**	**0.1 Hz**
Specimen	**Dynamic Modulus (MPa)**					
1	674.00	435.00	319.00	173.00	142.00	100.00
2						
3	792.00	516	378.00	208.00	169.00	120.00
Average	**733.00**	**475.50**	**348.50**	**190.50**	**155.50**	**110.00**
	Phase Angle (Degrees)					
1	42.50	40.00	37.80	30.20	26.60	22.80
2						
3	36.00	39.60	36.80	29.60	26.20	19.80
Average	**39.25**	**39.80**	**37.30**	**29.90**	**26.40**	**21.30**

Table 38: VTP2 Unconditioned Dynamic Modulus and Phase Angle Data at 4.4° C

	VTP2 Unconditioned 4.4° C					
	25 Hz	10 Hz	5 Hz	1 Hz	0.5 Hz	0.1 Hz
Specimen	**Dynamic Modulus (MPa)**					
1	11930	10541	9530	7015	6072	4017
2	12499	10965	9851	7334	6376	4246
3	12222	10801	9647	7153	6033	3947
Average	**12217.00**	**10769.00**	**9676.00**	**7167.33**	**6160.33**	**4070.00**
	Phase Angle (Degrees)					
1	18	14	15.8	19	21.4	27.6
2	9	14	15.4	18.4	21.2	28.2
3	13.5	14.2	16.4	20.2	22	29.2
Average	**13.50**	**14.07**	**15.87**	**19.20**	**21.53**	**28.33**

Table 39: VTP2 Unconditioned Dynamic Modulus and Phase Angle Data at 21.1° C

	VTP2 Unconditioned 21.1° C					
	25 Hz	10 Hz	5 Hz	1 Hz	0.5 Hz	0.1 Hz
Specimen	**Dynamic Modulus (MPa)**					
1	3807	2864	2263	1216	924	484
2	4852	3704	2923	1553	1173	616
3	4257	3192	2503	1322	996	519
Average	**4305.33**	**3253.33**	**2563.00**	**1363.67**	**1031.00**	**539.67**
	Phase Angle (Degrees)					
1	35	32.2	34.2	37.2	37.8	36.4
2	27	31.4	33.8	37.4	37.2	36.6
3	34	33	34.6	38.4	37.6	36.6
Average	**32.00**	**32.20**	**34.20**	**37.67**	**37.53**	**36.53**

Table 40: VTP2 Unconditioned Dynamic Modulus and Phase Angle Data at 37.8° C

	VTP2 Unconditioned 37.8° C					
	25 Hz	**10 Hz**	**5 Hz**	**1 Hz**	**0.5 Hz**	**0.1 Hz**
Specimen	**Dynamic Modulus (MPa)**					
1	944.00	632.00	466.00	255.00	211.00	147.00
2	1108.00	738.00	542.00	299.00	243.00	168.00
3	1131.00	752	551.00	302.00	245.00	169.00
Average	**1061.00**	**707.33**	**519.67**	**285.33**	**233.00**	**161.33**
	Phase Angle (Degrees)					
1	36.50	38.00	36.60	30.20	26.80	23.40
2	42.00	38.80	36.60	30.00	26.60	24.90
3	36.00	37.60	35.60	29.60	26.40	20.80
Average	**38.17**	**38.13**	**36.27**	**29.93**	**26.60**	**23.03**

Table 41: VTP2 MiST Conditioned Dynamic Modulus and Phase Angle Data at 4.4° C

	VTP2 MiST 4.4° C					
	25 Hz	**10 Hz**	**5 Hz**	**1 Hz**	**0.5 Hz**	**0.1 Hz**
Specimen	**Dynamic Modulus (MPa)**					
1	9215	7955	7045	5023	4293	2693
2	8954	7757	6859	4867	4084	2523
3	10246	8941	7949	5712	4827	3016
Average	**9471.67**	**8217.67**	**7284.33**	**5200.67**	**4401.33**	**2744.00**
	Phase Angle (Degrees)					
1	10.5	16.2	18	21.6	24	31
2	12	17.2	19.8	24.6	26.4	32.4
3	18	16	17.4	21.8	24.8	31.6
Average	**13.50**	**16.47**	**18.40**	**22.67**	**25.07**	**31.67**

Table 42: VTP2 MiST Conditioned Dynamic Modulus and Phase Angle Data at 21.1° C

	VTP2 MiST 21.1° C					
	25 Hz	**10 Hz**	**5 Hz**	**1 Hz**	**0.5 Hz**	**0.1 Hz**
Specimen	**Dynamic Modulus (MPa)**					
1	2785	2023	1557	790	588	296
2	2699	1967	1522	772	584	297
3	3064	2241	1715	861	635	316
Average	**2849.33**	**2077.00**	**1598.00**	**807.67**	**602.33**	**303.00**
	Phase Angle (Degrees)					
1	27	35	36.6	39.6	39	37
2	36	35.4	37.6	39.4	38.4	36.4
3	28.5	35.4	37.6	39.6	39.4	37.4
Average	**30.50**	**35.27**	**37.27**	**39.53**	**38.93**	**36.93**

Table 43: VTP2 MiST Conditioned Dynamic Modulus and Phase Angle Data at 37.8° C

	VTP2 MiST 37.8° C					
	25 Hz	**10 Hz**	**5 Hz**	**1 Hz**	**0.5 Hz**	**0.1 Hz**
Specimen	**Dynamic Modulus (MPa)**					
1	600.00	392.00	290.00	158.00	130.00	68.00
2	578.00	378.00	279.00	156.00	129.00	85.00
3	597.00	390	286.00	161.00	134.00	94.00
Average	**591.67**	**386.67**	**285.00**	**158.33**	**131.00**	**82.33**
	Phase Angle (Degrees)					
1	45.00	39.20	37.20	29.40	27.20	22.80
2	45.00	39.80	37.40	30.20	27.40	26.50
3	41.00	39.60	37.00	28.80	25.40	22.00
Average	**43.67**	**39.53**	**37.20**	**29.47**	**26.67**	**23.77**

Table 44: MEG1 Unconditioned Dynamic Modulus and Phase Angle Data at 4.4° C

	MEG1 Unconditioned 4.4° C					
	25 Hz	**10 Hz**	**5 Hz**	**1 Hz**	**0.5 Hz**	**0.1 Hz**
Specimen	**Dynamic Modulus (MPa)**					
1	11231	10085	9218	7235	6406	4726
2	10301	9188	8378	6576	5838	4269
3	10938	9715	8801	6705	5909	4279
Average	**10823.33**	**9662.67**	**8799.00**	**6838.67**	**6051.00**	**4424.67**
	Phase Angle (Degrees)					
1	9	12.2	13.2	15.8	17.2	21
2	9	12.8	13.6	16.2	17.2	20.4
3	9	13.4	13.8	16.4	17.8	21.6
Average	**9.00**	**12.80**	**13.53**	**16.13**	**17.40**	**21.00**

Table 45: MEG1 Unconditioned Dynamic Modulus and Phase Angle Data at 21.1° C

	MEG1 Unconditioned 21.1° C					
	25 Hz	**10 Hz**	**5 Hz**	**1 Hz**	**0.5 Hz**	**0.1 Hz**
Specimen	**Dynamic Modulus (MPa)**					
1	4324	3406	2820	1741	1397	821
2	3715	2921	2417	1473	1197	701
3	4176	3261	2655	1607	1289	752
Average	**4071.67**	**3196.00**	**2630.67**	**1607.00**	**1294.33**	**758.00**
	Phase Angle (Degrees)					
1	18	26.2	28.2	30.2	31	33
2	27	28.2	28.6	31.8	32	34.8
3	18	27.2	28	30.8	31.2	32.8
Average	**21.00**	**27.20**	**28.27**	**30.93**	**31.40**	**33.53**

Table 46: MEG1 Unconditioned Dynamic Modulus and Phase Angle Data at 37.8° C

	MEG1 Unconditioned 37.8° C					
	25 Hz	**10 Hz**	**5 Hz**	**1 Hz**	**0.5 Hz**	**0.1 Hz**
Specimen	**Dynamic Modulus (MPa)**					
1	1218.00	873.00	684.00	397.00	329.00	222.00
2	1075.00	772.00	601.00	349.00	290.00	192.00
3	1091.00	787	615.00	363.00	299.00	200.00
Average	**1128.00**	**810.67**	**633.33**	**369.67**	**306.00**	**204.67**
	Phase Angle (Degrees)					
1	36.00	34.20	33.80	30.20	28.20	26.00
2	36.00	35.60	34.80	32.00	30.00	28.60
3	39.00	34.40	34.20	31.40	29.00	28.70
Average	**37.00**	**34.73**	**34.27**	**31.20**	**29.07**	**27.77**

Table 47: MEG1 MiST Conditioned Dynamic Modulus and Phase Angle Data at 4.4° C

	MEG1 MiST 4.4° C					
	25 Hz	**10 Hz**	**5 Hz**	**1 Hz**	**0.5 Hz**	**0.1 Hz**
Specimen	**Dynamic Modulus (MPa)**					
1	11179	9773	8773	6725	5826	4114
2						
3						
Average	**11179.00**	**9773.00**	**8773.00**	**6725.00**	**5826.00**	**4114.00**
	Phase Angle (Degrees)					
1	11.5	13.4	14.2	18	18.2	23.4
2						
3						
Average	**11.50**	**13.40**	**14.20**	**18.00**	**18.20**	**23.40**

Table 48: MEG1 MiST Conditioned Dynamic Modulus and Phase Angle Data at 21.1° C

	MEG1 MiST 21.1° C					
	25 Hz	**10 Hz**	**5 Hz**	**1 Hz**	**0.5 Hz**	**0.1 Hz**
Specimen	**Dynamic Modulus (MPa)**					
1	3765	2904	2355	1398	1121	645
2						
3						
Average	**3765.00**	**2904.00**	**2355.00**	**1398.00**	**1121.00**	**645.00**
	Phase Angle (Degrees)					
1	27	28.2	29.2	31.8	31.8	32.8
2						
3						
Average	**27.00**	**28.20**	**29.20**	**31.80**	**31.80**	**32.80**

Table 49: MEG1 MiST Conditioned Dynamic Modulus and Phase Angle Data at 37.8° C

	MEG1 MiST 37.8° C					
	25 Hz	**10 Hz**	**5 Hz**	**1 Hz**	**0.5 Hz**	**0.1 Hz**
Specimen	**Dynamic Modulus (MPa)**					
1	1011.00	711.00	537.00	299.00	239.00	107.00
2						
3						
Average	**1011.00**	**711.00**	**537.00**	**299.00**	**239.00**	**107.00**
	Phase Angle (Degrees)					
1	40.50	36.30	34.80	31.20	28.80	26.70
2						
3						
Average	**40.50**	**36.30**	**34.80**	**31.20**	**28.80**	**26.70**

Table 50: MEP4 Unconditioned Dynamic Modulus and Phase Angle Data at 4.4° C

	MEP4 Unconditioned 4.4° C					
	25 Hz	10 Hz	5 Hz	1 Hz	0.5 Hz	0.1 Hz
Specimen	**Dynamic Modulus (MPa)**					
1	11596	10544	9718	7813	7078	5395
2	11434	10381	9593	7793	7013	5386
3	11805	10664	9814	7831	7019	5281
Average	**11611.67**	**10529.67**	**9708.33**	**7812.33**	**7036.67**	**5354.00**
	Phase Angle (Degrees)					
1	9	11.6	12.8	14.6	15.8	19.2
2	12	11.4	11.8	13.8	15	18.2
3	9	11.2	12	14.2	15.2	18.8
Average	**10.00**	**11.40**	**12.20**	**14.20**	**15.33**	**18.73**

Table 51: MEP4 Unconditioned Dynamic Modulus and Phase Angle Data at 21.1° C

	MEP4 Unconditioned 21.1° C					
	25 Hz	10 Hz	5 Hz	1 Hz	0.5 Hz	0.1 Hz
Specimen	**Dynamic Modulus (MPa)**					
1	4816	3927	3323	2155	1785	1096
2	4733	3862	3247	2121	1739	1055
3	4776	3845	3222	2040	1678	1002
Average	**4775.00**	**3878.00**	**3264.00**	**2105.33**	**1734.00**	**1051.00**
	Phase Angle (Degrees)					
1	18	23.2	24.4	28	28.2	31.8
2	15	22.2	24.2	27.6	28.8	31.8
3	25.5	24.2	25.8	29.8	29.4	32.4
Average	**19.50**	**23.20**	**24.80**	**28.47**	**28.80**	**32.00**

Table 52: MEP4 Unconditioned Dynamic Modulus and Phase Angle Data at 37.8° C

	MEP4 Unconditioned 37.8° C					
	25 Hz	**10 Hz**	**5 Hz**	**1 Hz**	**0.5 Hz**	**0.1 Hz**
Specimen	**Dynamic Modulus (MPa)**					
1	1623.00	1210.00	970.00	586.00	489.00	327.00
2	1589.00	1182.00	943.00	574.00	475.00	316.00
3	1492.00	1100	876.00	515.00	435.00	290.00
Average	**1568.00**	**1164.00**	**929.67**	**558.33**	**466.33**	**311.00**
	Phase Angle (Degrees)					
1	36.00	32.40	31.60	30.60	28.80	28.40
2	36.00	33.20	32.20	31.20	28.80	29.00
3	35.50	33.00	32.20	31.40	29.20	28.20
Average	**35.83**	**32.87**	**32.00**	**31.07**	**28.93**	**28.53**

Table 53: MEP4 MiST Conditioned Dynamic Modulus and Phase Angle Data at 4.4° C

	MEP4 MiST 4.4° C					
	25 Hz	**10 Hz**	**5 Hz**	**1 Hz**	**0.5 Hz**	**0.1 Hz**
Specimen	**Dynamic Modulus (MPa)**					
1	9844	9016	8267	6616	5959	4514
2	10022	9654	8841	6866	6202	4677
3						
Average	**9933.00**	**9335.00**	**8554.00**	**6741.00**	**6080.50**	**4595.50**
	Phase Angle (Degrees)					
1	9	11	12.6	13	15.2	18
2	9	11.8	12.6	15	16	19.8
3						
Average	**9.00**	**11.40**	**12.60**	**14.00**	**15.60**	**18.90**

Table 54: MEP4 MiST Conditioned Dynamic Modulus and Phase Angle Data at 21.1° C

	MEP4 MiST 21.1° C					
	25 Hz	**10 Hz**	**5 Hz**	**1 Hz**	**0.5 Hz**	**0.1 Hz**
Specimen	**Dynamic Modulus (MPa)**					
1	4266	3447	2902	1852	1517	907
2						
3						
Average	**4266.00**	**3447.00**	**2902.00**	**1852.00**	**1517.00**	**907.00**
	Phase Angle (Degrees)					
1	18	23.6	24.6	28	29.4	32.4
2						
3						
Average	**18.00**	**23.60**	**24.60**	**28.00**	**29.40**	**32.40**

Table 55: MEP4 MiST Conditioned Dynamic Modulus and Phase Angle Data at 37.8° C

	MEP4 MiST 37.8° C					
	25 Hz	**10 Hz**	**5 Hz**	**1 Hz**	**0.5 Hz**	**0.1 Hz**
Specimen	**Dynamic Modulus (MPa)**					
1	1335.00	955.00	747.00	427.00	343.00	216.00
2						
3						
Average	**1335.00**	**955.00**	**747.00**	**427.00**	**343.00**	**216.00**
	Phase Angle (Degrees)					
1	36.00	35.40	34.50	33.00	30.30	29.10
2						
3						
Average	**36.00**	**35.40**	**34.50**	**33.00**	**30.30**	**29.10**

Table 56: MEP1 Unconditioned Dynamic Modulus and Phase Angle Data at 4.4° C

	MEP1 Unconditioned 4.4° C					
	25 Hz	**10 Hz**	**5 Hz**	**1 Hz**	**0.5 Hz**	**0.1 Hz**
Specimen	**Dynamic Modulus (MPa)**					
1	9210	8100	7280	5536	4814	3382
2	10875	9581	8657	6606	5743	4106
3	10583	9404	8519	6558	5744	4128
Average	**10222.67**	**9028.33**	**8152.00**	**6233.33**	**5433.67**	**3872.00**
	Phase Angle (Degrees)					
1	18	13.6	14.2	17.4	18.6	22.8
2	12	13.4	14.4	16.8	18.6	21.6
3	9	13.2	15	16.8	18.8	22.2
Average	**13.00**	**13.40**	**14.53**	**17.00**	**18.67**	**22.20**

Table 57: MEP1 Unconditioned Dynamic Modulus and Phase Angle Data at 21.1° C

	MEP1 Unconditioned 21.1° C					
	25 Hz	**10 Hz**	**5 Hz**	**1 Hz**	**0.5 Hz**	**0.1 Hz**
Specimen	**Dynamic Modulus (MPa)**					
1	3369	2628	2169	1338	1090	668
2	3811	2961	2434	1493	1220	747
3	3785	2966	2439	1511	1236	759
Average	**3655.00**	**2851.67**	**2347.33**	**1447.33**	**1182.00**	**724.67**
	Phase Angle (Degrees)					
1	27	27.8	28.4	30	30.4	29.6
2	27	27.4	28.6	30.2	29.8	30.2
3	27	27.6	28.2	29.8	29.8	30
Average	**27.00**	**27.60**	**28.40**	**30.00**	**30.00**	**29.93**

Table 58: MEP1 Unconditioned Dynamic Modulus and Phase Angle Data at 37.8° C

	MEP1 Unconditioned 37.8° C					
	25 Hz	**10 Hz**	**5 Hz**	**1 Hz**	**0.5 Hz**	**0.1 Hz**
Specimen	**Dynamic Modulus (MPa)**					
1	1097.00	811.00	648.00	408.00	352.00	254.00
2						
3	1116.00	825	666.00	426.00	369.00	273.00
Average	**1106.50**	**818.00**	**657.00**	**417.00**	**360.50**	**263.50**
	Phase Angle (Degrees)					
1	36.00	32.60	31.40	27.40	25.20	24.60
2						
3	34.00	31.40	30.40	26.40	24.00	22.20
Average	**35.00**	**32.00**	**30.90**	**26.90**	**24.60**	**23.40**

Table 59: MEP1 MiST Conditioned Dynamic Modulus and Phase Angle Data at 4.4° C

	MEP1 MiST 4.4° C					
	25 Hz	**10 Hz**	**5 Hz**	**1 Hz**	**0.5 Hz**	**0.1 Hz**
Specimen	**Dynamic Modulus (MPa)**					
1	8798.2	7601.83	6773.05	4994.79	4301.06	2968.05
2	9320.74	8253.77	7429	5521	5521	3345.67
3						
Average	**9059.47**	**7927.80**	**7101.03**	**5257.90**	**4911.03**	**3156.86**
	Phase Angle (Degrees)					
1	18	15.2	15.8	19.4	19.2	24.6
2	9	15.8	16.4	19	19.8	24.2
3						
Average	**13.50**	**15.50**	**16.10**	**19.20**	**19.50**	**24.40**

Table 60: MEP1 MiST Conditioned Dynamic Modulus and Phase Angle Data at 21.1° C

	MEP1 MiST 21.1° C					
	25 Hz	**10 Hz**	**5 Hz**	**1 Hz**	**0.5 Hz**	**0.1 Hz**
Specimen	**Dynamic Modulus (MPa)**					
1	2978.76	2252.82	1811.68	1062.75	856.57	501.37
2	2833.01	2160.16	1754.63	1044.29	844.81	498.67
3						
Average	**2905.89**	**2206.49**	**1783.16**	**1053.52**	**850.69**	**500.02**
	Phase Angle (Degrees)					
1	27	29.6	30.2	32.4	32.4	33.8
2	27	29	29.6	31.2	31.6	32.4
3						
Average	**27.00**	**29.30**	**29.90**	**31.80**	**32.00**	**33.10**

Table 61: MEP1 MiST Conditioned Dynamic Modulus and Phase Angle Data at 37.8° C

	MEP1 MiST 37.8° C					
	25 Hz	**10 Hz**	**5 Hz**	**1 Hz**	**0.5 Hz**	**0.1 Hz**
Specimen	**Dynamic Modulus (MPa)**					
1	597.00	390	286.00	161.00	134.00	94.00
2						
3						
Average	**597.00**	**390.00**	**286.00**	**161.00**	**134.00**	**94.00**
	Phase Angle (Degrees)					
1	45.00	39.20	37.20	29.40	27.20	22.80
2						
3						
Average	**45.00**	**39.20**	**37.20**	**29.40**	**27.20**	**22.80**

Appendix D: Pavement Analysis Inputs

The following section contains the inputs used in PavementME to perform pavement analysis simulations. Anything that is not specifically listed in this section was not changed from the default setting in the program. PavementME Version 2.3.1 was used in this research.

Table 62: PavementME Traffic and Climate Inputs

Traffic Input	Thin Pavement Structure	Thick Pavement Structure
2 Way AADT	3000	8000
Total Lanes	2	4
Trucks in Design Direction	50%	50%
Trucks in Design Lane	100%	95%
Operational Speed (mph)	60	60
Truck Class Distribution	Default Values	Default Values
Axle Configuration	Default Values	Default Values
Lateral Wander	Default Values	Default Values
Wheelbase Dimensions	Default Values	Default Values
Climate Station:	Burlington, VT Station No. 14742	Burlington, VT Station No. 14742

Table 63: PavementME Pavement Structure and Material Property Inputs

Layer	Property	Thin Pavement Structure	Thick Pavement Structure
Asphalt Concrete Surface	Thickness (in)	3	6
	Percent Binder (Volume-based)	11.6	
	Air Voids (%)	7	
	Density (lb/ft^3)	150	
	Poissons's Ratio	0.35	
	Binder	Level 1 Input: See Table 64	
	Creep Compliance	Default Level 3 Input	
	Dynamic Modulus	Level 1 Input: Lab Measured Properties	
Crushed Stone Base	Thickness (in)	6	12
	Pavement ME Material Input	Crushed Stone	
	Lateral Pressure Coefficient (K0)	0.5	
	Resilient Modulus (psi)	30000	
	Poisson's Ratio	0.35	
	Gradation Properties	A-1-a	
Subgrade	Thickness (in)	Semi-Infinite	
	Pavement ME Material Input	A-2-4	
	Lateral Pressure Coefficient (K0)	0.5	
	Resilient Modulus (psi)	16500	
	Gradation Properties	A-2-4	

Table 64: PavementME Binder Property Inputs

PG58-28 Binders (VTP1 And VTP2)		
Temperature (°F)	Complex Shear Modulus (Pa)	Phase Angle (degrees)
136.4	1320	80
147.2	663	84
158	330	88

PG70-28 Binders (VTG1)		
Temperature (°F)	Complex Shear Modulus (Pa)	Phase Angle (degrees)
158	1320	80
168.8	663	84
179.6	330	88

Appendix E: Disk-Shaped Compact Tension (DCT) Specimen Data

The following section contains individual specimen data from the DCT testing. This includes the specimen I.D., conditioning method, dimensions, air voids, and calculated fracture energy.

Table 65: VTP1 DCT Individual Specimen Data

Mix	Specimen I.D.	Conditioning Method	Air Voids (%)	Avg. Ligament Length (mm)	Avg. Specimen Height (mm)	Fracture Energy (J/m^2)
VTP1	DCT 1.1	Freeze-Thaw	6.6	80.7	49.2	777.9
	DCT 3.2	Freeze-Thaw	6.7	81.8	50.3	743.1
	DCT 4.2	Freeze-Thaw	6.9	82.0	50.3	496.2
	DCT 2.1	Unconditioned	6.5	81.9	49.7	523.0
	DCT 3.1	Unconditioned	7.0	81.8	48.7	515.8
	DCT 4.1	Unconditioned	6.8	82.5	49.9	620.1

Table 66: VTP2 DCT Individual Specimen Data

Mix	Specimen I.D.	Conditioning Method	Air Voids (%)	Avg. Ligament Length (mm)	Avg. Specimen Height (mm)	Fracture Energy (J/m^2)
VTP2	DCT 1.2	Freeze-Thaw	6.9	82.3	50.8	640.1
	DCT 2.2	Freeze-Thaw	7.5	81.4	49.0	546.4
	DCT 3.1	Freeze-Thaw	7.4	82.7	49.0	431.6
	DCT 1.1	Unconditioned	7.2	82.7	48.9	511.8
	DCT 2.1	Unconditioned	7.0	81.0	49.9	Pre-Test Crack
	DCT 3.2	Unconditioned	7.1	80.2	50.8	576.3

Table 67: MEP1 DCT Individual Specimen Data

Mix	Specimen I.D.	Conditioning Method	Air Voids (%)	Avg. Ligament Length (mm)	Avg. Specimen Height (mm)	Fracture Energy (J/m^2)
MEP1	DCT 1.2	Freeze-Thaw	7.3	81.6	51.3	679.6
	DCT 3.1	Freeze-Thaw	6.8	80.6	49.1	602.4
	DCT 4.2	Freeze-Thaw	7.0	80.8	50.3	650
	DCT 1.1	Unconditioned	6.9	80.8	50.5	651.6
	DCT 2.1	Unconditioned	7.0	83.1	49.3	650.3
	DCT 4.1	Unconditioned	6.9	81.8	49.7	608.7

Table 68: MEP2 DCT Individual Specimen Data

Mix	Specimen I.D.	Conditioning Method	Air Voids (%)	Avg. Ligament Length (mm)	Avg. Specimen Height (mm)	Fracture Energy (J/m^2)
MEP2	DCT 4.2	Freeze-Thaw	6.6	81.6	50.0	556.7
	DCT 5.1	Freeze-Thaw	7.1	81.6	48.3	722.9
	DCT 7.1	Freeze-Thaw	6.9	81.8	49.1	668.1
	DCT 5.2	Unconditioned	7.4	80.8	50.4	637.4
	DCT 6.1	Unconditioned	7.2	83.1	49.2	Pre-Test Crack
	DCT 6.2	Unconditioned	7.5	80.8	49.7	634.2

Table 69: NHG1 DCT Individual Specimen Data

Mix	Specimen I.D.	Conditioning Method	Air Voids (%)	Avg. Ligament Length (mm)	Avg. Specimen Height (mm)	Fracture Energy (J/m^2)
NHG1	DCT 1.1	Freeze-Thaw	6.7	82.2	49.5	626.4
	DCT 2.2	Freeze-Thaw	7.1	82.4	49.1	585.3
	DCT 4.2	Freeze-Thaw	7.0	82.3	49.5	493.7
	DCT 2.1	Unconditioned	7.3	81.3	49.9	563.9
	DCT 3.1	Unconditioned	7.2	81.1	49.7	426.1
	DCT 3.2	Unconditioned	7.2	83.4	49.8	670.9

Appendix F: Hamburg Wheel Tracker Individual Specimen Results

The following section contains individual specimen results from Hamburg testing. Results from both traditional analysis and TTI analysis are included. It should be noted that the average passes to failure and stripping inflection point results in Chapter 3 are not arithmetic averages of the results in Table 70. A spreadsheet containing an algorithm, which uses weighting factors, was used to find the average values.

Table 70: Traditional Hamburg Analysis Results

Mix	Specimen	Air Voids (%)	Passes to Failure	Stripping Inflection Point	Avg. Creep Slope (mm/1K pass)	Avg. Stripping Slope (mm/1K pass)
VTG1	Left	7.0	No Failure	None	0.3	0.33
	Right	7.2	No Failure	None		
VTP1	Left	6.9	No Failure	None	0.26	0.89
	Right	7.2	No Failure	16467		
VTP2	Left	7.1	18448	14739	0.31	1.7
	Right	7.2	15366	12488		
MEG1	Left	7.1	No Failure	None	0.33	0.77
	Right	7.4	18680	None		
MEP1	Left	7.1	19810	14984	0.45	1.17
	Right	7.3	13324	None		
MEP2	Left	6.8	No Failure	None	0.37	0.43
	Right	7.1	No Failure	None		
MEP3	Left	7.0	11650	9781	0.25	4.38
	Right	7.2	13230	11761		
MEP4	Left	7.2	No Failure	15941	0.22	0.66
	Right	7.3	No Failure	None		
CTP1	Left	6.7	No Failure	None	0.21	0.38
	Right	6.8	No Failure	None		
NHG1	Left	6.8	No Failure	None	0.11	0.08
	Right	7.1	No Failure	None		

For the TTI analysis results, the values reported in Chapter 3 are arithmetic averages of the individual results. For specimens that did not experience a stripping number or reach the stripping life, values of 25,000 passes were used for the calculations of the mixture average.

Table 71: TTI Hamburg Analysis Results

Mix	Specimen	Air Voids (%)	Stripping Number (LC sn)	Stripping Life (LC st)
VTG1	Left	7	None	No Failure
	Right	7.2	None	No Failure
VTP1	Left	6.89	8078	20775
	Right	7.22	8126	18843
VTP2	Left	7.13	6948	17013
	Right	7.2	6609	14415
MEG1	Left	7.08	None	No Failure
	Right	7.44	7829	16691
MEP1	Left	7.1	7914	12543
	Right	7.3	4720	12190
MEP2	Left	6.8	None	No Failure
	Right	7.1	None	No Failure
MEP3	Left	7	3439	10668
	Right	7.2	4948	12570
MEP4	Left	7.15	7706	20157
	Right	7.33	None	No Failure
CTP1	Left	6.7	8987	27124
	Right	6.8	None	No Failure
NHG1	Left	6.8	None	No Failure
	Right	7.1	None	No Failure